Available online at www.sciencedirect.com

SciVerse ScienceDirect

Journal of Electrocardiology 46 (2013) e1 – e37

JOURNAL OF Electrocardiology

www.jecgonline.com

ICE 2013 Oral Abstracts

A novel approach to determine atrial repolarization in electrocardiograms

J. Sivaraman[a], G. Uma[a], S. Venakatesan[b], M. Umapathy[a], V.E. Dhandapani[b]

[a]*Department of Instrumentation and Control Engineering, National Institute of Technology, Trichy, India*

[b]*Department of Cardiology, Madras Medical College, Government General Hospital, Chennai, India*

Introduction: The observation of atrial activity is critical in the case of atrial arrhythmias. Since the ventricular QRS potential may obscure that of the P wave, much information about the atrial phase is not well determined in the standard 12 lead ECG. A novel Modified Limb Lead (MLL) system is proposed to enhance the atrial P and Ta waves in healthy subjects and patients with AV block.

Methods: Sixty healthy male subjects (mean age 38 ± 8.76 years) and fifteen male patients with AV block (mean age 68 ± 5.43 years) were studied. In addition to a standard 12-lead ECG, an MLL ECG was recorded with the RA electrode placed at the 3rd right intercostal space a little to the right of the parasternal line, the LA electrode placed in the 5th right intercostal space slightly to the right of the mid clavicular line, and the LL electrode placed in the 5th right intercostal space on the mid clavicular line. ECGs were recorded for 60 s each with an EDAN SE-1010 PC ECG system.

Results: The average R wave amplitude and duration in standard leads I–aVF were 0.44 ± 0.25 mV and 89.61 ± 17.07 ms respectively. The average P wave amplitude and duration were 0.04 ± 0.05 mV and 91.83 ± 7.12 ms respectively. Corresponding MLL R and P wave amplitude and duration measurements were 0.13 ± 0.09 mV, 89.64 ± 11.45 ms and 0.07 ± 0.09 mV, 86.84 ± 5.41 ms. A negative wave was observed after the P wave in the PR segment of the MLL trace. This was regarded as the atrial Ta wave. The polarity of the Ta wave was opposite to that of the P wave and the duration was longer. A significant correlation was found between P and Ta wave amplitudes ($r = 0.30$, $p = 0.01$). In all cases of AV block, the Ta wave was observed more clearly in the MLL ECG than in the standard ECG.

Conclusion: The MLL system allows easier recognition of the atrial Ta wave than the standard 12 lead ECG.

http://dx.doi.org/10.1016/j.jelectrocard.2013.05.009

Advanced interatrial block is associated with atrial fibrillation recurrence after successful pulmonary vein isolation for paroxysmal atrial fibrillation

J.C. Caldwell, S. Koppikar, W. Barake, D.P. Redfearn, K. Michael, C. Simpson, W. Hopman, A. Baranchuk

Kingston General Hospital, Ontario

Introduction: Pulmonary vein isolation (PVI) for paroxysmal AF (PAF) is successful in ~70–80% of cases often requiring repeat procedures. This suggests that electrical abnormalities outside the pulmonary veins are involved. Interatrial block (IAB), with resultant left atrial (LA) electrical heterogeneity, is known to be associated with AF development. This study aimed to assess the association between IAB and AF recurrence post PVI.

Methods: Twelve lead ECGs were analysed blindly on PVI patients from Aug 2007–Aug 2011; patients with persistent AF, mitral valve disease, undergoing redo procedures or with no sinus rhythm (SR) ECG within 1 year of the procedure were excluded. ECGs were scanned at 300 DPI, amplified × 10 before maximum and minimum p-wave duration (PWD) were measured. Advanced IAB was defined as max PWD >140 ms. Medical records were examined for demographics, duration of AF, presence of co-morbid conditions and echocardiographic parameters prior to ablation.

Results: The selective cohort consisted of 100 patients: age 58 ± 11 years, 72% male, LVEF 62 ± 9%, 18% ischaemic heart disease and 13% diabetic. Thirty-five had advanced IAB. Advanced IAB was associated with greater AF recurrence rates (63% vs 35%, $p < 0.05$ compared to those without advanced IAB). Similarly, AF recurrence was associated with greater maximum PWD (139 ± 17 vs 129 ± 14, $p < 0.01$), p-wave dispersion (58 ± 21 vs 49 ± 15, $p < 0.01$), LA dimension (41 ± 6 vs. 38 ± 5, $p < 0.05$) and LA volumes (40 ± 14 vs 34 ± 11, $p < 0.05$) compared to those in who remained in SR.

Conclusion: The presence of pre-existent advanced IAB is associated with a higher risk of AF recurrence post ablation for paroxysmal AF.

http://dx.doi.org/10.1016/j.jelectrocard.2013.05.010

Novel body surface electrical restitution based marker is predictive of sudden cardiac death risk independent of existing risk markers

W.B. Nicolson[a], M.I. Smith[b], G. Chu[b], A.J. Sandilands[c], P.J. Stafford[c], F.S. Schlindwein[b], N.J. Samani[a], G.P. McCann[a], G.A. Ng[a]

[a]*Leicester Cardiovascular Biomedical Research Unit*

[b]*University of Leicester*

[c]*University Hospitals of Leicester NHS Trust*

Introduction: Better sudden cardiac death (SCD) risk markers are needed. We have developed the Regional Restitution Instability Index (R2I2) and retrospectively demonstrated its potential utility for risk stratification of patients with ischaemic cardiomyopathy. The R2I2 quantifies cardiac electrical instability by measuring heterogeneity in electrical restitution. We present the first prospective evidence of R2I2's potential.

Methods: We conducted a blinded prospective study of 60 ischaemic cardiomyopathy patients undergoing risk stratification for implantable cardioverter defibrillator and 15 control patients having an electrophysiological study (EPS) for assessment of supraventricular tachycardia. The R2I2 technique has been described previously: a 12 lead ECG is recorded during an EPS and APD restitution gradient heterogeneity across the ECG is calculated using surrogates for action potential duration and diastolic interval.

Results: R2I2 was significantly higher in IHD patients compared with controls (mean ± SEM: 0.91 ± 0.04 vs. 0.67 ± 0.05, $p = 0.006$) and higher in 16 patients with endpoint of ventricular arrhythmia/SCD than the rest (1.11 ± 0.09 vs. 0.84 ± 0.04, $p = 0.003$, median 22 months follow up).

R2I2 was predictive of endpoint independent of EPS result, LVEF or QRS duration (Cox model p = 0.003). Using a predefined cut-off R2I2 value of ≥1.03 identified patients with a significantly higher risk of ventricular arrhythmia/SCD (63%) compared with R2I2 <1.03 (18%) (p < 0.0001).

Conclusions: The R2I2, replicating a predefined technique, identified patients at very high risk of developing ventricular arrhythmias. R2I2 is a straightforward, potentially non-invasive test that could add considerable value to existing sudden cardiac death risk markers.

http://dx.doi.org/10.1016/j.jelectrocard.2013.05.011

Body surface restitution gradient predicts sudden cardiac death risk in a clinical study

W.B. Nicolson[a], M.I. Smith[b], G. Chu[b], P.B. Brown[b], A.J. Sandilands[c], P.J. Stafford[c], F.S. Schlindwein[b], N.J. Samani[a], G.P. McCann[a], G.A. Ng[a]
[a]*Leicester Cardiovascular Biomedical Research Unit*
[b]*University of Leicester*
[c]*University Hospitals of Leicester NHS Trust*

Introduction: Peak action potential duration (APD) restitution gradient greater than unity has been mathematically linked to ventricular arrhythmogenesis. This abstract investigates peak body surface and peak intracardiac APD restitution gradients as predictors of sudden cardiac death (SCD).

Methods: We conducted a prospective, blinded study of 60 patients with ischaemic heart disease being assessed for ICD implantation and 15 control patients. Standard APD restitution curves were constructed for each lead of the 12 lead ECG using surrogates for APD (QRS onset to T wave peak, QTp) and diastolic interval (T wave peak to the following QRS onset, TpQ) and for the unipolar signal (45/60 patients). Peak mean 12 lead body surface restitution gradients were calculated from the mean of the gradients across the 12 ECG leads taken at each S1S2 coupling interval.

Results: Peak mean 12 lead body surface restitution gradient was significantly higher in study patients experiencing appropriate ICD therapy (Ax)/SCD (16/60) than in those not (1.35 [0.60] vs. 1.08 [0.52], p = 0.01) and similarly in study patients compared with controls (1.11 [0.60] vs. 0.98 [0.31], p = 0.431). Peak unipolar APD restitution gradients were non-significantly higher in study patients receiving Ax/SCD (13/45) than those not (2.94 [3.26] vs. 2.06[2.19], p = 0.43) and similar in study versus control patients (2.21 [2.49] vs. 2.00 [1.03], p = 0.27).

Conclusions: Peak mean body surface restitution gradient shows potential as a marker of SCD. Its superiority over intracardiac data may be due to the tighter distribution of values. Also, an intracardiac catheter can be proximate to or distant from pathology whereas the body surface signal summates cardiac electrical activity.

http://dx.doi.org/10.1016/j.jelectrocard.2013.05.012

Global cardiovascular risk and arrhythmic electrocardiographic markers in hypertensive patients without coronary artery disease

A. Morales-Salinas[a], E. León-Aliz[b], R. Carmona-Puerta[c]
[a]*Cardiocentro "Ernesto Che Guevara", Cuba*
[b]*Cardiocentro "Ernesto Che Guevara", Cuba*
[c]*Cardiocentro "Ernesto Che Guevara", Cuba*

Background: Arrhythmias are a major cause of morbidity and mortality in acute coronary ischemia. However, arrhythmic electrocardiographic markers are underutilized in the prediction of global cardiovascular risk. The aim of this study, therefore, was to analyze the relationship between global cardiovascular risk and some major electrocardiographic markers of arrhythmias.

Methods: This was a cross sectional study. The sample included 48 hypertensive patients without personal history of coronary artery disease. The main variables were clinical (age, sex, personal history, etc), laboratory (cholesterol, glucose, etc) and electrocardiogram (P wave dispersion – DP, QT interval, QT dispersion – ΔQT, T peak-T end – Tp-e and QRS duration). All electrocardiogram variables were corrected for heart rate. Global cardiovascular risk was calculated according to quantitative-qualitative score of the European Society of Hypertension. Exclusion criteria were: atrial fibrillation, left bundle branch block, pacemaker, chronic obstructive pulmonary disease and asthma.

Results: Mean age was 59.4 years, women, 52.1%. Prevalence of smoking, hypercholesterolemia, diabetes and obesity was 18.8%, 27.1%, 25% and 56.3% respectively. 25%, 22.9% and 31.3% of patients were classified as "moderate", "high" and "very high" risk subgroups in each case, according to the global cardiovascular risk. We found a significant relationship between global cardiovascular risk and the following electrocardiographic markers: dP (p = 0.013), QT (p = 0.010) and Tp-Te (p = 0.000).

Conclusion: There is a relationship between markers of ischemia and arrhythmias in hypertensive patients with "moderate", "high" and "very high" global cardiovascular risk.

http://dx.doi.org/10.1016/j.jelectrocard.2013.05.013

Modeling of presymptomatic and symptomatic stages of Parkinsonism in MPTP-treated mice: heart contraction adrenergic regulation and catecholamines content in blood

R.R. Nigmatullina[a], T.S. Fedoseeva[a], G.R. Khakimova[b], V.S. Kudrin[c], S.N. Zemskova[a], M.V. Ugrumov[b]
[a]*Kazan State Medical University, Kazan, Russia*
[b]*Institute of Developmental Biology RAS*
[c]*Institute of Pharmacology RAMS, Moscow, Russia*

Introduction: Parkinson's disease (PD) in humans is characterized by a long-term development at the preclinical (presymptomatic) stage and a widespread occurrence of pathological processes besides a degeneration of nigrostriatal dopaminergic (DA-ergic) neurons. It was thought that testing of peripheral manifestations of the systemic pathology might be useful for the development of a preclinical diagnosis of PD. To this end, the peripheral markers should be sought in humans just after the appearance of motor symptoms and before the onset of specific treatment and in Parkinsonian animals at the pre-symptomatic (PSS) stage and the early symptomatic stage (ESS). The goal was to evaluate: i.) functional activity of the heart with focus on catecholaminergic (CA) regulation; ii.) catecholamine contents [CA] in plasma at the PSS and ESS.

Methods: Models of the pre-symptomatic and the early symptomatic stages of Parkinsonism were recently developed (Ugrumov et al., 2011) by sub-cutaneous MPTP injections.

Results: Heart failure was induced in MPTP-treated mice under a transition from the PSS to the ESS. Indeed, the weight and contraction force of the left ventricle were not changed at the PSS compared to the control whereas a noradrenaline (NA) stimulating influence on its contraction increased significantly. Conversely, at the ESS, the weight and contraction of the left ventricle decreased and were accompanied by a decrease of an NA influence on the ventricular contraction. The presumptive changes in [CA] in plasma were considered as a manifestation of the MPTP-induced perturbations of peripheral CA systems. The DA concentration decreased by 28% at the PSS and tripled at the ESS. The other [CA] remained unchanged at the PSS and increased significantly at the ESS.

Conclusion: Transition of the PSS of Parkinsonism to the ESS in MPTP-treated mice was manifested by the development of heart failure as well as by an increase of the [CA] in plasma.

http://dx.doi.org/10.1016/j.jelectrocard.2013.05.014

Estimation of variability in manual QT interval measurements by a group of readers: comparison of two study designs

V.S. Salvi, D.R. Karnad, V. Kerkar, G.K. Panicker, M. Natekar, S. Kothari
Quintiles Cardiac Safety Services

Introduction: Inter- and intra-reader variability (RV) in QT interval measurement should be quantified in each Thorough QT study; two methods

are commonly used for this. However, the performance of these methods has never been compared.

Methods: In the grouped analysis design (GAD), a set of 40 ECGs was read twice by 12 readers. In the pairwise analysis design (PAD), 40 ECGs analyzed by each reader in a clinical trial were analyzed again by the same reader (intra-RV) and also by another reader (inter-RV); thus, 40 different ECGs were used to estimate variability between each pair of readers (totaling 480 ECGs). Using data from 500 ECGs that had been analyzed twice by 12 readers, we bootstrapped 1000 datasets each for both methods. Inter- and intra-RV were estimated by means and standard deviations of actual and absolute differences, and also by an ANOVA interaction model.

Results:

Table
Mean (95% CI) of reader variability in QT interval measurement from 1000 datasets of 480 ECGs read twice by 12 readers.

Statistical method	Inter-reader variability (ms)		Intra-reader variability (ms)	
	GAD	PAD	GAD	PAD
Actual difference	0 (−0.5 to 0.4)	0 (−0.7 to 0.6)	0 (−0.8 to 0.7)	0 (−0.8 to 0.7)
Absolute difference	7.7 (6.2 to 9.8)	7.7 (6.6 to 9.1)	5.2 (4.3 to 6.3)	5.1 (4.4 to 6.0)
ANOVA model	3.9 (2.1 to 5.5)	4.1 (2.6 to 5.4)	4.4 (3.6 to 5.9)	4.3 (3.7 to 5.3)

Conclusions: Reader variability estimates by both study designs are comparable; pairwise analysis design, which uses more ECGs, may be preferred for quantifying study-specific RV while grouped analysis design, which uses a small number but of same ECGs for all readers, may be preferred for benchmarking performance of a group of readers as in a central laboratory.

http://dx.doi.org/10.1016/j.jelectrocard.2013.05.015

Reader variability in QT interval measurement due to measurement error and variability in leads selection: a simulation study comparing 2-way vs. 3-way interaction ANOVA model

V.S. Salvi, M. Natekar, D.R. Karnad, A. Ramasamy, V. Kerkar, G.K. Panicker, S. Kothari
Quintiles Cardiac Safety Services

Introduction: QT interval is usually measured in lead II by trained readers; however if a reader considers lead II unsatisfactory, it is measured in another ECG lead. Reader variability (RV) results from measurement differences or variability in lead section; the latter is not reflected in conventional methods for estimating RV.

Methods: The mean and SD of QT intervals in 12-leads of 100 ECGs measured twice (Read1 and Read2) by 25 readers were used to simulate datasets with inter-RV of 5, 10, 15, 20, 25 ms and intra-RV of 3, 6, 9, 12, 15 ms. 625 datasets were simulated such that different leads were used in Read1 and Read2 in 0, 10, 20, 30, 40% of ECGs by 25 readers. RV was estimated using ANOVA interaction models: a 3-way model using reader, ECG and lead as factors, and a 2-way model using reader and ECG as factors.

Results: Estimates from the 3-way model accurately matched the inter- and intra-RV that were introduced during simulation for all combinations of intra- and inter-reader measurement variability regardless of percent of ECGs with lead selection variability. The 2-way model showed increasing RV estimates as the proportion of ECGs read in different leads increased (Table).

Conclusion: Although a 3-way model provides an accurate estimate of measurement variability, it only uses measurements made in the same lead in Read I and Read II. The 2-way model provides identical estimates when both reads are in same leads, but higher, more realistic estimates when measurements are made in different leads.

Table
RV estimates (ms) by 2-way model for measurement variability of 5 ms inter-RV and 3 ms intra-RV introduced during simulation in 25 ECGs read twice by 25 readers.

ECGs with QT in a different lead	Intra-RV					Inter-RV				
Read2 (%) → Read1 (%)↓	0	10	20	30	40	0	10	20	30	40
0	2.9					5.8				
10	2.9	5.6	7.3	8.6	10	10.4	9	9.6	9.9	10.8
20	2.9	5.5	7.6	8.9	10.4	10.1	10.4	10.9	11	11.5
30	2.9	5.6	7.8	9.2	10.6	11.6	11.7	12	12.3	12.3
40	2.9	5.9	7.9	9.5	10.7	13.2	13.2	13.4	13.4	13.4

Similar results were observed for other combinations of measurement variability.

http://dx.doi.org/10.1016/j.jelectrocard.2013.05.016

Prevalence of normal electrocardiograms in primary care patients: a study by a telecardiology service

M.S. Marcolino[a], D.M.F. Palhares[b], M.B.M. Alkmim[c], A.L. Ribeiro[a]
[a]Department of Internal Medicine, Medical School, Universidade Federal de Minas Gerais, Brazil
[b]Medical School, Universidade Federal de Minas Gerais, Brazil
[c]Telehealth Center Network of Minas Gerais, Brazil

Introduction: The electrocardiogram (ECG) is an easy exam to perform, has low-cost and significant clinical usefulness. A knowledge of the proportion of normal and abnormal ECGs in primary care patients allows the estimation of the proportion of exams that can be analyzed by a general practitioner with minimal training in ECG interpretation, in addition to being of epidemiological relevance. The objective of this study was to assess the prevalence of normal ECGs in primary care patients.

Methods: In this observational and retrospective study, all 12-lead standard digital ECGs analyzed by cardiologists of a public telemedicine service in Brazil from January to December 2011 were assessed. This service supports primary care in 660 cities in the province of Minas Gerais. ECGs were sent by IT professionals from the remote sites over the internet to be analyzed centrally by cardiologists who were trained and experienced in the analysis and interpretation of ECG. The prevalence of normal ECGs was assessed.

Results: During the study period, 290,795 ECGs were analyzed (mean age 50.9 ± 19.0 years), and 57.6% of them were found to be normal. This proportion was higher in women (60.1 vs 53.8%, $p < 0.001$) and lower in patients with hypertension (45.8% vs 63.2%, $p < 0.001$) or diabetes (43.3% vs 58.4%, $p < 0.001$). There was a progressive reduction of the prevalence of normal ECG with increasing age (Table 1). Among the ECGs of patients under investigation for chest pain, 58.7% had no abnormalities.

Conclusion: The prevalence of normal ECGs in primary care patients is over 50% and this proportion decreases with age and comorbidities. Most ECGs performed for investigation of chest pain in primary care have no abnormalities.

Table 1
Prevalence of normal electrocardiograms according to age distribution.

Age group (years)	N	Prevalence (%)
30–39	35,885	74.6
40–49	51,095	66.7
50–59	57,885	56.4
60–69	49,092	45.2
70–79	34,426	34.4
80–89	13,394	24.6
≥90	1,837	20.5

http://dx.doi.org/10.1016/j.jelectrocard.2013.05.017

Frequent electrocardiographic abnormalities and associated conditions in Chagas disease patients

M.S. Marcolino[a], T.G.P. Assis[a], E.V. Santos[a], L.R. Ferreira[a], D.M.F. Palhares[a], M.B.M. Alkmim[b], A.L. Ribeiro[a]
[a]*Medical School, Universidade Federal de Minas Gerais, Brazil*
[b]*Telehealth Center Network of Minas Gerais, Brazil*

Introduction: Chagas disease (ChD) is endemic in Latin American countries, but has become a worldwide problem due to migration of infected individuals to developed countries. Electrocardiography has been considered an essential exam to evaluate ChD patients. The objective of this study is to identify prevalent abnormalities in the electrocardiogram (ECG) and common associated conditions in patients with ChD.

Methods: In this observational and retrospective study, all 12-lead standard digital ECGs analyzed by cardiologists of a public telemedicine service in Brazil, from January to December 2011 were assessed. This service attends primary care of 660 cities in Minas Gerais province. ECGs were sent by IT professionals in remote sites over the internet to be analyzed centrally by cardiologists who were trained and experienced in the analysis and interpretation of ECGs. The prevalence of ECG abnormalities in patients known to have ChD was assessed.

Results: During the study period, 264,324 patients were assessed; 7590 were ChD patients (mean age 57.0 ± 13.7 years, 64.1% women). Hypertension was the most frequent comorbidity (61.3% of the ChD patients), followed by diabetes (9.1%) and dyslipidemia (6.9%). Family history of coronary disease was reported by 32.6% of the patients, and 10.7% were smokers. Only 30.1% of them had normal ECGs. Regarding the rhythm, 86.9% had normal sinus rhythm, 5.3% atrial fibrillation or flutter, 5.4% ventricular premature beats, 2.5% supraventricular premature beats and 3.5% were pacemaker users. Right bundle branch block (RBBB) was observed in 22.7% of the ECGs, left bundle block in 3.1% and left anterior hemiblock (LAH) in 22.5%.The presence of first degree atrioventricular block was found in 4.9%, second and third degrees in 0.2% each. There was electrocardiographic evidence of left ventricular and atrial hypertrophy in 3.6% and 2.5% of patients, respectively.

Conclusion: In this large sample of primary care patients with ChD, there was a high prevalence of ECG abnormalities. As expected, the most common abnormalities were RBBB and LAH.

http://dx.doi.org/10.1016/j.jelectrocard.2013.05.018

Atrial fibrillation: prevalence in primary care patients in Brazil

M.S. Marcolino[a], D.M.F. Palhares[a], M.B.M. Alkmim[b], A.L. Ribeiro[a]
[a]*Medical School, Universidade Federal de Minas Gerais, Brazil*
[b]*Telehealth Center Network of Minas Gerais, Brazil*

Introduction: Atrial fibrillation (AF) is a growing public health problem. Although an increasing prevalence has been reported, the actual prevalence is uncertain, and there is a lack of studies in the South American population. As anticoagulation in AF can consistently reduce the possibility of thromboembolic events, the study of its prevalence assumes great importance in primary care. The objective of this study was to assess the prevalence of AF in patients who attended primary care centres of 658 cities in Minas Gerais, Brazil.

Methods: In this observational and retrospective study, all 12-lead standard digital electrocardiograms (ECGs) analyzed by cardiologists of the Telehealth Network of Minas Gerais, a public telemedicine service in Brazil, from January to December 2011, were assessed. In that period, the service supported primary care in 658 cities in Minas Gerais province. ECGs were sent by remote professionals over the internet to be analyzed by cardiologists who were trained and experienced in the analysis and interpretation of ECGs. The prevalence of AF was assessed.

Results: During the study period, 264,324 primary care patients underwent ECG recording (mean age 50.6 ± 19.0 years, 5% were ≥80 years-old, and 59.6% were female). The overall prevalence of AF was 1.8%; 2.4% in men and 1.3% in women ($p < 0.001$). There was a progressive increase in prevalence with age, and the prevalence was higher in men than women in all age groups (Table 1). The most common comorbidities in patients with AF were hypertension (51.8%), Chagas disease (8.8%) and diabetes (7.3%). When compared to other population studies, AF prevalence was similar to that in all age groups in the Anticoagulaton and Risk Factors In Atrial Fibrilation (ATRIA) Study, and similar to the Rotterdam study, except for a lower prevalence in octogenarians in the present study.

Table 1
Prevalence of atrial fibrillation according to age distribution and gender.

Age group (years)	N	Prevalence (%)	
		Males	Females
50–59	52,658	1.6	0.7
60–69	44,126	3.2	1.9
70–79	30,349	6.3	4.1
80–89	11,702	9.8	6.7
≥90	1,574	14.6	8.7

Conclusion: In this study in a large sample of primary care patients, prevalence of AF increased progressively with age and was higher in men than in women. The prevalence and age distribution of AF were similar European and North American studies.

http://dx.doi.org/10.1016/j.jelectrocard.2013.05.019

Electrocardiographic abnormalities in elderly Chagas disease patients: a population-based study (the Bambuí study)

A.L. Ribeiro, M.S. Marcolino, M.F. Lima-Costa
Medical School, Universidade Federal de Minas Gerais, Brazil

Introduction: Electrocardiography has been considered as an important tool in the management of Chagas disease (ChD) patients, although its value in elderly infected patients is unknown. This study was designed to investigate the prevalence and prognostic value of electrocardiographic abnormalities in *Trypanosoma cruzi* chronically infected and non-infected individuals in a community-based cohort of older adults.

Methods: There were 1462 participants (84% of the total) aged 60 and over, who were residents in Bambui City, Brazil, with electrocardiogram (ECG) records coded according to the Minnesota Code. They were followed for 10 years; the endpoint was mortality. Adjustment for potential confounding variables included age, gender, conventional risk factors and B-type natriuretic peptide (BNP).

Results: The mean age was 69 years, with women predominating (60.9%). The prevalence of ChD was 38.1% (n = 557). ECG abnormalities were more frequently found in ChD patients (87.6% vs. 77.7%, $p < 0.001$); the presence of right bundle branch block (RBBB) and left anterior hemiblock was strongly related to ChD (OR: 11.99 [5.60–25.69]). From a total of 556 deaths, 253 occurred in ChD subjects (45.0%). ECG variables independently associated with prognosis in ChD included sinus rhythm, frequent ventricular and supraventricular ectopic beats, atrial fibrillation, RBBB, possible old myocardial infarction, and left ventricular hypertrophy. The presence of any major ECG abnormalities doubled the risk of death in ChD patients (HR: 2.18 [1.35–3.53]), but it also increased the risk in non ChD subjects (HR: 1.50 [1.07–2.10]; the risk of death increased with the number of major abnormalities in the same patient.

Conclusion: The ECG is a powerful method for diagnostic and prognostic evaluation of elderly patients with ChD.

http://dx.doi.org/10.1016/j.jelectrocard.2013.05.020

Arrhythmia telemonitoring in asymptomatic patients

T. Gegenava, M. Gegenava, Z. Kirtava
Tbilisi State Medical University, Georgia

Introduction: Asymptomatic arrhythmias can be a challenge to diagnose. The goal of the present study was to assess asymptomatic episodes of

arrhythmia with the help of mobile telemonitoring, which is an uncomplicated technology that facilitates the continuous monitoring and recording of arrhythmias.

Methods: We investigated 54 outpatients in the Republic of Georgia with different types of arrhythmia (32 male, 22 female, age range – 12–80 years). Among them were patients with unexplained syncope, epilepsy, and asymptomatic patients who underwent radiofrequency catheter ablation. In addition, there were asymptomatic patients after aorto-coronary bypass graft surgery and 10 healthy sportsmen. Investigations were made by 3-lead electrocardiograph-ECG loop recorder in automatic recording/transmitting mode.

Results: Arrhythmias were registered during 7–68 hours of observation. 52% of arrhythmia episodes were asymptomatic. Arrhythmia relapse was detected in 3/6 patients who underwent radiofrequency catheter ablation for SVT or SVPCs, but mostly they were asymptomatic. Asymptomatic episodes of ventricular premature complexes were detected in patients who underwent aorto-coronary bypass graft surgery. In 10 patients with epilepsy, there were 3 patients with supraventricular tachycardia (SVT) and 2 patients with sinus tachycardia. Among 10 patients with unexplained syncope, there were 2 patients with sinus tachycardia, 2 patients with SVT and 1 patient with sick-sinus syndrome. Asymptomatic episodes of supraventricular tachycardia were detected in 1 sportsman. Asymptomatic episodes were detected in the majority of cases ($p = 0.001$). No difference between genders in the frequency of arrhythmias was found ($p = 0.05$).

Conclusions: Mobile telecardiology offers a feasible methodology for monitoring arrhythmia outpatients in Georgia. It is also a useful tool for detecting a relapse, or symptomatic and asymptomatic episodes of life-threatening arrhythmia.

http://dx.doi.org/10.1016/j.jelectrocard.2013.05.021

The response of the pumping function of the heart to the orthostatic test and monoamines plasma level may serve as markers of early-stage Parkinson's disease

R.R. Nigmatullina[a], M.V. Ugrumov[b], N.I. Abzalov[c], S.N. Zemskova[a], O.I. Kuzmina[a]
[a]*Kazan State Medical University, Kazan, Russia*
[b]*Institute of Developmental Biology RAS*
[c]*Kazan Federal (Volga Region) University*

Introduction: Currently, the diagnosis of Parkinson's disease (PD) is made too late, after the appearance of regulatory and compensatory mechanisms, so that therapy does not cure patients. The objective of this study was to develop early (pre-clinical) diagnosis based on revealing peripheral biomarkers. We aimed (1) to identify the sympathetic denervation by studying the heart pumping function (HPF); (2) to reveal the dependence of the HPF on the type of PD; (3) to determine the plasma catecholamines level (CCh) of PD patients.

Methods: To study HPF and to identify the sympathectomy, the tetrapolar chest rheography and orthostatic tests were used. To measure CCh, we used liquid chromatography with electrochemical detection (HELC-ED). Patients with tremor (n = 25) and rigid (n = 10) forms of PD were observed along with a control group (n = 18).

Results: It was found that at the initial stages of PD at rest conditions, the values of HR were higher than in the control group. The lowest HR response to the orthostatic test was found in PD patients with tremor. Stroke volume (SV) in PD was significantly lower. After moving to the standing position, intergroup differences in SV disappeared. In PD plasma, in comparison with controls, we found: 1) an increased level of dopamine (DA); 2) a reduced level of DA precursor – DOPA; and 3) a reduced level of DA metabolite – 3.4-dihydroxyphenyl-acetic acid. Parkinson patients showed the reduced NE and increased EP levels. The increased plasma DA level points to the activation of compensatory mechanisms at the earliest stages of PD, and their dependence on the PD form.

Conclusion: The alteration of the heart pumping function and the catecholamines level occurs in the very early stages of PD, and depends on the type of the disease. Parameters of the pumping function of the heart during the orthostatic test and determination of the level of monoamines in the blood plasma may serve as markers of early-stage PD.

http://dx.doi.org/10.1016/j.jelectrocard.2013.05.022

Electrocardiographic changes in patients with schizophrenia

M. Gegenava, T. Gegenava
Tbilisi State Medical University, Georgia

Introduction: Some antipsychotics are associated with QT interval prolongation on the electrocardiogram (ECG), which increases the risk of sudden death in other populations from potentially fatal ventricular arrhythmias. The aim of present work was to reveal electrocardiographic changes in patients with schizophrenia.

Methods: 71 patients, 30 females and 41 males, with ages varying from 35 to 70 years, with the diagnosis of schizophrenia were investigated. They all received neuroleptics and other psychotropic drugs.

Results: The following changes were detected by electrocardiography: Sinus tachycardia n = 32 (45%); sinus bradycardia n = 8, (11.26%); QTc was prolonged in 21.4 %, nonspecific ST changes were found in n = 13 (18,3%) $p = 0.047$, nonspecific T wave changes in n = 7 (9.8%), ST depression in n = 13, (18.3%), $p = 0.047$, post infarction scarring Q wave and QS complex were detected in n = 14 (19.71%). Extrasystolic arrhythmia was revealed in n = 6 (8.45%) and ventricular extrasystoles in 2.8%. Conduction block was detected in n = 4 (5.63%), mostly manifested as His bundle block. PQ interval was slightly prolonged in the study group. QRS complex duration and QTc interval were also slightly prolonged in patients with schizophrenia. A high correlation was found between QTc prolongation and Haloperidol dosage $p < 0.001$. Such a correlation between other groups of psychotropic medications was not detected. In total, electrocardiographic changes were manifested in 44.3% of the patients. Out of 30 healthy people only 2 (6.6%) showed electrocardiographic changes ($p = 0.035$).

Conclusions: As the results have shown, ECG changes occurred frequently among patients with schizophrenia. Use of electrocardiograms (ECGs) to monitor the safety of pharmacotherapy is the best way to achieve this in psychiatric clinics. Because neuroleptics affect cardiac repolarization, QTc has been found to be an accurate indicator of their effect on the heart.

http://dx.doi.org/10.1016/j.jelectrocard.2013.05.023

Beta-blockade and a1-adenosine receptor blockade effects on atrioventricular conduction in patients with atrial fibrillation

V.D.A. Corino[a], F. Holmqvist[b], P.G. Platonov[b]
[a]*Politecnico di Milano*
[b]*Lund University*

Introduction: Reduced RR irregularity in atrial fibrillation (AF) has been associated with poor outcome. However, whether modification of atrioventricular (AV) conduction using rate control drugs affects RR is not known. We aimed to study whether variability and irregularity of RR are modified by a selective A1 adenosine receptor agonist tecadenoson (tec), beta-blocker esmolol and their combination.

Methods: Seven patients (age 58 ± 8 y, 4 men) with AF were assigned to 300 μg i.v. tec that was given alone and during esmolol infusion (50 μg/kg/min). Heart rate (HR), variability and irregularity of RR intervals were assessed at baseline (B1), after 1st tec bolus (T), tec wash-out (B2), during esmolol infusion alone (E) and in combination with 2nd tec bolus (T + E). Variability was assessed by SDNN, pNN20, pNN50, pNN80 and rMSSD, whereas irregularity was determined by nonlinear measures (regularity index and approximate entropy (ApEn)).

Results: Tec decreases HR and increases all RR variability parameters. Addition of tec to esmolol results in greater RR variability than with tec alone. Irregularity parameters did not change after tec. No significant difference was observed between different dosages. Results are shown in Table 1: rMSSD and R exemplify the behaviour of RR variability and irregularity measures respectively.

Conclusion: Modification of AV node conduction using i.v. A1-receptor blocker and beta-blocker results in increase of RR intervals and their variability but does not affect irregularity of RR series during AF. Relative stability of RR-irregularity measures during AF supports the use of non-linear indices of RR behaviour for assessment of clinical outcome.

Table 1

	B1	T	B2	E	T + E
Normalized HR	1 ± 0	0.92 ± 0.04*	1 ± 0	0.98 ± 0.04°	0.88 ± 0.04°
rMSSD (ms)	161 ± 38	183 ± 39*	191 ± 17	196 ± 28°	235 ± 37°
R (a.u.)	0.08 ± 0.03	0.06 ± 0.02	0.04 ± 0.01	0.05 ± 0.03	0.06 ± 0.03

* $p < 0.05$ compared to B1.
° $p < 0.05$ compared to B2.

http://dx.doi.org/10.1016/j.jelectrocard.2013.05.024

Fragmented QRS as a predictor of arrhythmic events in patients with hypertrophic obstructive cardiomyopathy

D.D. Anselm[a], M. Arce[b], J. Van Grieken[b], E. Trucco[c], L. Mont[c], M. Abello[d], J.L. Merino[e], M. Rivero-Ayerza[f], G. Bulent[g], C. Rodriguez[h], W.M. Hopman[a], F. Femenía[b], A. Baranchuk[a]
[a]*Queen's University, Kingston General Hospital*
[b]*Hospital Español de Mendoza, Argentina*
[c]*Thorax Institute, Hospital Clinic, Universitat de Barcelona*
[d]*Electrophysiology Section, FLENI, Buenos Aires, Argentina*
[e]*Hospital Universitario La Paz, Madrid, Spain*
[f]*Transnational University Limburg, Belgium*
[g]*Osmangazi Eskisehir University, Eskisehir, Turkey*
[h]*Instituto IECTAS Maracaibo, Venezuela*

Introduction: Hypertrophic obstructive cardiomyopathy (HOCM) is a genetic disorder associated with life-threatening arrhythmias frequently requiring an implantable cardioverter-defibrillator (ICD). Seeking a non-invasive method of risk stratification remains a challenge. Our objectives were to determine whether fragmented QRS (fQRS) in the surface ECG at implant can predict arrhythmic events using appropriate therapy delivered by the ICD as a surrogate.
Methods: This was a retrospective multicentre study of patients with HOCM and ICD. Surface 12-lead ECGs were analyzed. Appropriate therapy was validated by a blinded core lab. Univariate and multivariate analyses were performed. A p value <0.05 was considered significant.
Results: We included 102 patients from 13 centres. Mean age at implant was 41.1 ± 18.2 years, 52 % were male. Mean left ventricular ejection fraction was 61.5 ± 9.4%, and two thirds had heart failure NYHA class I. Secondary prophylaxis ICD implantation was the indication for implant in 40.2% of cases. About half received a single chamber ICD. fQRS was present at the time of diagnosis in 21% and 54% at ICD implant. At a mean follow-up of 47.8 ± 39.3 months 41 patients (40.2%) presented with appropriate therapy. In a multivariate logistic regression, predictors of appropriate therapy included fQRS at implant (odds ratio [OR] 16.4, 95% confidence interval [CI] 3.6–74.0, p = 0.0003), a history of combined ventricular tachycardia/fibrillation/sudden death (OR 14.3, 95% CI 3.2–-69.3, p = 0.001) and a history of syncope (OR 5.5, 95% CI 1.5–20.4, p = 0.009). Ten deaths (9.8 %) occurred during the follow-up. fQRS in the lateral location increased the risk of appropriate therapies (p < 0.0001).
Conclusions: fQRS predicts arrhythmic events in patients with HOCM and should be considered in a model of risk stratification.

http://dx.doi.org/10.1016/j.jelectrocard.2013.05.025

Effects of human atrial ionic remodelling by β-blocker therapy on mechanisms of atrial fibrillation: a computer simulation

S.R. Kharche[a], T. Stary[a], I.V. Biktasheva[b], A.J. Workman[c], A.C. Rankin[c], A.V. Holden[d], H. Zhang[e]
[a]*University of Exeter*
[b]*University of Liverpool*
[c]*University of Glasgow*
[d]*University of Leeds*
[e]*University of Manchester*

Introduction: Atrial anti-arrhythmic effects of beta-adrenoceptor antagonists (β-blockers) probably involve both an acute suppression of pro-arrhythmic effects of catecholamines, and an adaptational electrophysiological response to chronic β-blocker use — so-called "pharmacological remodelling". In human atrium, such remodelling involves a decrease in transient outward (I_{TO}) and inward rectifier (I_{K1}) K^+ currents and an increase in cellular action potential duration (APD) and effective refractory period (ERP). However, the consequences of these changes on mechanisms of genesis and maintenance of atrial fibrillation (AF) are unknown. Using mathematical modelling, we tested the hypothesis that human atrial ion current changes resulting from chronic β-blocker therapy suppress AF by inhibiting re-entry through increasing ERP.

Methods: Contemporary, biophysically detailed human atrial cell and tissue (1D, 2D and 3D) models, were used to investigate effects of reducing whole-cell density of I_{TO} and I_{K1} by equivalent magnitudes as in atrial cells from patients taking β-blockers.

Results: Chronic β-blockade-remodelling prolonged simulated atrial cell APD and ERP, and reduced the incidence of cellular APD alternans. At the 1D tissue level, β-blocker-remodelling decreased the maximum pacing rate at which APs could be conducted. At the 2D tissue level, β-blocker-remodelling increased reentry spiral wave-meander, and reduced the rate of localised excitation. At the 3D organ level, β-blocker-remodelling reduced the life span of reentry scroll waves.

Conclusion: This study improves our understanding of the mechanisms of suppression of human AF by chronic β-blocker therapy. We show, with mathematical modelling, that AF suppression may involve a reduced propensity for initiation and maintenance of spiral wave re-entry, as a consequence of increased APD and ERP and suppression of alternans.

http://dx.doi.org/10.1016/j.jelectrocard.2013.05.026

Computer simulation of the role of fibre orientation in cardioversion of chronic atrial fibrillation

S.R. Kharche[a], T. Stary[a], I.V. Biktasheva[b], H. Zhang[c], V.N. Biktashev[a]
[a]*University of Exeter*
[b]*University of Liverpool*
[c]*University of Manchester*

Introduction: Fibre orientation anisotropy in the human atria influences successful electrical cardioversion. This study quantifies the effectiveness of an established cardioversion method using a novel cardiac simulation environment, BeatBox.

Methods: A biophysical human atrial cell model was used to simulate Control and chronic atrial fibrillation (CAF) action potentials (APs). The cell model was combined with human atrial geometry to construct a 3D realistic human atrial model with fibre directions. Cardioversion parameters of threshold stimulus and low energy stimulation strength required for scroll wave termination were evaluated. The obtained results were compared to a previous isotropic case study.

Results: CAF reduced the AP from 306 ms to 120 ms. Scroll waves were initiated at two locations (L1 and L2) and the electrical activity registered at a point registration electrode. Under CAF isotropic conditions, the scroll waves became pinned. In contrast, anisotropy caused the scroll wave to degenerate into multiple scrolls with each scroll evolving erratically or pinning to anatomical defects. Recurrence cycle maps show that under CAF, isotropy leads to a monomorphic tachycardia while anisotropy promoted a polymorphic tachycardia. The single shock stimulation threshold to eliminate CAF scroll waves was found to be 4.5 pA/pF. For CAF scroll waves initiated at location L1, a series of small amplitude global stimuli of strength 0.4 pA/pF were sufficient in terminating the scroll waves. However CAF scroll waves initiated at L2 required a stimulation strength of 2 pA/pF for

termination within 10 s. In all CAF simulations, the localized pacing at the registration electrode was approximately 8 Hz.

Conclusions: Inherent atrial anisotropy plays an important role in atrial electrical properties. The low energy stimulus strength has a strong correlation to the scroll wave location. The low energy stimulation strength was always lower than the threshold stimulus. Anisotropy aggravated CAF and led to high frequency erratic propagations. The efficacy of cardioversion is significantly affected by anatomical defects as well as anisotropy. The novel multifunction simulation package, BeatBox, is an ideal simulation environment that facilitates such extensive large scale simulation studies.

http://dx.doi.org/10.1016/j.jelectrocard.2013.05.027

5-HT2B receptor expression and its role in an embryonic development of human myocardium

D.F. Bilalova
Kazan State Medical University, Kazan, Russia

Introduction: Serotonin plays an important role in the development (Nebigil, 2003) of myocardial fibro-elastic component (FEC). It was postulated that one of the mechanisms of acquired defects (AD) is the activation of endothelial cells (EC) by serotonin.

Goal: Identification of 5HT2b serotonin receptor (5-HT2bR) expression and its intensity in the human embryo (HE) in the fetal period of development (FPD).

Objectives: 1. To estimate the morphological changes of the heart in the FPD; 2. To estimate the 5HT2b receptor expression intensity, including in the EC; 3. To reveal the dependence between heart development and intensity of 5HT2b expression throughout the FPD.

Results: At 11–12 weeks of embryonal development, a strong expression of 5-HT2bR is observed in all of the human myocardium. However, initially, expression of 5-HT2bR is manifested in the thickness of the whole heart, while later it is more peripheral, being closer to the epicardium (Ep), and in the atria (AT). Further, there is a decrease of intensity. However, the atria continues to express a large number of 5HT2bR. Probably, 5-HT2bR at 10–12 weeks is responsible for the differentiation of structures and hence the expression of 5-HT2bR is observed in all parts of the heart. These changes occur at the end of the second trimester. The 15–16th weeks are characterized by a lack of expression of 5-HT2bR in the endocardium and epicardium. It was also found that there was migration of the 5-HT2bR expression closer to Ep, as well as weakening with conversion to the negativity of the coloring of the 5HT2bR in the FEC structures of the heart. In the ventricles, due to cell differentiation, which is located closer to the Ep, the immunopositive cells remain in the midline structures. In the third trimester, the expression of 5HT2bR is observed in the EC of the valves, but the ventricular EC still remains immunonegative.

Conclusion: It could be assumed that the cells of such type can serve as a generator that stimulates the growth and differentiation in the myocardium of the human embryo as well as providing a further backup restore mechanism.

http://dx.doi.org/10.1016/j.jelectrocard.2013.05.028

Usability study to assess the ability of randomly selected untrained target users to operate public access defibrillators in the United States

P. O'Hare[a], P. McCanny[a], H. Torney[a], G. Crispino[b], L. Crawford[c], A. McIntyre[a], C. McIntyre[a], DiR. Maio[a]
[a]*HeartSine Technologies Ltd*
[b]*University College Dublin*
[c]*University of Ulster*

Introduction: The design of public access, automatic external defibrillators (AED) must be intuitive, offer clear and easy-to-follow instructions and is assessed as part of the regulatory approval process. This usability study was designed to assess if a new AED could be safely and correctly used by a representative sample of target users in the North American market.

Methods: Randomly selected untrained users (15–65+ years old, n = 81) were assessed for time to turn on the device, time to place electrodes, electrode placement, time to first shock, participant contact during "shock delivery" and CPR efficacy. Qualitative and quantitative data were collected including both participant self and investigator observer evaluation. Audio-visual data were gathered to analyse and evaluate all parameters. Results were compared to previously published studies. Statistical analysis was performed using the R statistical package.

Results: All participants successfully delivered a shock. Average time to place electrodes was 66.9, 63.0 and 64.6 seconds for the 15–21, 22–64 and 65+ age groups, respectively. Average time to first shock was 92.8, 88.8 and 89.1 seconds for the 15–21, 22–64 and 65+ age groups, respectively. Average time to first shock was either equal to or significantly quicker ($P < 0.01$) when compared to those in reference study (134 seconds). First-to-shock-times were comparable to studies of minimally trained AEDs users.

Table 1
Summary table of primary efficacy variables.

	Ages 15–21	Ages 22–64	Ages 65+	CPR trained	Not CPR trained	Defib trained	Not Defib trained	All participants
Time to switch on (seconds)	4.8 (−17, 11.3)	3.7 (1.2, 6.2)	3.5 (0.3, 6.7)	4.9 (−06, 10.4)	3.3 (1.2, 5.4)	N/A	4 (0, 7.9)	4 (0, 7.9)
Time to place electrodes (seconds)	66.9 (40.9, 92.9)	63 (37.8, 88.2)	64.6 (53.7 75.4)	65.4 (42.9, 87.9)	63.4 (39.2, 87.6)	N/A	64.2 (40.8, 87.6)	64.2 (40.8, 87.6)
Time to first shock (seconds)	92.8 (66, 1 19.6)	88.8 (60.6, 117)	89.1 (79.3, 100)	90.7 (67.7, 113.7)	89.3 (62, 116.6)	N/A	89.9 (64.4, 115.3)	89.9 (64.4, 115.3)
n	20	47	14	33	48	0	81	81

Discussion: It can be concluded that time-to-first-shock in the assessed system is at least analogous to systems referenced in the literature for untrained users and comparable to minimally trained users. There was no significant difference in shock times between age groups. CPR training did not significantly impact time to first shock or time to place electrodes.

http://dx.doi.org/10.1016/j.jelectrocard.2013.05.029

Conventional ECG markers do not predict ventricular fibrillation during ST-elevation myocardial infarction

M.M. Demidova[a], J. Carlson[b], D. Erlinge[b], P.G. Platonov[b]
[a]*Federal Center of Heart, St. Petersburg, Russia and Lund University, Lund, Sweden*
[b]*Lund University, Lund, Sweden*

Introduction: Ventricular fibrillation (VF) is a common cause of early mortality in acute ST-elevation myocardial infarction (STEMI). However, its predictors remain largely unknown. Prolonged QTc time is an established risk factor for sudden death but its relation to VF in the settings of STEMI is poorly understood. Our aim was to analyse whether basic ECG characteristics, including QTc, before STEMI can predict VF before reperfusion in STEMI.

Methods: Consecutive STEMI patients admitted to a Swedish tertiary care hospital for primary PCI during a 12-month period were included (n = 627). Information about the presence of VF was obtained using the Register of Information and Knowledge about Swedish Heart Intensive Care Admissions (RIKS-HIA). Medical records were analysed for VF timing in relation to infarct-related artery opening. Regional ECG databases containing all 10-sec long snapshot ECGs taken in the hospital catchment area since 1988 were reviewed and the latest ECG registered before admission with STEMI was chosen. Only patients having a previous ECG available were included in the analysis. QTc was calculated using the Bazett formula.

Results: VF during early hours of STEMI before reperfusion (both at the prehospital stage and after admission to the hospital) occurred in 28 patients. In 18 of them, an ECG prior to STEMI was available (age 71 ± 11, 78% male). Of the remaining 599 patients, 458 had a previous ECG available and were used as a control group (age 69 ± 12, 66% male). Median time between a previous ECG and admission with STEMI was 20 (range 1–228) months. QTc interval was 416 ± 25 ms in the VF group compared to 424 ± 25 ms in the control group (OR = 0.99 95% CI 0.97–1.01 p = 0.24). Mean QRS duration was 95 ± 17 ms in both groups. The percentage of patients with QRS width more than 120 ms (due to LBBB, RBBB) did not differ between groups — 11% in VF group and 7.8% in the no VF group (OR = 1.46 95% CI 0.32–6.58 p = 0.63). Heart rate, P-wave duration and PR interval did not differ either.

Conclusion: VF occurring during the early hours of STEMI before reperfusion therapy is not associated with standard ECG markers on an ECG recorded prior to STEMI.

http://dx.doi.org/10.1016/j.jelectrocard.2013.05.030

ECG characteristics in dogs of hunting breeds (spaniels, terriers)

V.I. Maximov, V.D. Fomina
Moscow State Academy of Veterinary Medicine and Biotechnology

Introduction: The method of electrocardiography is becoming more important for the diagnosis of canine heart disease and assessment of the functional state of the dog body, especially in heart pathologies due to heavy physical loads, injuries, diseases of respiratory and excretory organs, past infectious diseases, etc. Depolarization and repolarization in different animal species and breeds have their own characteristics, which affect the parameters of electrocardiogram (ECG) intervals. That is why the study of the features of the ECG in health and disease of the heart in different species and breeds of animals is urgently needed and requires a detailed study. The purpose of this research is studying the ECG in dogs of hunting breeds (Spaniels, Terriers) in the trunk sagittal leads according to M.P. Roshchevsky and identifying the connection of the Q-T interval with heart rate.

Methods: The study was conducted with the help of a specialized biological system «CONAN» on 10 physiologically healthy dogs aged 5–6 years. In the electrocardiogram, we evaluated the source of the heart rate and regularity of its activation, the heart rate (HR) itself, analyzed the amplitude, shape of the peak and duration of ECG intervals and established a relationship of the Q-T interval with the HR.

Results: The studies on dogs showed that all the ECG elements are most clearly recorded in the 2nd and 3rd sagittal leads. The ECG analysis in these leads in dogs of studied breeds showed the features of activation in the sinus node, which is expressed by frequent arrhythmia. Ventricular depolarization in the 2nd lead appears as a complex QRs, and in the 3rd as qRS. The Q-T interval duration is independent of the HR and is 0.16 s.

Conclusion: The ECG in healthy dogs of hunting breeds (Spaniels, Terriers) is different from other breeds. The Q-T interval duration is independent of the HR and the most stable element of the ECG remaining unchanged in arrhythmia and tachycardia.

http://dx.doi.org/10.1016/j.jelectrocard.2013.05.031

Chronic myocardial infarction promotes atrial action potential alternans, afterdepolarisations and fibrillation

S. Kettlewell, F.L. Burton, G.L. Smith, A.J. Workman
University of Glasgow

Introduction: Atrial fibrillation (AF) is increased in patients with heart failure resulting from myocardial infarction (MI). We aimed to determine the effects of chronic ventricular MI in rabbits on the susceptibility to AF, and underlying atrial electrophysiological and intracellular Ca^{2+} (Ca^{2+}_i)-handling mechanisms.

Methods: Atrial electrograms, action potentials, ion currents or Ca^{2+}_i were measured in rabbit isolated perfused hearts or cardiomyocytes, using standard electrophysiological and optical techniques.

Results: In isolated hearts, under β-adrenergic-stimulation with isoproterenol (1 μM; ISO), 8 weeks MI decreased AF threshold, indicating increased AF-susceptibility. This was associated with increased atrial action potential duration (APD)-alternans at 90% repolarisation, by 147%, and no significant change in mean APD or global conduction velocity (n = 6–13 non-MI hearts, 5–12 MI). In atrial isolated myocytes, also under β-stimulation, L-type Ca^{2+} current (I_{CaL}) density and Ca^{2+}_i-transient amplitude were decreased by MI, by 35% and 41%, respectively, and the frequency of spontaneous depolarisations (SDs) was substantially increased. MI increased myocyte size and capacity, and markedly decreased transverse-tubule density. In non-MI hearts perfused with ISO, the I_{CaL}-blocker nifedipine, at a concentration (0.02 μM) causing an equivalent I_{CaL}-reduction (35%) to that from the MI, did not affect AF-susceptibility, and decreased APD.

Conclusion: Chronic MI in rabbits remodels atrial structure, electrophysiology and Ca^{2+}_i-handling. Increased susceptibility to AF by MI, under β-adrenergic-stimulation, may result from associated production of atrial APD-alternans and SDs, since steady-state APD and global conduction velocity were unchanged under these conditions, and may be unrelated to the associated reduction in whole-cell I_{CaL}.

http://dx.doi.org/10.1016/j.jelectrocard.2013.05.032

Does fragmented surface ECG predict appropriate ICD therapy in patients with Chagas cardiomyopathy (the FECHA study)?

D.D. Anselm[a], F. Femenía[b], J.C. Lopez-Diez[c], C. Muratore[d], M. Valentino[e], E. Retyk[f], N. Galizio[g], D. Di Toro[h], K. Alonso[i], W.M. Hopman[a], R. Miranda[j], A. Baranchuk[a]
[a]*Queen's University, Kingston General Hospital, Ontario, Canada*
[b]*Hospital Español de Mendoza, Argentina*
[c]*Hospital Militar, Buenos Aires, Argentina*
[d]*Hospital Fernández, Buenos Aires, Argentina*
[e]*Sanatorio Parque, Rosario, Santa Fe, Argentina*
[f]*Hospital Castex, Buenos Aires, Argentina*
[g]*Fundacion Favaloro, Buenos Aires, Argentina*
[h]*Hospital Argerich, Buenos Aires, Argentina*
[i]*Sanatorio Franchin, Buenos Aires, Argentina*
[j]*Universidad de la Frontera, Temuco, Chile*

Introduction: Main causes of death in chronic Chagas cardiomyopathy (CChC) are progressive congestive heart failure and sudden cardiac death. Implantable cardioverter defibrillators (ICD) have been proven to be an effective therapy to prevent sudden death in patients with CChC. Identification of predictors of sudden death, however, remains a challenge. In the Fragmented ECG in CHAgas cardiomyopathy (FECHA) study, our objective was to determine whether surface fragmented ECG (fQRS) helps identify patients with CChC and ICDs at higher risk of presenting appropriate ICD therapies.

Methods: This was a multicentre retrospective study. All patients with CChC and ICDs were analyzed. Clinical demographics, surface ECG and ICD therapies were collected.

Results: A total of 98 patients were analyzed. Other four cases were excluded due to pacing dependency. Mean age was 55.5 ± 10.4 years, male gender 65%, heart failure NYHA class I 47% and II 38%. Mean LVEF 39.6 ± 11.8%. The indication for ICD was secondary prevention in 70% of patients. fQRS was found in 56 patients (59.6%). Location of fragmentation was inferior (57.1%), lateral (35.7%) and anterior (44.6%). Rsr pattern was the more prevalent (57.1%). Predictors of appropriate therapy in the multivariate model were: increased age (p = 0.01), secondary prevention indication (p = 0.01), ventricular pacing >50% of the time (p = 0.004) and LVEF <30% (p = 0.01). The presence of fQRS did not identify patients at higher risk of presenting appropriate therapies delivered by the ICD (p = 0.87), regardless of QRS interval duration.

Conclusions: fQRS is highly prevalent among patients with CChC. It has been found to be a poor predictor of appropriate therapies delivered by the ICD in this population.

http://dx.doi.org/10.1016/j.jelectrocard.2013.05.033

ECG QT interval in mitral valve prolapse syndrome patients in Taiwan

C.H. Hsu[a], Y.C. Chen[a], L.W. Tsai[b], I.F. Yang[c], C.K. Tseng[d], T.F. Yang[a,b]
[a]*National Chiao Tung University*
[b]*Taipei Medical University and Hospital, Taipei, Taiwan*
[c]*Jen Chi General Hospital, Taipei, Taiwan*
[d]*China Medical University Hospital, Taichung, Taiwan*

Introduction: Until recently, there has been no study to assess the difference of QT interval between patients with mitral valve prolapse syndrome (MVPS) and normal Taiwanese. The QT interval is dependent on the heart rate (the faster the heart rate the shorter the QT interval) and corrected QT (QTc) can be easily calculated by computer-based ECG machines to improve the detection of ventricular arrhythmia(VA) and Sudden Cardiac Death (SCD). Different correction formulae such as Bazett, Fridericia, Framingham, Hodges etc have been adopted. MVPS has been reported to produce significantly more repolarization abnormalities and VA than normal. The aim of this study was to evaluate whether there was any differences in QT between MVPS and normal Taiwanese.

Methods: ECG data were recorded with a BURDICK Atria 6100® and analyzed in 581 normal subjects (239 males (26 ± 10 years) and 342 females (36 ± 14 years)) as well as in 86 echocardiographically documented MVP patients (8 males (33 ± 15 years) and 78 females (43 ± 14 years)) at a cardiology clinic. All the ECG signals were collected to a desktop PC for further SPSS-19 software statistical analysis. The two tail student-t test was adopted to differentiate the QT corrected formulae. $P < 0.05$ was regarded as statistically significant.

Results:

Table 1
QT and QTc (derived from 4 formulae) in normal subjects and patients with MVPS.

	Number	QTint (ms)	QTcBaz (ms)	QTcFri (ms)	QTcFra (ms)	QTcHod (ms)
Normal	581	392.23	424.06 ± 36.68	412.92 ± 42.25	364.32 ± 53.13	378.10 ± 43.12
MVPS	86	402.60	433.96 ± 25.16	423.03 ± 37.62	375.68 ± 47.23	388.65 ± 35.18
P		<0.01	<0.01	<0.01	<0.05	<0.05

Conclusions:
1. There is no significant difference in QTc between MVPS and normal in women.
2. In men, there was a significant difference in QTc Bazett and Fridericia.
3. There are not enough males with MVPS in this study, which might introduce some bias.

http://dx.doi.org/10.1016/j.jelectrocard.2013.05.034

Gender differences of heart rate variability between symptomatic mitral valve prolapse syndrome and normal Taiwanese

Y.C. Chen[a], C.H. Hsu[a], L.W. Tsai[b], I.F. Yang[c], C.K. Tseng[d], T.F. Yang[a,b]
[a]*National Chiao Tung University, Hsin Chu, Taiwan*
[b]*Taipei Medical University and Hospital, Taipei, Taiwan*
[c]*Jen Chi General Hospital, Taipei, Taiwan*
[d]*China Medical University Hospital, Taichung, Taiwan*

Introduction: Short term heart rate variability (HRV) can provide non-invasive information on the autonomic nervous system (ANS), including its vagal and sympathetic components, which has a strong association with the pathogenesis of ventricular arrhythmias and sudden cardiac death (SCD) in the general population. Short term HRV is claimed to be similar to 24 hour HRV in men and can provide predictive information similar in strength to an entire 24 hour record. Mitral Valve Prolapse Syndrome (MVPS) was reported to be associated with significant ANS dysfunction in Caucasians. Gender variation of HRV was also previously reported. The aim of this study was to evaluate the effect of gender on HRV parameters in Taiwanese symptomatic MVPS patients.

Methods: A total of 118 MVP patients (7 males and 111 females) who had been echocardiographically documented at a cardiology clinic and 148 healthy university students (54 males and 94 females) were recruited for the study. A local HRV system with modified lead II ECG was used. HRV was performed during the daytime to avoid diurnal effects. The subjects were asked to rest at least 5 minutes before recording HRV with lying, sitting and standing posture. The paired Student t test was used to characterize changes in HRV variables between MVPS patients and the normal control group. All HRV variables were expressed as mean ± SD. All statistical analyses were performed using Microsoft Excel 2007. A P value <0.05 was determined as statistically significant.

Results: For MVPS, no difference was found in time domain measures between male and female except in the lying position. For the normals, all frequency domain parameters were statistically significantly different between male and female, except total power.

Conclusion:
1. Gender specific HRV diagnostic MVPS criteria should be established in Taiwanese.
2. One limitation of the study is the relatively small number of males with MVPS.

http://dx.doi.org/10.1016/j.jelectrocard.2013.05.035

Electrocardiographic and echocardiographic correlations in patients with pulmonary arterial hypertension

E. Blinova, T. Sakhnova, M. Saidova, A. Loskutova, Z. Dadacheva, O. Archipova, T. Martynyuk, I. Chazova
Cardiology Research Complex

Objective: To study the interrelations of electrocardiographic (ECG) and echocardiographic parameters in patients with pulmonary arterial hypertension (PAH).

Methods: We examined 30 PAH patients (4 males and 26 females; age (mean ± SE) 38.0 ± 2.0 years). Systolic pulmonary artery pressure (SPAP), right ventricular (RV) dimensions, systolic and diastolic function were assessed using comprehensive echocardiographic examination, including Tissue Doppler Imaging and two-dimensional Speckle Tracking. ECG parameters under investigation were: QRS and T axes, frontal plane QRS-T angle (QRS-Tf), QRS duration (QRSd), R and S wave amplitudes in leads V1 and V5.

Results: QRS-Tf, QRSd and RV1 correlated positively with RV anterior-posterior, basal and middle dimensions ($r = 0.6$; $p < 0.01$ for QRSd; r from 0.4 to 0.7; $p < 0.05$ for QRS-Tf; r from 0.4 to 0.5; $p < 0.05$ for RV1). QRS-Tf and RV1 correlated with RV anterior wall thickness ($r = 0.5$; $p < 0.05$) and SPAP ($r = 0.6$; $p < 0.01$). QRS-Tf and QRSd correlated negatively with parameters of RV systolic function: RV fractional area change (FAC), TAPSE, RV and interventricular septum systolic velocities (r from −0.4 to −0.7; $p < 0.05$). QRS-Tf and QRSd correlated positively with parameters of RV diastolic function: RV and interventricular septum diastolic velocities (r from 0.4 to 0.6; $p < 0.05$). QRS-Tf and QRSd correlated positively with RV longitudinal strain ($r = 0.5$; $p < 0.05$).

Conclusion: In patients with PAH, ECG parameters QRS-Tf and QRSd correlate with RV dimensions and parameters of RV systolic and diastolic function.

http://dx.doi.org/10.1016/j.jelectrocard.2013.05.036

Decartographic detection of presence and severity of right ventricular overload in patients with pulmonary hypertension

T. Sakhnova[a], E. Blinova[a], V. Trunov[b], E. Aidu[b], E. Yurasova[a], M. Saidova[a], T. Martynyuk[a], I. Chazova[a]
[a]*Cardiology Research Complex*
[b]*Institute for Information Transmission Problems RAS*

Introduction: The aim of this study was to examine the value of decartographic parameters of repolarization for the assessment of right

ventricular overload severity in patients with pulmonary arterial hypertension (PAH).
Methods: We examined 120 PAH patients (23% males; age (mean ± SE) 39.5 ± 1.2 years). 120 healthy subjects (32% males; age 33.6 ± 0.9 years) comprised the control group. Systolic pulmonary artery pressure (SPAP) was calculated using Doppler echocardiography. Moderate PAH was defined as SPAP between 30–50 mm Hg; severe PAH as SPAP >50 mm Hg. Digital orthogonal electrocardiograms were recorded. We studied the magnitude G (in ms) and spatial components Gx, Gy, Gz of the "recovery acceleration" vector (directed to the left, inferior, and anterior).
Results: In 30 patients with moderate PAH G, Gx and Gz were lower as compared with the normal group, and G, Gx and Gy were greater as compared with 90 patients with severe PAH. When used for discriminating between the moderate PAH and the normal group, Gz had an area under the ROC curve of 0.83, SE 0.05. The threshold Gz <10 ms provided 77% sensitivity and 83% specificity. For discriminating moderate and severe PAH, Gy had an area under the ROC curve of 0.87, SE 0.04. The threshold Gy <25 ms provided 82% sensitivity and 90% specificity. Gx and Gy had moderate correlation with SPAP ($r = -0.5$; $p < 0.01$).
Conclusion: The use of decartographic parameters of repolarization may be helpful not only for detection of right ventricular overload in patients with PAH, but also for the assessment of its severity.

http://dx.doi.org/10.1016/j.jelectrocard.2013.05.037

Heart rate variability as predictor of atrial fibrillation in middle-aged population

J.S. Perkiömäki[a,b], O. Ukkola[b,c], A. Kiviniemi[d], M. Tulppo[d], A. Ylitalo[e], Y.A. Kesäniemi[b,c], H.V. Huikuri[a,b]
[a]*Division of Cardiology, University of Oulu, Oulu, Finland*
[b]*University Central Hospital of Oulu, Finland*
[c]*Dept. of Internal Medicine, University of Oulu, Finland*
[d]*Department of Exercise and Medical Physiology, Verve Research, Oulu, Finland*
[e]*Heart Center, Satakunta Central Hospital, Pori, Finland*

Introduction: Elevated resting heart rate (HR) has been suggested to predict the occurrence of atrial fibrillation (AF) in patients with hypertension, but there is less information about the HR variability as a predictor of new-onset AF. We studied the prognostic value of HR and HR variability measured from a 45-minute standardized ECG recording in a middle-aged population.
Methods: The study population consisted of 600 hypertensive and 600 age and sex matched control subjects at the time of recruitment in 1990 (Opera study). HR and HR variability was measured in 789 subjects (mean age 50 ± 6 years, 54% males) from a standardized 45-minute period, including 15 minutes at supine position, 15 minutes sitting, and 15 minutes during slow walking.
Results: During a mean follow-up of 17 ± 4 years, 76 subjects (9.6%) had developed symptomatic AF needing hospitalization. HR during the 45-minute period, or at any 15-minute period, did not predict the occurrence of AF. Among the various spectral and time-domain HR variability indexes, only the low-frequency (LF) spectral component predicted AF ($p < 0.001$). In the Cox regression analysis, the hazard ratio of reduced HR corrected LF (LFCCV <2.56%, optimal cutoff from the ROC curve) in predicting the AF was 3.2 (95% CI: 1.8–5.7, $p < 0.001$). In the multiple Cox regression model, including LFCCV and other predictors of AF, such as age, gender, body mass index, history of coronary artery disease, hypertension, or diabetes, systolic blood pressure, fasting glucose, gamma-GT, beta-blocking medication, left atrial size and left ventricular mass index obtained by echocardiography, only LFCCV (hazard ratio 2.6, 95% CI: 1.2–5.8, $p = 0.018$) and age ($p = 0.020$) remained as significant predictors of AF.
Conclusion: Impaired LF oscillation of HR predicts new-onset AF in a middle-aged population. The present data suggest that the independent prognostic power of altered autonomic regulation of HR is as strong as age in predicting the AF.

http://dx.doi.org/10.1016/j.jelectrocard.2013.05.038

Differences in drug-induced QT prolongation in men and women when QT interval is measured in each of the 12 leads of the ECG in a thorough QT study

G.K. Panicker, V.S. Salvi, D.R. Karnad, S.S. Chakraborty, D. Manohar, Y.Y. Lokhandwala, S.N. Kothari
Quintiles Cardiac Safety Services, Mumbai

Introduction: When evaluating new drugs for QT prolongation, precise QT interval measurements are done in a pre-specified single lead in a core laboratory; lead II is commonly used. Whether other ECG leads also show comparable QT prolongation is not known.
Methods: We studied moxifloxacin-induced QT prolongation in a crossover thorough QT study with 97 healthy subjects (54 males, 43 females). Placebo-subtracted 'change from baseline' in QTc corrected by Fridericia's method ($\Delta\Delta$QTcF) 1, 1.5, 2 and 4 hours after moxifloxacin was calculated from the QT measurements in each of the 12 leads. A linear mixed effects model was used to assess differences in $\Delta\Delta$QTcF in males and females.
Results: Unacceptably wide 90% CI for $\Delta\Delta$QTcF was seen in some leads; these leads also had high proportions of ECGs with flat T waves (60% in aVL, 45% in Lead III and 42% in V1). The presence of flat T waves increases variability in QT measurement; therefore ECGs with T amplitude <0.1 mV were excluded. After excluding ECGs with flat T waves, assay sensitivity (90% lower CI of $\Delta\Delta$QTcF ≥ 5 ms) was demonstrated by all the leads, except Leads III, aVL and V1 in men. These leads did not demonstrate assay sensitivity, even after excluding ECGs with flat T waves, as the confidence intervals for $\Delta\Delta$QTcF were widest in these leads. The 90% LCL exceeded 5 ms in these 3 leads in women despite wide 90% CIs because of greater drug-induced QTcF prolongation in women. Leads III (axis +120°) and aVL (axis −30°) had their axes almost perpendicular to the mean frontal T wave axis (43° in males and 46° in females), which explains many of our observations.
Conclusion: Moxifloxacin-induced QT prolongation is not satisfactorily demonstrated when QT intervals are measured in Leads III, aVL and V1. These leads should be avoided when measuring QT interval in thorough QT studies.

http://dx.doi.org/10.1016/j.jelectrocard.2013.05.039

Realistic heterogeneous and anisotropic canine atrial model for the study of atrial arrhythmias

M. Varela[a], M.A. Colman[b], H. Zhang[b], O.V. Aslanidi[a]
[a]*Biomedical Engineering, Division of Imaging Sciences, King's College London, London, UK*
[b]*Biological Physics Group, School of Physics and Astronomy, University of Manchester, Manchester, UK*

Introduction: Myocardial fibre orientation and heterogeneity of action potential (AP) characteristics across different atrial tissues can play an important role in the mechanisms of atrial fibrillation. However, few computational studies of the entire atria have accounted for these in detail.
Methods: A 3D canine atrial geometry was generated using contrast-enhanced 36-μm resolution microCT images, from which fibre orientation was also estimated using structure tensor analysis. The atria were segmented into the left atrium (LA), right atrium (RA), pulmonary vein (PV) sleeves and Bachmann's bundle (BB). Specific canine cell models based on recently published experimental data were created and assigned to each tissue. The monodomain equation was solved using a finite differences method in a Cartesian grid. Simulations in physiological conditions were performed by stimulating the sino-atrial node region at a cycle length (CL) of 1 s. To study arrhythmia initiation, the PV region was stimulated at 192 ms.
Results: The AP duration (APD_{90}) of the developed cell models agreed well with published experimental data in the dog (RA: 184, LA: 170, BB: 235, PV: 135 ms, CL = 1 s). Tissue activation sequence and timings in physiological conditions also showed good agreement with experimental data with a total activation time of 76 ms and a mean conduction velocity of 96 cm/s. Fast pacing near the PVs gave rise to rapid re-entrant activity, due to the high local fibre anisotropy and the APD gradient between the PV sleeves and the surrounding LA tissue.

Conclusion: We developed a detailed 3D model of the canine atria with realistic anatomical and electrophysiological properties. This model can be used to further investigate the mechanisms underlying atrial arrhythmias, namely the characteristics of the rapid activation sources observed clinically near the PV sleeves during atrial fibrillation.

http://dx.doi.org/10.1016/j.jelectrocard.2013.05.040

Effect of pacing rate on cardiac output and pulse wave velocity at rest

L. Soukup[a], V. Vondra[b], I. Viscor[b], P. Jurak[b], J. Halamek[b]
[a]*FNUSA-ICRC Brno*
[b]*Institute of Scientific Instruments AS CR*

Introduction: Cardiac output (CO) and pulse wave velocity (PWV) are recognised markers for classification of the cardiovascular system. Several studies proved the dependence of PWV and CO on heart rate (HR). However, this dependence is poorly described in patients with an implanted pacemaker. The aim of this study was to extend knowledge about the effect of pacing rate on the cardiovascular system. At the same time, we wished to test using of the bioimpedance method for PWV measurement by the device designed in the ISI Brno in clinical research.

Methods: Biological signals were measured continuously in 24 volunteers with implanted pacemakers. Blood pressure (by Finapres-2300), phonocardiogram, ECG (12 leads), as well as bioimpedance of thorax and calf, were recorded. During the experiment, patients were in the supine position and pacing rate was changed between 80, 100 and 120 bpm repetitively. Pulse wave velocity and cardiac output (or stroke volume) were determined by the bioimpedance method.

Results: Only those intervals where all signals did not have errors or artefacts (signal interruption or corruption, extrasystoles, etc.) were chosen, in order to obtain maximally valid results. All parameters at each heart rate (80, 100 and 120) were necessary for evaluation. The study group consisted of 20 men and 4 women, average age 74.6 ± 9.4 years. Systolic pressure, diastolic pressure, mean arterial pressure and pulse pressure were also computed. All parameters were normalized for comparison of trends. After normalization, it was ascertained that the CO (2.9% decrease) and PWV (1.2% decrease) do not significantly depend on pacing rate at rest. On the other hand, pulse pressure decreased about 13% with pacing rate.

Conclusion: Dependence of CO and PWV on pacing rate was investigated in this study. The bioimpedance method used for evaluation of CO and PWV was non invasive and easily tolerated by patients.

http://dx.doi.org/10.1016/j.jelectrocard.2013.05.041

Changes of electrocardiogram in low-renin hypertension

E. Blinova[a], T. Sakhnova[a], N. Chikhladze[a], V. Trunov[b], E. Aidu[b], Z. Valieva[a], M. Saidova[a], A. Rogoza[a], I. Chazova[a]
[a]*Cardiology Research Complex*
[b]*Institute for Information Transmission Problems RAS*

Objective: To study the changes of ECG in hypertensive patients in comparison with the plasma renin activity (PRA), echocardiographic data and ambulatory blood pressure monitoring (ABPM).

Methods: Parameters of 12 lead and orthogonal ECG, echocardiography and ABPM were evaluated in 40 patients with arterial hypertension (57% male), 30 patients with PRA less than 1 ng/ml/h in the supine position (group 1) and 10 with PRA more than 1 ng/ml/h (group 2).

Results: Characteristics of the groups are shown in Table 1.

Patients with low PRA were characterized by significantly greater values of spatial QRS-T angle and significantly lower magnitude (G) and components X, Y, Z (Gx, Gy, Gz) of the "recovery acceleration" vector. There were no statistically significant differences in Cornell product, Sokolow-Lyon voltage, QRS duration and QRS maximal vector amplitude between the groups. We revealed statistically significant correlations between PRA and spatial QRS-T angle ($r = -0.5$; $p < 0.01$); G, Gx and Gy ($r = 0.5$; $p < 0.01$); Gz ($r = 0.4$; $p < 0.02$). Gx correlated with WT and RWT ($r = -0.5$; $p < 0.01$); LVMM and indexed LVMM ($r = -0.4$; $p < 0.02$). Gy correlated with diastolic BP at ABPM ($r = -0.4$; $p < 0.02$).

Table 1
Characteristics of the groups.

	Group 1	Group 2	p
Age, years	47 ± 3	35 ± 4	0.02
AH duration, years	14 ± 2	9 ± 3	>0.1
SBP, mm Hg	153 ± 5	140 ± 4	>0.1
DBP, mm Hg	91 ± 3	86 ± 4	>0.1
K+, mmol/l	4.5 ± 0.1	4.8 ± 0.2	>0.1
PRA, ng/ml/h	0.34 ± 0.05	1.78 ± 0.29	<0.01
PAC, pg/ml	219 ± 76	148 ± 43	>0.1
SBP24hr, mm Hg	141 ± 3	141 ± 3	>0.1
DBP24hr, mmHg	88 ± 2	83 ± 4	>0.1
EDV, mm	5.1 ± 0.1	5.2 ± 0.1	>0.1
WT, mm	1.07 ± 0.04	0.93 ± 0.03	0.09
RWT	0.42 ± 0.01	0.36 ± 0.02	0.03
LVMM, g	214 ± 17	178 ± 11	>0.1
ILVMM, g/m^2	109 ± 7	92 ± 6	>0.1
HR, bpm	66 ± 2	65 ± 4	>0.1

Conclusion: Hypertensive patients with low PRA in comparison with medium PRA were characterized by more pronounced changes in ECG parameters which describe cardiac repolarization in its relation to the preceding depolarization.

http://dx.doi.org/10.1016/j.jelectrocard.2013.05.042

Automatic detection of end QRS notching or slurring

E.N. Clark, P.W. Macfarlane
University of Glasgow

Introduction: There has recently been a resurgence of interest in the significance of end QRS notching or slurring. However, there is no agreed definition of this morphology and so there is variation in reporting this feature visually. The purpose of the present study is to evaluate the accuracy of automated detection of notching and slurring.

Method: 100 resting 12 lead ECGs from young adult men (mean age 24.8 ± 3.2 years) were split randomly into equal training and test sets. To establish a gold standard, the waveforms for the training set were examined independently by two reviewers for the presence of end QRS notches and slurs using the following definitions. A notch was defined as a low amplitude short duration reversal of QRS slope distinguishable to the eye, and a slur as a change of QRS slope, each on the terminal component of an R wave in leads II, III, aVF, V4–V6. To qualify, the amplitude at the apex of the notch or at the inflection point of the slur had to be less than 0.5 mV with respect to QRS onset. Where reviewers differed initially, consensus was reached by re-examination. Logic was added to the Glasgow ECG analysis program to automate the detection of notching and slurring. The automated output for the training set was compared with the manual results on a lead by lead basis and sensitivities and specificities calculated. Discrepancies were reviewed and improvements made to the automated process. The test set was then analysed.

Results: Reviewers initially disagreed in 5% of cases. After revision, the training set exhibited a notch or slur in 63/300 leads (21%). After training, the automated detection had a sensitivity (SE) of 92.1% and a specificity (SP) of 96.6% with respect to the gold standard. For the test set, SE was 90.7% and SP was 94.9%.

Conclusion: The detection of end QRS notching or slurring can be automated with a high degree of accuracy. This approach could be used to improve the automated diagnosis of "early repolarisation".

http://dx.doi.org/10.1016/j.jelectrocard.2013.05.043

Comparison of the spatial QRS-T angle derived from the conventional 12-lead ECG using standard electrode positions with that derived from the Holter ECG using Mason Likar electrode positions

V. Salvi[a], E. Clark[b], D.R. Karnad[a], P. Macfarlane[b], G.K. Panicker[a], P. Hingorani[a], S. Kothari[a], Y.Y. Lokhandwala[a]
[a]*Quintiles Cardiac Safety Services, Mumbai, India*
[b]*University of Glasgow, Glasgow, UK*

Introduction: The spatial QRS-T angle derived from orthogonal leads is a marker for cardiac mortality. Data from 12-lead ECGs are often used to reconstruct orthogonal leads and derive the spatial QRS-T angle. The effect on the spatial QRS-T angle of using Mason Likar (M-L) electrode positions as used in Holter ECGs was studied.

Methods: 12-lead ECGs were recorded simultaneously with standard limb lead positions using an ECG device and M-L lead positions using a 12-lead Holter recorder in 100 volunteers. Spatial QRS-T angles were calculated by 2 methods — a vector method within the Glasgow algorithm and a net amplitude method where net QRS [R amplitude minus Q or S amplitude (whichever is greater)] and T wave amplitudes were manually measured in derived orthogonal leads.

Results: There was a small, statistically significant difference in spatial QRS-T angles from standard and M-L ECGs (57º ± 18º vs. 48º ± 20º respectively using the net amplitude method and 53º ± 28º vs. 48º ± 23º respectively by the vector method). This was due to differences in QRS and T amplitudes in derived leads Y and Z probably resulting from differences in leads I and II (Table 1). Although dual snap electrodes were used, QRS and T amplitudes in leads V4–V6 also differed between the two lead systems probably due to a difference in potential at the central terminal.

Table 1
QRS and T wave amplitudes in standard and M-L ECGs by net amplitude method.

Parameter	QRS amplitude (μV)		T amplitude (μV)	
	Standard leads	M-L Leads	Standard leads	M-L leads
Lead X	1209 ± 362	1218 ± 376	388 ± 122*	413 ± 134
Lead Y	672 ± 266*	1059 ± 365	200 ± 86*	318 ± 118
Lead Z	400 ± 380*	451 ± 395	330 ± 184*	344 ± 179
Lead I	567 ± 324*	253 ± 237	287 ± 95*	208 ± 82
Lead II	915 ± 297*	1248 ± 414	357 ± 109*	471 ± 148

* $p < 0.001$ vs. M-L leads by paired t-test.

Conclusion: There is a small, statistically significant difference in spatial QRS-T angles derived from 12-lead ECGs using standard and M-L lead systems. However, this difference may not be clinically significant.

http://dx.doi.org/10.1016/j.jelectrocard.2013.05.044

Cardiac arrhythmia induced by hypothermia in a cardiac model in vitro

B. Xu[a], S. Jacquir[b], O. Pont[a], H. Yahia[a]
[a]*Team GeoStat - INRIA Bordeaux Sud-Ouest*
[b]*CNRS UMR 5158 Dijon France, LE2I Université de Bourgogne*

Introduction: The neurological damage after cardiac arrest (CA) has presented a big challenge to hospital discharge for many years. The therapeutic hypothermia therapy (34 °C–32 °C) has shown its benefit to reduce cerebral oxygen demand and improve neurological outcomes after cardiac arrest. Despite the fact that induced hypothermia after CA has been shown to increase the hospital survival rate, it can have many adverse effects, among which the generation of cardiac arrhythmias represents an important part (up to 34%, according to different clinical studies). Compared to studies in vivo, cardiac culture in vitro provides a better spatial resolution at cellular level, which could bring some insights into the mechanism of post–hypothermia arrhythmia (PHA) generation.

Method: Monolayer cardiac culture is prepared with cardiomyocytes from the new-born rat (1–4 days) directly on the MEA at 37 °C. The experiments consist of culture cooling (37 °C–30 °C) and re-warming (30 °C–37 °C). The acquired signals are then analyzed with detrended fluctuation analysis (DFA) and phase space reconstruction (PSR).

Results: Both experiments showed that period-doubling phenomena are present at 35 °C, which can be translated as a transit point from the normal state to the chaos state, from the point view of nonlinear dynamics. Spiral waves are observed in the reconstructed activation map which is commonly considered as a sign of cardiac arrhythmia. Below 35 °C, the signals became regular. However, another transit point is found between 30 °C–33 °C, which agreed with other studies that hypothermia below 32 °C could induce arrhythmia. These results are confirmed by DFA and PSR methods.

Conclusion: The general hypothermia therapy uses constant cooling or re-warming. Results in this study showed that a variable speed, especially fast passing 35 °C, would help to reduce the rate of post-hypothermia arrhythmia.

http://dx.doi.org/10.1016/j.jelectrocard.2013.05.045

Electrocardiography of Takotsubo syndrome

J.E.M. Madias
Mount Sinai School of Medicine of the New York University/Cardiology Division, Elmhurst Hospital Center

Introduction: The electrocardiogram (ECG) in patients presenting with the Takotsubo syndrome (TTS) does not show specific features for this disorder which are adequate to differentiate it from those encountered in acute coronary syndromes (ACS) or acute pericarditis (AP). The literature emphasizes the transient ST-segment elevation, followed by T-wave inversion and QTc interval prolongation, all of which may even be absent early in the clinical course of patients with TTS. Some recent insight associates myocardial edema, as detected by cardiac magnetic resonance imaging in patients with TTS, with attenuation (ATT) in the ECG voltage (J Electrocariol. 2012;45:795–6).

Methods: The entire literature of 614 published papers, searched for in PubMed, via the MeSH term "electrocardiogram in takotsubo syndrome", was reviewed and analyzed for the presence of low voltage ECG (LVECG) based on 1 ECG, or ATT based on ≥2 ECGs, in 368 patients who presented to the hospital with documented TTS.

Results: LVECG was seen in 91.5% of 200 patients with TTS and 1 ECG, and ATT was seen in 93.5% of 168 patients with TTS and ≥2 ECGs.

Conclusion: LVECG and ATT are very sensitive and specific ECG signs for TTS, and may be employed to differentiate TTS from ACS and AP.

http://dx.doi.org/10.1016/j.jelectrocard.2013.05.046

Signal averaged electrocardiography in elderly hypertensive patients

I. Mozos, M. Hancu, L. Susan
"Victor Babes" University of Medicine and Pharmacy, Timisoara, Romania

Introduction: Signal averaged electrocardiography detects late ventricular potentials, as markers of sudden cardiac death risk. The present study hypothesized that aging increases the prevalence of late ventricular potentials.

Methods: A total of 40 hypertensive patients, 73% males, underwent signal averaged electrocardiography. The ages of the participants were 61 ± 12 years, 43% of them being elderly (≥65 years). The positive criteria for late ventricular potentials were: QRS duration (SA-QRS) >120 ms, LAS40 (the duration of the signal at the end of the QRS complex with an amplitude below 40 μV – "Low Amplitude Signal") >38 ms and RMS40 ("Root Mean Square" – the square root of the last 40 ms of the signal) <20 μV.

Results: SA-QRS was longer than 120 ms, LAS40 longer than 38 ms, and RMS40 up to 20 μV, in 25%, 38% and 60% of the patients, respectively. One and two positive criteria were detected in 60% and 40% of the patients, respectively (LVP1 and LVP2). Elderly patients were more likely to have longer SA-QRS (OR = 2.591, 95% CI: 0.598–11.234) and LAS40 (OR =

3.2, 95% CI: 0.81–12.647), and late ventricular potentials (OR = 1.667, 95% CI = 0.463–6.06).
Conclusion: Aging increases the prevalence of abnormal signal averaged electrocardiograms and late ventricular potentials in hypertensive patients.

http://dx.doi.org/10.1016/j.jelectrocard.2013.05.047

An individualised torso model further improves the accuracy of epicardial potentials derived from the body surface potential map using inverse electrocardiography in the diagnosis of acute myocardial infarction: a prospective study

M.J. Daly[a], D.D. Finlay[b], D. Guldenring[b], P.J. Scott[a], A.A.J. Adgey[a], M.T. Harbinson[c]
[a]The Heart Centre, Royal Victoria Hospital, Grosvenor Road, Belfast, Northern Ireland UK
[b]School of Computing and Mathematics and Computer Science Research Institute, University of Ulster, Northern Ireland, UK
[c]Centre for Vision and Vascular Sciences, Queen's University, Whitla Medical Building, Lisburn Road, Belfast, Northern Ireland, UK

Introduction: Epicardial potentials (EP) derived from body surface potentials using a standard thoracic volume conductor model (TVCM) improve acute myocardial infarction (AMI) diagnosis. In this study, we compared EP derived from the 80-lead body surface potential map (BSPM) using a standard TVCM developed from CT imaging with those derived using a patient-specific torso model (PSTM).
Methods: In this prospective study, consecutive patients presenting to both the ED and pre-hospital coronary care unit between August 2009 and August 2011 with acute ischaemic-type chest pain at rest were enrolled. At first medical contact, a 12-lead electrocardiogram (ECG) and BSPM were recorded. Patient height (m) and weight (kg) were recorded, and body mass index (BMI) calculated (kg m^{-2}). Cardiac troponin-T (cTnT) was sampled 12 h after symptom onset. AMI was diagnosed when cTnT $\geq$0.1 μg/L. Patients were excluded from analysis if they had bundle branch block, permanent pacemaker, left ventricular hypertrophy by voltage criteria or concomitant digitalis therapy. A cardiologist assessed the 12-lead ECG for STEMI by Minnesota criteria and the BSPM. BSPM ST-elevation (STE) was $\geq$0.2 mV in anterior, $\geq$0.1 mV in lateral, inferior, right ventricular (RV) or high right anterior and $\geq$0.05 mV in posterior territories indicating AMI. To derive EP, the 80-lead BSPM data were interpolated (Laplacian method) to yield values at 352-nodes of a Dalhouse torso. Using an inverse solution based on the boundary element method employing Tikhonov regularization, EP at 98 cardiac nodes positioned within a standard TVCM were estimated. The standard TVCM was scaled to produce a PSTM using a mathematical model developed from thoracic CT scans in 50 patients of varying BMIs. EP $\geq$0.4 mV defined STE. A cardiologist blinded to both the 12-lead ECG and BSPM interpreted the EP map.
Results: Enrolled were 400 patients (age 62 ± 13 y; 57% male): 80 patients had exclusion criteria. Of the remaining 320 patients, BMI was 27.8 ± 5.6 kg m^{-2}. Of these, 180 (56%) had AMI. Overall, 160 had BSPM STE (sensitivity 81%, specificity 90%). TVCM EP STE occurred in 165 patients (sensitivity 88%, specificity 95%, $p < 0.001$). PSTM EP STE occurred in 206 patients (sensitivity 98%, specificity 79%, $p < 0.001$). Of those with AMI and TVCM EP <0.4MV ($n = 22$), all patients had EP $\geq$0.4 mV when an individualised PSTM was used.
Conclusion: Among patients presenting with ischaemic-type chest pain at rest, EP derived from BSPM using inverse electrocardiography and a novel PSTM significantly improves sensitivity for AMI diagnosis.

http://dx.doi.org/10.1016/j.jelectrocard.2013.05.048

Visually estimating the spatial QRS-T angle from the conventional 12-lead ECG

D.L.C. Cortez[a], N. Sharma[b], C.D. Devers[c], E.D. Devers[c], T.S. Schlegel[d]
[a]CHOC Children's/Children's Hospital of Colorado
[b]Cleveland Clinic Foundation
[c]Indiana Wesleyan University
[d]NASA Johnson Space Center

Introduction: The 12-lead ECG-derived spatial QRS-T angle has notable prognostic and diagnostic utility, but most ECG machines currently fail to report it. The primary goal of this study was to determine if a reasonably accurate method exists for rapid *visual* estimations of the spatial peaks QRS-T angle from conventional 12-lead ECG tracings.
Methods: Simultaneous 12-lead and Frank XYZ-lead recordings were obtained from a publicly available database for 100 post-myocardial infarction patients and 50 controls. ANOVA, Pearson's correlation coefficients and concordance plots were used to evaluate relative agreement for spatial peaks QRS-T angle results from the true Frank leads versus from several *visually-applied* 12-to-Frank XYZ-lead transforms. The latter included Kors et al's regression and quasi-orthogonal, Bjerle and Arvedson's quasi-orthogonal, Dower's inverse, and Hyttinen et al's, Dawson et al's and Guillem et al's transforms.
Results: Spatial peaks QRS-T angles derived from the true Frank leads were not statistically significantly different than those derived from any visually-applied transform. Of the visually applied transforms, the Kors' regression and Kors' quasi-orthogonal yielded the highest Pearson correlation coefficients against the gold-standard results from the true Frank leads [0.88 and 0.81, respectively, when individuals with bundle branch blocks were excluded (N = 137), and 0.83 and 0.78, respectively, when individuals with bundle branch blocks were included (N = 150)].
Discussion: Even when strictly visually applied, the Kors' regression-related and quasi-orthogonal transforms can allow for reasonably precise estimates of the spatial peaks QRS-T angle. Such visual estimates may serve as a practical way for busy clinicians to quickly visually estimate the spatial peaks QRS-T angle from conventional 12-lead ECG tracings and printouts.

http://dx.doi.org/10.1016/j.jelectrocard.2013.05.049

Relation of preoperative heart rate turbulence parameters with ventricular arrhythmias after coronary artery bypass grafting

E.N. Dyuzheva, A.V. Sobolev, A.E. Vlasova, G.V. Ryabykina
Russian Cardiology Research and Production Complex

Introduction: The aim of this study was to determine the relationship of preoperative heart rate turbulence (HRT) parameters with ventricular arrhythmias (VA) after coronary artery bypass grafting (CABG).
Methods: We studied 58 patients with multiple coronary vessel disease: 16 with depressed LVEF = 32 ± 6% and 42 with preserved LVEF = 56 ± 7%. 44 (76%) had a history of myocardial infarction while 14 (24%) had diabetes mellitus. The control group consisted of 17 patients without coronary artery disease (CAD) with normal LVEF. All participants underwent Holter monitoring (HM). We determined turbulence onset (TO), turbulence slope (TS) (mean, maximum, minimum) before CABG. HM was repeated 7–14 days after CABG.
Results: There were significant differences in TOmean and TSmean between CAD and control groups: −1.1 vs −3.1, $p < 0.01$ (TO); 4.7 vs 12, $p < 0.01$ (TS). TOmax was significantly higher in depressed LVEF subgroup (LVEFs) compared with preserved LVEFs: 11.9 vs 7.2, $p < 0.05$. Preoperative TOmax moderately correlated with postoperative ventricular premature complexes (VPCs) ($r = -0.5$, $p < 0,05$). Patients with postoperative non-sustained ventricular tachycardia (VT) had significantly higher preoperative TOmax than those without; 11 vs 5.9, $p < 0.05$. Preoperative TSmin moderately correlated with postoperative ventricular premature complexes (VPCs) and ventricular pairs (VP) ($r = -0.6$, $p < 0.05$). If preoperative TSmin < −2, then there were significantly more postoperative VPCs: 1707 vs 99, $p < 0.01$; and VP: 35 vs 0.6, $p < 0.05$.
Conclusion: Interdependencies between preoperative TSmin, TOmax and postoperative VA were identified. These preoperative HRT parameters can be prognostic factors of early postoperative VA.

http://dx.doi.org/10.1016/j.jelectrocard.2013.05.050

Biophysical modeling of ST-T alterations under myocardial ischemia

O.V. Baum[a], V.I. Voloshin[a], L.A. Popov[a], G.A. Muromtseva[b]

[a]Institute of Theoretical and Experimental Biophysics, Russian Academy of Sciences, Pushchino
[b]National Research Centre for Preventive Medicine, Ministry of Health, Moscow, Russia

Introduction: A long-term priority of contemporary biomedicine is the problem of ischemic heart disease. The aim of our investigation was to study, with the use of mathematical and computer models, the tendencies of variation of the morphological characteristics of the T wave of the ECG following a change of parameters of the transmembrane action potential in an "ischemic" zone with evaluation of the possible use of the results in computer based diagnostic algorithms.

Methods: Computer experiments were executed on a system for 3D-modeling of the cardiac electrical activity with the aid of our earlier developed model of ECG genesis (cellular automaton of about a million elements of the Myocardium-His-Purkinje type), the parameters of which are electrophysiological, anatomical, and biophysical characteristics of heart muscle. Processing of the model ECG was carried out with our special program.

Results: Methods of segmentation of the model hearts on separate compartments (segments), as well as calculation and visualization of the partial contribution of any segment into the potential of the chosen lead against a background of the summary ECG have been developed and were used in the given work. For the modeled cardiosignals, some «medical» evaluation in terms of the Minnesota Code has been carried out and a set of characteristics, similar to parameters of the real ECG, has been measured and calculated. The most sensitive parameters of "ECG" for ischemia have been selected and analysed.

Conclusion: Systematic comparative investigations on the basis of modeling ischemia of various localization, extensiveness and degree of intensity are necessary. In conclusion, it should also be noted that the method of phase space is far from having exhausted itself and, as a preliminary consideration, may be developed into an *n*-dimensional area during a search for a complex of informative parameters for new diagnostic algorithms.

http://dx.doi.org/10.1016/j.jelectrocard.2013.05.051

Advances in inverse electrocardiography based imaging: from simple models to clinical applications

A.V. Kalinin[a], *L.I. Titomir*[a], *V.V. Kalinin*[b], *E.A.I. Aidu*[a], *V.G. Trunov*[a]
[a]Institute for Information Transmission Problems of the Russian Academy of Sciences
[b]Bakoulev Center for Cardiovascular Surgery Russian Academy of Medical Sciences

Introduction: Inverse electrocardiography based imaging is a new modality for cardiac electrophysiological studies providing non-invasive reconstruction of electrograms, isopotential maps, and activation sequence on the heart surface. Three approaches to the inverse ECG problem are considered. The first approach uses the orthogonal ECG as dipole components of the cardiac electric field (DECARTO). The second estimates several multipole components from multiple body surface ECGs (MULTECARTO). The model-based electrophysiological myocardium characteristics are then calculated and projected on a quasi epicardial surface. The latter method does not impose any limitations on the heart electric generator character, but, along with the body surface ECG, it requires accurate geometry of the human heart and torso (CT/MRI). Mathematically, this method is a generalization of the Cauchy problem for the Laplace equation. The first two methods are useful for preliminary diagnostics. The latter is designated for anatomically accurate diagnosis of cardiac disorders.

Methods: 89 patients, age range 16–76 years, with heart rhythm disorders were enrolled. Non-invasive inverse ECG-based imaging was performed in all patients. In patients demonstrating focal activity, ectopic foci and accessory pathways were localized with the use of this method and compared with the invasive electrophysiological examination data and results of radiofrequency ablation.

Results: Inverse ECG-based imaging helps to determine localization and depth of ectopic foci occurrence in the ventricles and atria, and provides detailed myocardial excitation patterns. The error of the method of ectopic foci localization was 6 ± 2 mm.

Conclusion: Inverse ECG-based imaging allows for accurate reconstruction of cardiac electric activity and can be used as a diagnostic tool for clinical management of cardiac arrhythmias.

http://dx.doi.org/10.1016/j.jelectrocard.2013.05.052

Computer modelling of beat-to-beat repolarization lability due to the diminished electrical coupling

G. Kozmann[a], *G. Tuboly*[a], *V. Szathmáry*[b], *J. Cvehlíková*[b], *M. Tysler*[b]
[a]University of Pannonia, Veszprém, Hungary
[b]Slovak Academy of Sciences, Bratislava, Slovakia

Introduction: A necessary prerequisite of malignant arrhythmias is the elevated static or dynamic repolarization dispersion (RD) of the ventricular myocardium. Body surface potential mapping provides a unique non-invasive method for the beat-to-beat exploration of spatial RD. In this study, the resultant RD properties were analyzed by the use of simulated QRST integral map sequences and non-dipolarity indices (NDIs).

Methods: A five-layer numerical heart model was used with globally or locally adjustable action potential duration (APD) and activation propagation properties, both expressed in model time units (mtu). Throughout the ventricular walls, APDs were characterized by their mean values and standard deviations (SDs). SD was assumed to be related to the strength of electrical coupling between the adjacent cells. A piecewise homogeneous thoracic model was used to compute the beat-to-beat QRST integral maps and NDIs. Modelling results were compared with clinical measurements taken from healthy and ICD patients.

Results: The instantaneous transmural gradient (TG) between the epicardial and endocardial layers was computed as $APD_{epi} - APD_{endo}$. In our reference case, the gradient was −15 mtu, yielding an NDI of 0.12. By the change of the transmural gradient in the apical part from −15 mtu up to +14 mtu, the NDI changed gradually from 0.12 up to 0.71. If simultaneous modulation of APD and propagation velocity was allowed, NDI could reach even the extreme value of 0.85.

Conclusion: In the healthy heart, the mean value of TG is large compared to the relevant SD value, and consequently the NDI is in the stable <0.2 range. In arrhythmia patients, the mean value of the gradient diminishes, while SD increases due to the poor electrical coupling. Consequently, NDI sequences will have temporally random, large amplitude beat-to-beat fluctuations.

http://dx.doi.org/10.1016/j.jelectrocard.2013.05.053

The effect of localized alteration of depolarization sequence on the QRS complex and ST segment patterns: a model study

L. Bacharova[a], *A. Mateasik*[a], *V. Szathmary*[b]
[a]International Laser Center, Bratislava, Slovakia
[b]Institute of Normal and Pathological Physiology, Slovak Academy of Sciences, Bratislava, Slovakia

Introduction:: Reduction or interruption of the blood supply to the myocardium due to occlusion of a coronary artery and consequent ischemia leads to changes of electrogenesis, namely changed action potentials and slowing of conduction velocity in the affected area. In this study, we simulated the effects of localized changes in depolarization sequence on the QRS and ST segment patterns, using computer modelling.

Methods: The model defines the geometry of cardiac ventricles analytically as parts of ellipsoids and allows the velocity of impulse propagation in the myocardium to be changed. An intramural electrically inactive area encircled by a transmural area with slowed impulse propagation velocity was introduced in anteroseptal and posterolateral locations. The effects on the QRS complex and the ST segment of the 12-lead electrocardiogram are presented.

Results: The intramural electrically inactive area caused QRS changes typical for corresponding locations which were further considerably modified by slowed impulse propagation velocity in the surrounding area.

Additionally, areas of slowed impulse propagation velocity led to ST segment deviations in the "reciprocal" leads, shifting the ST segment change towards the affected areas.

Conclusion: Using computer modeling we showed that the localized alteration of impulse propagation modified not only the QRS complex, but produced also changes in the ST segment consistent with changes which are usually interpreted as the effect of "injury current".

Supported by the grant VEGA 2/0131/13.

http://dx.doi.org/10.1016/j.jelectrocard.2013.05.054

Feature extraction of ECG signal using a support vector machine

I. Saini[a], V. Kumar[b], A. Khosla[a]
[a]*Dr B R Ambedkar National Institute of Technology, Jalandhar, India*
[b]*Indian Institute of Technology, Roorkee, India*

Introduction: Identification and delineation of clinically important parameters like occurrence, amplitude and duration of P, QRS-complex and T-wave to predict clinical conditions and for diagnostic purposes are well established. In this work, a Support Vector Machine (SVM), a classifier motivated from statistical learning theory, has been successfully applied for locating electrocardiographic fiducial points.

Methods: The algorithm was evaluated on two standard databases: (i) the 12-lead CSE DS-3 database (f_s = 500*Hz*) (ii) QT database (f_s = 250*Hz*) and also on an ECG dataset acquired using a BIOPAC® MP100 system (f_s = 500*Hz*) in laboratory settings. The mean (*m*) and standard deviation (std) of P-on, P-off, QRS-on, QRS-off and T-end were calculated as the average errors, taken as the time difference between the algorithmic results and the referee cardiologist annotations.

Results: The delineation results of CSE and QT databases have been compared with the accepted two standard deviation (2_{sCSE}) tolerances as recommended by CSE working party (Table 1). The results for ECG records acquired using BIOPAC® MP100 system, in terms of QRS duration, heart rate, QT-interval, P-wave duration and PR-interval using SVM algorithm have also been computed.

Table 1
Differences between SVM algorithm and gold standard expressed using different statistical parameters (mean difference ± std(ms)).

Database	P-on	P-off	QRS-on	QRS-off	T-end
CSE (25 records)	−0.16 ± 4.2	−1.2 ± 6.2	−1.8 ± 5.8	0.4 ± 6.0	2.6 ± 10.4
QT (30 records)	0.2 ± 13.2	1.3 ± 12.4	−1.4 ± 7.6	4.2 ± 8.6	2.7 ± 17.2
Tolerance (2_{sCSE})	10.2	12.7	6.5	11.6	30.6

Conclusion: In general, automated ECG diagnosis relies on accurate localisation of the ECG fiducial points. The method presented here for ECG wave delineation is efficient, simple and easily adaptable to a wide variety of ECG wave morphologies. The statistical measures, i.e. mean and standard deviation of differences between the algorithm and the gold standard have been computed for two databases and found to be well within the recommended tolerance limits.

http://dx.doi.org/10.1016/j.jelectrocard.2013.05.055

Impact of torso model fidelity on the inverse localization of ischemia

J. Lenkova, J. Svehlikova, M. Tysler
Institute of Measurement Science SAS

Introduction: The electrocardiographic inverse solution based on multi-channel ECG recordings and a dipole model of a local cardiac generator enables non-invasive localization of cardiac ischemia. Its accuracy is influenced by the torso model used. Whole-torso CT is desirable to create it; however, there is usually no CT or only cardiac CT with a part of the torso available. In this simulation study, we investigated the accuracy of an inverse solution if a common torso shape adjusted to the patient's chest dimensions, containing lungs and a heart model in various positions is used instead of the whole-torso CT based model.

Methods: Surface ECGs generated by a normal heart and a heart with one small ischemic lesion were simulated in 7 realistic inhomogeneous torso models. For each of them, 18 lesions in myocardial areas corresponding to occlusions of main coronary vessels were modelled. Inverse localization of each lesion was performed using difference QRST integral maps between normal and ischemic hearts and approximate torso shapes containing a common heart model: A – in standard position based on lead V2, B – vertically shifted using inverse localization of initial ventricular activation, C – shifted as B but properly rotated and scaled, and D – properly shifted, rotated and scaled.

Results: The mean errors of the vertical position of the heart model and the lesion localization for different torso-heart models are shown in Table 1.

Table 1
Mean errors in [cm].

Torso-heart model:	A	B	C	D	Torso CT
Error of vertical heart position:	1.6 ± 2.3	0.2 ± 1.2	0.2 ± 1.2	0.0	0.0
Error of lesion localization:	3.4 ± 0.9	3.9 ± 1.0	2.4 ± 0.7	1.1 ± 0.7	0.7 ± 0.7

Conclusions: Although the position of the heart within the torso model is important, its proper orientation and size also appear to be crucial. Thus, if whole-torso CT is unavailable, a properly oriented, scaled and placed heart model in a torso shape adjusted to the patient's chest dimensions can give acceptable inverse localization of ischemia.

http://dx.doi.org/10.1016/j.jelectrocard.2013.05.056

Respiratory sinus arrhythmia in Chagas disease

V.R. Neves[a], M. Peltola[b], M.O.C. Rocha[a], A.L.P. Ribeiro[a]
[a]*School of Medicine and University Hospital, Universidade Federal de Minas Gerais*
[b]*Faculty of Medicine, Institute of Clinical Medicine, University of Oulu*

Introduction: Chagas disease (ChD) is an endemic health problem in certain areas of Latin America and, recently, due to migratory movements of infected subjects, also in the United States and Europe. Damage of the autonomic nervous system, mainly the parasympathetic branch of the heart and the digestive tract, is an important pathological feature in patients with ChD. The respiratory sinus arrhythmia (RSA) index can be used as marker of vagal dysautonomia in cardiac disease. Therefore, we applied the RSA quantification algorithm to 24-hour ECG recordings in ChD patients. Our aim was to assess the autonomic control of heart rate by RSA in ChD patients with and without ventricular dysfunction.

Methods: ChD patients (181) and control subjects (Group 0, n = 28) underwent a standardized protocol including Holter monitoring, heart rate variability (HRV) analyses and quantification of RSA. ChD patients were divided according to the absence (group 1, n = 148) or presence (group 2, n = 33) of left ventricular (LV) dysfunction, defined as reduced LV ejection fraction (<55%). One-way ANOVA with Duncan correction and Pearson correlation were used.

Results: Both ChD groups displayed reduced RSA index (Group 0 = 1011 (288–2252); Group 1 = 299 (144–812); Group 2 = 335 (162–667), $p < 0.05$). RSA index was significantly correlated with HF power (Group 0, r = 0.830, $p < 0.001$; ChD patients, r = 0.794, $p < 0.001$), LF power (Group 0, r = 0.561, $p < 0.01$; ChD patients, r = 0.271, $p < 0.002$), RMSSD (Group 0, r = 0.873, $p < 0.001$; ChD patients, r = 0.729, $p < 0.001$) and SDNN (Group 0, r = 0.768, $p < 0.001$; ChD patients, r = 0.541, $p < 0.001$).

Conclusion: The RSA index is a useful marker of vagal modulation in ChD patients; cardiac parasympathetic dysfunction occurs in both groups of ChD patients, with and without LV dysfunction.

http://dx.doi.org/10.1016/j.jelectrocard.2013.05.057

Fusion of biventricular incomplete bundle branch block, in healthy young adults and in patients with moderate pulmonary hypertension. Fragmented depolarization – a new real ECG entity

L. Regos[a], A. Simon[b], B. Garai[c], I. Berényi[d], Z. Antalóczy[e]
[a]*Ujpesti Health Nonprofit Kft*
[b]*Szt Imre Hospital*
[c]*Karolyi Sandor Hospital*
[d]*Balatonfüred Heart Hospital*
[e]*Postgraduate Medical School*

Introduction: Within the QRS complex, the vector components either compete with each other or can appear at the same time. The two best examples of rewriting the original ECG curves are preexcitation and complete left bundle branch block. In contrast, the rS complex of left anterior hemiblock (LAH) and the Q wave of postero-inferior myocardial infarction (PI MI) can be observed simultaneously forming a W complex in the inferior leads.
Methods: First, variants of incomplete right bundle branch blocks (IRBBB) were studied in healthy young adults and in patients with moderate pulmonary hypertension. According to the QRS morphology in the frontal plane (59 patients), three IRBBB patterns were formed: 1. SI-SII-SIII (n = 20); 2. SI-QIII (n = 18); 3. Both 1 and 2 patterns (n = 8). Presence or absence of IRBBB signs in lead V1 was meanwhile registered. Secondly, two further patterns were formed relating to comparison of biventricular incomplete blocks with arborization block. Both are characterized by depolarization inhomogeneity. 4. IRBBB + LAH (n = 11); 5. IRBBB + LAH + PI MI (n = 2).
Results: In pattern 3, initial and terminal vectors (QIII-SIII) occurred simultaneously in the ECG lead III. Frequently, waves occurring in the same period of the depolarization in certain leads remained separable (two-component S-wave). In pattern 4, after the initial "r" wave, a two component S wave (rW complex) appeared in the inferior leads. Such separation of the depolarization vector components does not mean high electrical inhomogeneity if the width of QRS remains under 110 ms. In pattern 5, the ventricular depolarization is fragmented, and appears as three negative waves in the inferior leads (VW complex). In these cases, the duration of ventricular depolarization is also not wider than 110 ms. In contrast, the arborization block is characterized by fragmented depolarization, but the duration of QRS is wider than 140 ms, resulting in extreme inhomogeneity.
Conclusion: By wave form analysis of biventricular incomplete blocks, we could describe a new ECG entity, of less dangerous "arborization block-like" form.

http://dx.doi.org/10.1016/j.jelectrocard.2013.05.058

Accuracy of electrocardiological inverse solutions: a model study

G. Kozmann[a], G. Tuboly[a], I. Maros[a], D. Wei[b], X. Zhu[b]
[a]*University of Pannonia, Veszprém, Hungary*
[b]*University of Aizu, Aizu-Wakamatsu, Japan*

Introduction: Non-invasive electrocardiographic imaging is usually based on the boundary element approach with zero-order Tikhonov regularization. The principal aim of this paper is the study of the achievable epicardial potential estimation quality.
Methods: Reference body surface and epicardial electrocardiograms were generated in 1003 epicardial and 344 body surface points by the Wei model. The inverse problem has been solved for the inhomogeneous and homogeneous chest model by the Tikhonov zero-type regularization procedure. The impact of the properly selected regularization parameter has been explored by the systematic exploration of its optimal value in each time instant. The impact of the method selected for the solution of the linear system of equations has been studied by the use of Gaussian elimination, conjugate gradient, minimum residual, quasi minimal residual, LSQR and symmetric LQ methods all taken from the MATLAB library. The quality of the inverse solution was characterized by the correlation coefficient of the real and the estimated epicardial potential distributions throughout the QRS interval.
Results: Both the suboptimal regularization parameter selection and the suboptimal equation solution methods resulted in a loss of estimation quality. The highest correlations (>0.9) were in the first half of the QRS interval. Later, the mean correlation was typically between 0.5 and 0.8. The range of deviations from the mean was 0.05, increasing up to 0.2 at the end of the QRS. The largest error source was the inadequate volume conductor model when the resultant correlation fell below 0.5.
Discussion: The individual contribution of the effects discussed suggests the need of appropriate validation procedures before solving clinically meaningful problems. According to our experience, the sensitivity of the solution to the different equation solving methods was the most surprising factor.

http://dx.doi.org/10.1016/j.jelectrocard.2013.05.059

In silico investigation of the electromechanical consequences of the short QT syndrome

I. Adeniran[a], J.C.H. Hancox[b], H. Zhang[a]
[a]*The University of Manchester*
[b]*University of Bristol*

Introduction: The Short QT Syndrome (SQTS) is a cardiac ion channelopathy associated with accelerated ventricular repolarization, arrhythmias and sudden death. Studies suggest that transmural consequences of accelerated repolarization lead to a substrate favourable to re-entry. Electromechanical consequences of the SQTS are less well understood. Therefore, this study employed electromechanical human ventricular models to explore electromechanical consequences of the SQTS.
Methods: The ventricular models were produced by coupling the Rice et al. (2008) mechanics model with the ten Tusscher et al. (2006) ventricular cell model, incorporating K^+ channel formulations based on *in vitro* consequences of SQT variants 1–3. Single cell functional effects of the SQTS mutations on Ca^{2+} transients, sarcomere length shortening and contractile force were evaluated with and without stretch-activated channel current (I_{SAC}).
Results: Without I_{SAC}, the SQTS mutations produced dramatic reductions in the amplitude of Ca^{2+} transients, sarcomere length shortening and contractile force. With I_{SAC}, there was considerable attenuation of these effects. Single cell models were incorporated into 2D and 3D models, which showed that timing of maximum deformation was delayed in the SQTS setting compared to control.
Conclusion: Our simulation matches qualitatively to the experimental data on the dissociation between ventricular repolarization and the end of mechanical systole in SQT patients. The striking difference between simulations incorporating or lacking I_{SAC} suggests that I_{SAC} modulates the functional effects of SQT 1–3 on ventricular mechanical dynamics. It raises a question as to whether compensatory changes occur in the SQTS that offset a negative inotropic effect of ventricular action potential abbreviation that might occur.

http://dx.doi.org/10.1016/j.jelectrocard.2013.05.060

Correlation of SPECT examination and high signal resolution electrocardiography

R.K. Krzyminiewski[a], B.D. Dobosz[a], R.S. Stepien[b]
[a]*Medical Physics Division, Adam Mickiewicz University*
[b]*Ministry of Internal Affairs Hospital*

Introduction: In view of the high rate of myocardial ischemic disease, early diagnosis and identification of patients requiring coronary arteriography and/or surgical treatment are of great importance.

Methods: We propose a computer method based on Fourier and linear transformation of ECG records, called NURSE-ECG, which increases resolution of the QRS complex. The high-resolution ECG proposed in this work combines the records from particular electrodes, each of computer enhanced resolution. NURSE-ECG provides an opportunity to detect even relatively small changes in electrical activity of particular segments of the cardiac muscle. In order to perform quantitative analysis, the heart muscle was divided into particular segments.

Results: The correct NURSE-ECG and standard activities of cardiac muscle segments were calculated. The quantitative analyses of NURSE-ECG records of people with ischemia were undertaken. The results obtained for people subjected to SPECT examination show a good correlation between the results of SPECT examination and the decrease in electrical activity of the cardiac muscle fragments observed by the HRVEC method (SE = 96%, SP = 92%).

Conclusion: Preliminary analysis of the sensitivity and specificity of the high signal resolution NURSE-ECG in IHD diagnostics has proved the method to be very promising in the diagnosis of ischemic heart disease.

http://dx.doi.org/10.1016/j.jelectrocard.2013.05.061

New algorithms and new technologies in computerized ECG analysis: a challenge in long-term follow-up studies

S. Perz[a], C. Meisinger[a], S. Kääb[b], M.F. Sinner[b], R. Küfner[a], K.H. Englmeier[a]
[a]*Helmholtz Zentrum München*
[b]*University Hospital Munich, Großhadern*

Introduction: Epidemiologic studies require consistently operating methods of data collection and analysis. In principle, this is provided by computerized ECG analysis largely avoiding intra- and inter-observer variability, but only if the same system has always been used. To determine electrocardiographic changes over a 25 year follow-up, the results of the population-based Monica Augsburg Survey 1984/85 (N = 4022) have to be compared with the results of the KORA Age study. In the baseline examination, the Sicard 803 system was used, whereas in the follow-up study, the HES Amedtec ECG pro system (HES) was used. Both systems analysed the 12 lead resting ECG, but using different hardware and software.

Methods: To adjust for systematic differences in the performance of the two systems, we analysed the ECGs of a subsample of 50 study participants using both systems simultaneously and compared the measurements of the quantitative analysis applying matched pairs T tests.

Results: Of the global measurements, PQ duration and QRS duration did not show significant differences when comparing the HES with the Sicard 803 results (Table 1). However, QT intervals were considerably (18.1 ms) longer when using the HES system. For lead specific parameters (lead II), measurements were partly smaller, partly almost identical and partly larger according to HES. As a consequence, all parameters of interest have to be evaluated.

Table 1
Comparison of HES and Sicard 803 measurement distributions (n = 50).

Measurement	HES	Sicard 803	Difference	P
PQ dur (ms)	166.5 ± 24.7	165.4 ± 25.8	1.1 ± 6.8	0.323
QRS dur (ms)	94.4 ± 15.6	93.6 ± 17.0	0.8 ± 7.3	0.455
QT interval (ms)	410.9 ± 29.6	392.8 ± 26.3	18.1 ± 9.6	0.000
R wave dur II (ms)	56.7 ± 19.9	67.5 ± 19.1	−10.8 ± 13.6	0.000
R wave amp II (μV)	922.0 ± 329.3	922.0 ± 373.7	0.0 ± 60.8	1.000
S wave dur II (ms)	37.1 ± 20.9	31.7 ± 19.7	5.4 ± 16.2	0.118
S wave amp II (μV)	211.7 ± 149.5	179.2 ± 145.8	32.5 ± 61.0	0.016

Conclusion: Appropriate interpretation of ECG measurement changes – determined in follow-up studies – requires systematic control of possible bias according to technology change of the ECG analysis systems used.

http://dx.doi.org/10.1016/j.jelectrocard.2013.05.062

Comparison of RR-intervals in rabbit heart in in-vivo, ex-vivo and under ischemia

O. Janoušek[a], M. Ronzhina[a], J. Kolářová[a], M. Nováková[b], P. Scheer[c], I. Provazník[a]
[a]*Brno University of Technology, Brno, Czech Republic*
[b]*Masaryk University, Brno, Czech Republic*
[c]*University of Veterinary and Pharmaceutical Sciences, Brno, Czech Republic*

Introduction: Use of heart rate variability for diagnostic purposes is highly topical. Although many studies of heart rate variability in-vivo have been published, only a few studies pay attention to isolated hearts, mainly because it can be studied only in patients with cardiac denervation. Ischemia is believed to influence nonautonomic mechanism of the heart. Detailed analysis of the both denervation and ischemia influence may have significant diagnostic contribution.

Methods: Seven isolated New Zealand rabbit hearts in Langendorff setup and five in-vivo New Zealand rabbit hearts were studied. Control period (15 min) was recorded for both groups. In addition, each isolated heart underwent episodes (15 min) of coronary artery occlusion, followed by three reperfusion periods (15 min). Electrograms from isolated hearts were recorded by three orthogonal leads positioned orthogonally around the heart. Signals were amplified and digitized with sampling rate 2 kHz and 16-bit analogue-to-digital converter. Electrocardiograms from in-vivo hearts were recorded by a SEIVA recording system with body surface wire electrodes attached to the skin with miniature clips in the position duplicating orthogonal leads in the ex-vivo setup. Five-minute long segments of electrograms have been manually evaluated from each phase of the experiment and inaccurate R-peaks were excluded from analysis.

Results: The histogram and boxplot have been used for comparison of RR-intervals of in-vivo and ex-vivo hearts and RR-intervals of the isolated hearts under normal and ischemic condition. The typical value of RR-interval prolonged from 250 ms in the in-vivo heart to 350 ms in the ex-vivo heart. During ischemia, the RR-interval dramatically prolonged to 600 ms. Subsequent reperfusion had no significant effect on the RR-interval, and no effect was observed during repeated ischemia and reperfusion periods. Variability of RR-intervals slightly decreased after heart excision from 226–273 ms in-vivo to 329–368 ms ex-vivo and significantly rose to 532–680 ms in the first episode of ischemia. RR-interval variability remained almost the same in subsequent ischemia and reperfusion repetitions.

Conclusions: The results show that denervation of the heart causes only prolongation of heart rate; however its regularity remains comparable with that of in-vivo hearts. It supports the hypothesis that heart rate variability persists in excited hearts. Ischemia causes irreversible changes of intracardiac mechanisms regulating heart activity. RR-intervals in ischemia significantly differ from those in-vivo and ex-vivo.

http://dx.doi.org/10.1016/j.jelectrocard.2013.05.063

Multi-scale integrative model of the human atria and torso: a platform for the investigation of atrial arrhythmias

E.A. Perez Alday[a], M.A. Colman[a], P. Langley[b], A.V. Holden[c], H. Zhang[a]
[a]*University of Manchester*
[b]*Newcastle University*
[c]*University of Leeds*

Introduction: Atrial tachycardia (AT), resulting from rapid ectopic atrial activity, may predispose to atrial fibrillation (AF). The regions of the pulmonary veins (PV) are identified as a major source of AF and AT. Such abnormal origin of atrial excitation may be reflected as an alteration in the P-wave morphology (PWM) of the electrocardiogram (ECG). Identifying the presence and the location of the ectopic atrial activity can help to diagnose the early onset of AF. In this study, we develop a biophysically detailed computational model of the human atria and torso, to investigate the relation between PWM and the different origins of atrial ectopic activity.

Methods: We apply a recently developed 3D human atrial model to simulate ectopic activity. The 3D model is then placed into a newly developed torso model, taken from the visible human dataset and considers the lungs and liver. A boundary element method is used to compute the electrical activity

from the surface of the atria to the surface of the torso. Elements of the torso mesh corresponding to the locations of the electrode placement are selected to simulate 12 and 64 lead ECG. PWM morphology associated with ectopic and rotor wave activity from a variety of regions throughout the atria and in the PV is analysed.

Results: During sinus rhythm conditions, the simulated P-waves and body surface potentials dipole direction show strong agreement with experimental data. Marked changes in PWM are observed in both 12 and 64 lead ECG associated with ectopic atrial activity and the presence of rotor waves.

Conclusion: Our simulation data suggested that ectopic activity originating from the PV can be identified based on changes of PWM. The correlation between PWM and rapid ectopic activity or the presence of rotor waves in the PV requires more detailed analysis and validation.

http://dx.doi.org/10.1016/j.jelectrocard.2013.05.064

The effect of AF-induced electrical remodelling on regional electrical heterogeneity and tissue vulnerability to atrial fibrillation—insights from modelling

M.A. Colman, O.V. Aslanidi, S.R. Kharche, M.R. Boyett, H. Zhang
University of Manchester

Introduction: Atrial fibrillation (AF) is the commonest sustained cardiac arrhythmia. Shortening of the action potential duration (APD) associated with AF-induced electrical remodelling (AFER) is known to promote re-entrant arrhythmias. Previous studies have shown that intrinsic regional heterogeneity within the atria plays an important role in arrhythmogenesis. However, the effect of AFER on regional heterogeneity in the atria has yet to be characterised. The aim of this study is to apply a model of the 3D human atria for investigating the functional impact of AFER on atrial electrical heterogeneity and tissue vulnerability to initiation of re-entrant excitation waves.

Methods: A family of previously developed models for variant atrial cell types was extended and modified to incorporate multiple data sets of AFER. The cell models are then incorporated into a segmented 3D model of the human atria. Vulnerability windows (VW) for unidirectional conduction block leading to re-entry are computed at major heterogeneous junctions of the pulmonary veins (PV) with the left atrium (LA) and the crista terminalis (CT) with the pectinate muscles (PM).

Results: AFER abbreviated atrial APD for all regions, but preserved dramatic regional heterogeneity in both single cell and in tissue. Importantly, in all AF conditions, APD gradients in the PV/LA and CT/PM junctions remain, resulting in an increase in the measured VW.

Conclusions: The functional effect of AFER on regional heterogeneity within the atria increases tissue susceptibility to arrhythmogenesis. This is due to preserved APD gradients and shortened excitation wavelengths, both contributing to initiation of re-entrant excitation waves. This study provides insights towards better understanding the high AF reoccurrence rates in patients with chronic AF after ablation therapy.

http://dx.doi.org/10.1016/j.jelectrocard.2013.05.065

Determination of local activation time in bipolar endocardial electrograms: a comparison of clinical criteria and a new method based on the non-linear energy operator

T.G. Oesterlein[a], M.W. Keller[a], S. Schuler[a], A. Luik[b], M. Krüger[a], G. Seemann[a], G. Seemann[a], C. Schmitt[b], O. Dössel[a]
[a]*Institute of Biomedical Engineering, Karlsruhe Institute of Technology (KIT), Karlsruhe, Germany*
[b]*IV. Medizinische Klinik, Städtisches Klinikum Karlsruhe, Karlsruhe, Germany*

Introduction: Local activation time (LAT) maps help to understand the path of electrical excitation in cardiac arrhythmias. They can be generated automatically from intracardiac electrograms using various criteria provided by commercial electroanatomical mapping systems. This study compares existing criteria and a novel method based on the non-linear energy operator (NLEO) with respect to their precision and robustness.

Methods: Bipolar electrograms were simulated for five catheter orientations ((anti-)parallel to tissue, orthogonal and ±45° tilt). In addition, clinically measured LAT maps comprising 489 signals were analyzed. LAT was determined from voltage V or its derivative dV/dt by common criteria like max, min or absolute value. NLEO was used to estimate the signal energy based on amplitude and frequency. NLEO based LATs were defined as maximum or barocentre of the low pass filtered NLEO signal. Known LATs from simulations were used to benchmark the algorithms.

Results: The time between min and max peak of simulated signals was 6.4 ± 0.6 ms, and 9.4 ± 5.8 ms for clinical signals. The absolute peak LAT performed best of all common criteria (total error: 1.0 ± 1.2 ms) but deviated strongly for orthogonal tilt of the catheter. The absolute derivative performed best only in this orthogonal orientation (1.7 ± 1.0 ms). LAT using maximum NLEO was superior to all common methods (0.5 ± 0.3 ms) considering all tilts.

Conclusion: Detection of LAT based only on max or min peak is expected to result in a direction dependent error of 10 ms, distorting the shape of isochrones. Using the maximum peak of any polarity performed best of all common criteria but deviated if the catheter was not aligned parallel to endocardium. Using the NLEO based method provides a robust solution to determine the LAT for any catheter angle.

http://dx.doi.org/10.1016/j.jelectrocard.2013.05.066

Measured and simulated P waves in normal subjects reflect complex atrial anatomy

M. Potse[a], T.A.R. Lankveld[b], S. Zeemering[b], N.H.L. Kuijpers[c], U. Schotten[b]
[a]*University of Lugano, Switzerland*
[b]*Maastricht University, Maastricht, The Netherlands*
[c]*Fontys Hogeschool ICT, Eindhoven, The Netherlands*

Introduction: The shape of the P wave can yield important information about the substrate of atrial fibrillation (AF). On the routine 12-lead ECG, obtained using standard equipment, P waves have a smooth appearance. Computer simulation studies with realistic atrial models, in contrast, have shown highly complex P-wave shapes with details that were linked to structural features of the atria. Therefore we evaluated P-wave shapes using high-resolution, unfiltered ECG recordings and sophisticated averaging techniques in control subjects.

Methods: We recorded 10-minute 184-channel high-resolution ECGs in 6 healthy volunteers (all male, age 26–43). Neither high-pass nor low-pass filters were used. Instead, signal averaging over more than 300 beats was used to cancel noise. To avoid smearing-out due to variations in PQ interval, beats were aligned on their P waves. Alignment was based on a compound signal of all 184 channels to reduce the effect of noise on alignment. In addition, 12-lead ECGs were simulated using a single patient-tailored heart-torso model with detailed atrial anatomy at 0.2-mm resolution.

Results: Averaging reduced the noise level to less than 2 microvolt (μV) peak-to-peak. Signal features of a few μV amplitude and less than 5 milliseconds (ms) duration could be reliably distinguished. Measured P waves had 4–5 separate peaks that were reproducible between recordings. Simulated P waves demonstrated similar complexity, which was related to structural features in the computer model of the atria.

Conclusion: The true shape of the P wave is very irregular and reflects the complex anatomy of the atria. This finding necessitates a reconsideration of the idea that an AF substrate can be recognized in the ECG by increased signal complexity, as high-resolution electrocardiography is necessary to reliably assess P-wave shape even in ECGs of healthy volunteers.

http://dx.doi.org/10.1016/j.jelectrocard.2013.05.067

Correlation between ECG and coronary angiography in patients with a sudden obstruction of the right coronary artery (RCA)—physiological and pathological myocardial remodeling

S. Sclarovsky[a], K. Nikus[b], Z.Q. Zhan[c], F.J. Feminia[d]

[a]Maccabi Health Center, Israel
[b]Tampere University Hospital, Finland
[c]Taihe Hospital, Hubei University, China
[d]Hospital Espanol, University of Mendoza, Argentina

Introduction: Changes occurring in non-involved myocardium with an isolated sudden obstruction of RCA and a normal or non-critical obstruction of coronary vessels supplying the non-involved area are considered as physiological remodelling. Changes occurring in non-involved myocardium during a sudden total obstruction of RCA and critical obstruction of other vessels supplying this area are considered as pathological remodelling. The aim of the study was to specify the ECG accuracy for predicting the different types of sudden obstruction of RCA, as determined by coronary angiography.

Methods: ECGs of patients with a non-anterior wall infarction from 3 medical centres were interpreted by a single blinded investigator. The ECG interpretation was sent back to the corresponding medical centres and compared to the coronary angiography findings. Patients with ECG signs of reperfusion or with previous myocardial infarction were excluded. The patients were divided into two groups: Group A – patients with ECG findings compatible with physiologic remodelling, and group B – patients with ECG findings compatible with pathological remodeling. Group B was then further divided into 3 groups: B1 – a dominant RCA supplying the low lateral, apical and low anteroseptal wall; B2 – the anterior wall is supplied by a chronic critical obstruction of LAD; and B3 – anterior and lateral wall supplied by a critical chronic obstruction of LMC or critical chronic obstruction of LAD and CX arteries.

Results: Of 155 ECG tracing with non-anterior wall infarction, 80 were recognized as a sudden obstruction of RCA.

P	ECG	Coronary angiography	Group Total-80
<0.01	33	33	A
<0.01	15	16	B1
<0.01	16	18	B2
<0.01	10	13	B3

Conclusion: The ECG is an accurate, non-invasive tool to predict coronary anatomy and pathophysiology of a sudden obstruction of RCA.

http://dx.doi.org/10.1016/j.jelectrocard.2013.05.068

The clinical and electrocardiographic characteristics of parasystolic idioventricular rhythm

M.P. Chmelevsky, E.A. Tsurinova, T.V. Treshkur
Almazov Federal Heart, Blood and Endocrinology Centre

Introduction: The purpose of the study was to assess the electrocardiographic features of parasystolic accelerated idioventricular rhythms (AIVR) and to analyse their relationship with the leading pacemaker.

Methods: An exercise training test (ETT) and Holter monitoring (HM) were undertaken in 640 patients with monomorphic ventricular parasystole. They included 65 men and 49 women aged from 17 to 68 (50 ± 12.4). 93 patients had structural heart disease, while 21 did not have any disease.

Results: AIVR were found in 114 patients (17%). There was sinus rhythm in 93.9% cases and atrial fibrillation in 6.1%. 29% of the patients complained of an irregular heartbeat. The electrocardiograms showed 62 patients (54%) with two completely independent pacemakers (sinus and parasystolic) manifesting as AV dissociation. In the other 52 cases (46%), sinus rhythm influenced the presence and regularity of the ectopic centre. Intermittent parasystolic activity was connected with (a) transient annihilation of the ectopic centre (10%), (b) incomplete entrance block in the ventricular automatic centre (43%), (c) incomplete exit block (40%), and (d) unknown reasons (7%). The 77% of AIVR were regular, while 23% were irregular. The reasons of irregularity were: exit block of the 2nd degree of type 1 (61%), incomplete entrance block in the ectopic centre (31%), modulation (23%), and unexplained parasystolic centre arrhythmia (8%). In 30% of cases, the rates of sinus rhythm and AIVR were identical. Among all AIVR registered during the ETT, 9% of AIVR were ischemic. In 12% of patients, ventricular arrhythmia disappeared during the test. During HM, 8% of AIVR were spontaneously transformed into non-sustained ventricular tachycardia.

Conclusion: The presence of AIVR of the same morphology as the premature ventricular beats with parasystole signs confirms the parasystolic origin of AIVR. It also helps the recognition of the variants of the relationship between the parasystolic ectopic and sinus centres and supports the assumption that the autonomic nervous system can influence the ectopic centre.

http://dx.doi.org/10.1016/j.jelectrocard.2013.05.069

The role of multi-diurnal telemonitoring ECG in the management of pregnant women with ventricular arrhythmia

E.A. Tsurinova, S.V. Popov, O.B. Irtyuga, T.V. Treshkur
Almazov Federal Heart, Blood and Endocrinology Centre

Introduction: Difficulties in the use of antiarrhythmic drugs (AAD) in the treatment of ventricular arrhythmia (VA) during pregnancy are increasing the risk of maternal and fetal complications. In the case presented, we analyzed the possibilities of multi-diurnal monitoring of the ECG (MM ECG) with telemetry to aid in the selection of AAD for a pregnant female with VA.

Methods: A 40-year-old woman, multigravida, who was 30 weeks pregnant, underwent radio frequency ablation of a focus of unstable idiopathic parasystolic ventricular tachycardia (VT) three months before this pregnancy. In the 30th week of pregnancy, 27000 VA per day reappeared. MM ECG was started using wireless telemetry with standard GSM, during which the selection of AAD was initiated.

Results: After administration of bisoprolol at the maximum dose of 10 mg, the daily amount of VA increased up to 39000 with renewed paroxysms of unstable VT, suggesting ineffectiveness, and perhaps, proarrhythmogenicity of bisoprolol which was therefore changed to sotalol. At a dose of 200 mg/day, the number of VA decreased to 10000 per day (efficiency of 75%), and the paroxysms of VT disappeared. At 39 weeks of pregnancy, in the ambulatory setting, MM ECG was reinstituted for controlling VA and determining the duration and mode of delivery. For 4 days, MM ECG registered 145 VAs. In consideration of the positive response to the received therapy and no obstetric contraindications for vaginal delivery, it was decided to avoid operative delivery. Full term delivery was without any complications. The MM ECG was continued in childbirth and in the postnatal period during which VA was not registered. The patient was discharged with the decreased dose of sotalol up to 80 mg/day, which permitted breast feeding.

Conclusion: MM ECG with telemetry should take its place in the management of pregnant women with rhythm disturbances, including outpatients. The technique will effectively and safely assist selection of the optimal AAD and may help to avoid unnecessary surgical treatment.

http://dx.doi.org/10.1016/j.jelectrocard.2013.05.070

Patient-specific MRI-based models of infarcted hearts can predict risk of sudden cardiac death

H.J. Arevalo, F. Vadakkumpadan, A. Jebb, K. Wu, N.A. Trayanavo
Johns Hopkins University, Baltimore, USA

Introduction: ICDs are an effective primary prevention strategy for patients with ischemic heart disease who are at high risk for sudden cardiac death (SCD). Unfortunately, current selection criteria that rely on left ventricular ejection fraction (LVEF) have low specificity, which has led to over implantation of this expensive device. The goal of this study was to demonstrate, in a retrospective analysis, that patient specific, MRI based heart models can be used to predict SCD risk in patients with prior infarction and low LVEF.

Methods: MRI and long term clinical follow-up data were acquired from 10 patients with ischemic cardiomyopathy who had ICDs implanted; 5 subsequently had appropriate ICD firings for ventricular tachycardia (VT) and 5 have had no VT events. Multiscale, biophysically-accurate heart

models, including inexcitable scar and electrically remodelled gray zone (GZ), were developed from the MRIs. SCD risk was assessed by simulating VT inducibility using programmed electrical stimulation (PES) delivered from 17 different endocardial sites.

Results: The simulations successfully predicted arrhythmia risk in all 10 patients. For the 5 patients with appropriate firings, simulations showed that PES from at least 1 endocardial site resulted in VT induction. All VTs were re-entries organized within the GZ. Simulations also correctly predicted that patients with no recorded VT events were non-inducible. Non-inducible patients had lower GZ volumes compared to those with firings (8.7 ± 9.7 cm^3 vs 19.2 ± 8.9 cm^3).

Conclusion: Simulations with patient-specific MRI-based models of hearts with infarction may provide a unique opportunity to noninvasively predict SCD risk in patients.

http://dx.doi.org/10.1016/j.jelectrocard.2013.05.071

The QT interval, arterial stiffness, endothelial function and vascular age

I. Mozos[a], *L. Filimon*[b]
[a]*"Victor Babes" University of Medicine and Pharmacy, Timisoara, Romania*
[b]*Military Hospital, Timisoara, Romania*

Introduction: The prolonged QT interval is a known predictor of sudden cardiac death. Arterial stiffness and endothelial dysfunction are markers of premature cardiovascular disease. The aim of the present study was to assess the relation between QT interval and arterial stiffness, endothelial function and arterial age, respectively.

Methods: A total of 32 patients with normal blood pressure, some being at the upper end of the normal range, together with others having grade 1 and 2 hypertension, underwent standard 12-lead ECG and arteriography. The mean age of the cohort was 34 ± 8 years and 69% were male. QT intervals were automatically measured and pulse wave velocity (PWV), brachial and aortic augmentation index (Aixbra and Aixao, respectively) and arterial age were assessed.

Results: Heart rate corrected QT interval (QTc) was: 422 ± 29 ms, arterial age: 44 ± 14 years, Aixbra: $-44 \pm 25\%$, Aixao: $15 \pm 2.31\%$, PWV: 8 ± 1.45 m/s. Multiple regression analysis revealed significant associations between heart rate corrected QT interval (QTc) and brachial and aortic regurgitation index (multiple R = 0.997, R square = 0.995, adjusted R = 0.961, significance $F < 0.01$). QTc was also significantly associated with arterial stiffness and increased arterial age (multiple R = 0.431 and 0.866, respectively, R square = 0.186 and 0.75, respectively, adjusted R = 0.153 and 0.717, respectively, significance F = 0.012 and <0.01, respectively).

Conclusion: Arterial stiffness, endothelial dysfunction and increased arterial age are associated with long QT intervals.

http://dx.doi.org/10.1016/j.jelectrocard.2013.05.072

Non-invasive myocardial imaging of PVCs and pacemakers using the 12 lead ECG

P.M. van Dam[a], *M. Laks*[b], *K. Shivkumar*[b]
[a]*University Nijmegen*
[b]*David Geffen School of Medicine at UCLA*

Introduction: Catheter ablation of abnormal focal activity requires a time consuming EP study to map its origin. The current non-invasive procedure, body surface mapping (BSM) is costly and complicated. In contrast, the 12 lead ECG is inexpensive, simple, and has never been quantitatively used for activation mapping. The standard 12 lead ECG was used to localize the origin of pacemakers and PVCs.

Method: We developed an automatic computer morphing tool to derive an accurate cardiac anatomical model from MRI for each patient. Using this model, ventricular activation maps of 5 ms isochrones were created from 65 lead BSM and the 12 lead ECG. From the activation map, the initial 5 ms focal site was compared to the electrode location derived from X-ray, the gold standard for pacemaker lead location or the electro-anatomical map, the gold standard for the PVC origin.

Results: In 8 patients, pacemaker leads were localized in 8 different regions of the right and left ventricles. The distance from the initial 5 ms focal activity to the pacemaker electrode was the same for BSM (range 3–20 mm, 14 ± 5 mm) and 12 lead ECG (range 4–24 mm, 17 ± 5 mm) $P > 0.05$. In 2 patients with PVCs, the initial 5 ms focal activity derived from 12 lead ECG was within 10 mm of the ablation site.

Conclusion: Our activation mapping technique using the 12 lead ECG is equivalent to BSM for the localization of focal activity. The 12 lead ECG can localize different positions of pacemaker leads and origins of PVCs. This non-invasive quantitative activation mapping technique can reduce mapping time in EP studies. It can also be updated rapidly with new data to establish and improve the localization of all abnormal cardiac focal activities. This isochrone producing technique creates a new investigative tool to visualize the activation sequence produced by the standard 12 lead ECG.

http://dx.doi.org/10.1016/j.jelectrocard.2013.05.073

Functional properties of complex fractionated atrial electrograms during atrial fibrillation can be explained by structural remodelling: a simulation study

T. Ashihara[a], *R. Haraguchi*[b], *K. Inada*[b], *S. Nakazawa*[b], *T. Ikeda*[c], *T. Ozawa*[a], *M. Ito*[a], *N. Trayanova*[d], *M. Horie*[a]
[a]*Shiga University of Medical Science*
[b]*National Cerebral and Cardiovascular Center Research Institute*
[c]*Toho University Faculty of Medicine*
[d]*Johns Hopkins University*

Introduction: Electrogram-based catheter ablation, targeting complex fractionated atrial electrograms (CFAE), is empirically known to be effective in halting chronic atrial fibrillation (AF). Since recent clinical studies have shown that non-fractionated electrograms were recorded during sinus rhythm at sites of CFAE during chronic AF and that block of the fast component of the delayed rectifier K current (IKr) diminished CFAE regions, a topic of debate remains whether the CFAE mechanisms are functional or structurally-based. We hypothesized that functional properties of CFAE during chronic AF can be explained by fibroblast proliferation as part of structural remodelling.

Methods: To address this issue, we investigated the electrophysiological mechanisms of CFAE using an in silico model of human chronic AF under heart failure, based on the fibroblast-CFAE hypothesis (Circ Res 2012) stating that fibroblast proliferation leads to the formation of CFAEs during chronic AF.

Results: (1) CFAEs were recorded in fibroblast proliferation area where spiral wave breakup was observed, because the small excitable gap, resulting from the short diastolic intervals, decreased myocardial excitability. (2) Non-fractionated electrograms were recorded in the same area during pacing because the larger excitable gap (longer diastolic intervals) recovered myocardial excitability, preventing wave breakup. (3) In the case of IKr block by 50%, spiral wave breakup was suppressed and the excitation intervals during AF were prolonged, resulting in the decrease in CFAE complexity. These simulation results are consistent with clinical studies in patients with chronic AF.

Conclusion: Since fibroblast proliferation alters electrotonically the electrophysiological properties of the atrial myocardium via myocyte-fibroblast coupling, structural remodelling in the atrial myocardium cannot be excluded even if CFAEs exhibit functional features.

http://dx.doi.org/10.1016/j.jelectrocard.2013.05.074

Species specific venom manifestations in ECG

R. Maheshwari[a], *V. Kumar*[b], *H.K. Verma*[c]
[a]*Rajasthan Technical University Kota*
[b]*IIT Roorkee*
[c]*Sharda University*

Introduction: The Tropics are home to human and venomous species. This cohabitation results in frequent survival encounters that may lead to venom interactions in human beings. The venom interacted victim's ECG signal exhibits species specific symptoms that may be useful in medical management.

Methods: A protocol was developed to obtain the ECG of the victims of venom interaction. 97 victims met the strict ethical guidelines and their ECG was obtained, in strict conformance with the CSE criteria. The ECG was analyzed using various software techniques. The onsets and offsets of all the fiducial points were recorded and standard parameters were obtained.
Results: It was observed that right pre-cordial leads were more susceptible in venom interactions, probably, due to wider surface area and thinner musculature of the right ventricle, compared to the left ventricle. The direct contact of the venom mixed blood may more prominently affect the right side as compared to the left. The krait (*Bungarus caeruleous*) bite cases manifested clear and distinct U waves. U waves, along with QTc prolongation and ST depression might be indicative of hypokalemia. The cobra (*Naja naja*) bite cases indicated ST-T change patterns similar to myocardial ischemia. The viper (*Echis carinatus* as well as *Vipera russelli*) venom influenced the QTc interval which might be because of potent cytotoxic effects on the cardiac muscles. The scorpion (*Mesobuthus tamulus pocock*) venom's 'autonomic storms' may cause dynamic and unstable features varying from electrolyte imbalance to hyperglycemia, hence no typical features in ECG could be identified, but in the majority, the tented T wave as found in hyperkalemia was seen. The recordings after completion of treatment revealed reversal of the abnormal parameters.
Conclusion: Distinct species specific features could be observed in the ECG. Prolongation of QTc was commonly found in the majority of cases, while many typical morphological features were identified.

http://dx.doi.org/10.1016/j.jelectrocard.2013.05.075

Effects of gender differences and aging on cardiac repolarization in mice

M. Kuwahara, S. Taniguchi, K. Ito
Department of Comparative Pathophysiology, Graduate School of Agricultural and Life Sciences, The University of Tokyo

Introduction: It is generally thought that sex hormones and aging affect cardiac repolarization. Although the density of repolarizing K^+ currents may be modified by sex hormones and aging, these effects are still a matter of controversy in murine models. Therefore, we evaluated the cardiac phenotype with ECGs and monophasic action potential (MAP) analysis in mice. Moreover, expression of KCNH2 and KCNQ1, the main subunits comprising the pore-forming region for IKr and IKs, was elucidated by PCR.
Methods: Both male and female C57BL/6 mice were used. Castration and oophorectomy were performed at 1 month of age. Standard limb lead ECGs were recorded in a prone position of a heated matte under pentobarbital anaesthesia from these mice during the period 3–12 months of age. MAPs were recorded under urethane anaesthesia at 13 months of age and analyzed with an ECG processor.
Results: There were no effects of castration and oophorectomy on most of the ECG parameters in mice at 3 months of age. QT intervals gradually increased with aging in all groups of mice. QT intervals in mice that had undergone oophorectomy were significantly prolonged compared to other groups of mice. The same tendency was observed in MAP analysis. The expression levels of KCNQ1 in females were higher than those in males. In contrast, expression levels of KCNH2 were almost the same in males and females. Although castration did not alter these expressions, KCNQ1 was decreased and KCNH2 was increased by oophorectomy. These data indicated that ventricular repolarization was altered with aging and sex hormones.
Conclusions: These results suggest that the effects of gender differences and aging on cardiac repolarization may be relevant to expression levels of K channels.

http://dx.doi.org/10.1016/j.jelectrocard.2013.05.076

ECG vs. blood pressure (systolic, diastolic, mean and pulse): an extended approach to baroreflex sensitivity

A.S. Amritpal Singh, B.S.S. Barjinder Singh Saini, G.S.D. Gurmej Singh Dhaliwal
Dr BR Ambedkar National Institute of Technology

Introduction: The cardiac baroreflex is the most important short-term mechanism for controlling blood pressure (BP) by altering the heart rate (HR). The vital role of baroreflex sensitivity (BRS) as a prognostic factor for various cardiovascular diseases is now well established. All measures of BP are strongly and directly related to risk of cardiovascular problems but their relative role in baroreflex control is yet to be fully understood.
Methods: The relative importance of systolic BP (SBP), diastolic BP (DBP), mean arterial pressure (MAP) and pulse pressure (PP) variation on baroreflex control was estimated using a mean coherence and weighted coherence ≥ 0.2 based transfer function approach by choosing BP as input variable and RR interval series derived from ECG as output variable. Correlation between BRS indices obtained using all BP measures was computed. 10 healthy subjects along with 21 subjects from the EuroBavar dataset were used for the analysis.
Results: The number of BRS determinations was more when SBP was used as compared to DBP, MAP and PP. Moreover, BRS indices obtained from RR-SBP were smaller than those obtained by RR-DBP, RR-MAP or RR-PP. In addition, all types of BRS estimates provided larger indices in the supine position than in the standing position. Correlation coefficients between DBP, MAP and PP based BRS estimation with SBP based BRS estimation were found to be 0.708, 0.816 and 0.952 respectively in the low frequency LF region and 0.674, 0.816 and 0.952 in the HF region.
Conclusions: Weighted coherence is a more sensitive measure than mean coherence and is a novel index for quantifying coherence between two related time series such as RR interval and blood pressure. Thus, a weighted coherence criterion provides enhanced coherence values as compared to mean coherence which results in an increased number of BRS responses. It was found that, except for SBP based BRS estimation, all other BRS estimates provided a decreased number of BRS responses especially for patients with an impaired baroreflex.

http://dx.doi.org/10.1016/j.jelectrocard.2013.05.077

Fractal dimension of electrocardiogram: distinguishing healthy and heart-failure patients

H.M.C. Mary, D. Singh
Dr B.R Ambedkar National Institute of Technology, India

Introduction: Determining the complexity of the cardiovascular system is a difficult task since it cannot be split into simpler subsystems without affecting the dynamic properties. The ECG is self-replicating, which means it looks similar at different level of magnification. Hence, the ECG signal is referred to as a fractal signal. Fractal dimension is an index for characterizing fractals and can reveal the complexity of the cardiovascular system.
Methods: Fractal dimension can be obtained using detrended fluctuation analysis (DFA). Since detrended fluctuation analysis is based on random walk theory, the noise level due to imperfect measurement in recording is reduced and it can systematically eliminate trends of different orders.
Results: The ECGs of patients were recorded using a BIOPAC MP100 system. DFA was applied to healthy and heart failure patients and the ranges of fractal dimension were obtained. The fractal dimension for healthy individuals was 1.66 ± 0.02 and for heart failure patients it was 1.9 ± 0.03. This indicates that as the complexity of the signal increases, the fractal dimension increases.
Conclusion: Fractal dimension can reflect changes in adaptability of physiological processes and can lead to successful diagnosis of pathological conditions. Fractal analysis is therefore a promising diagnostic tool in cardiovascular disease diagnosis and evaluation.

http://dx.doi.org/10.1016/j.jelectrocard.2013.05.078

Heart check-ups with pocket size event ECG recorder in citizen's marathon rally

Y.K. Kasamaki, M.O. Ohta, I.W. Watanabe, M.S. Soma, Y.O. Ozawa, M.N. Nagashima, T.N. Nakai, S.K. Kunimoto
Nihon University School of Medicine

Introduction: Participants in a marathon occasionally suffer a sudden death. We have enforced a simple heart examination with a pocket sized ECG

recorder on the day of a marathon to look for ECG abnormalities that might be linked with sudden cardiac death.
Methods: An ECG recording area was installed at the starting point of the Okinawa marathon, the Sapporo marathon and 5 other big rallies in total. Lead I of the ECG was recorded for 32 seconds using the CG2100 pocket sized ECG device in 2,596 runners (1,558 men and 1,038 women: 10–80 years old). An ECG specialist reviewed the ECGs at a later date and classified the ECGs according to the severity of the findings.
Results: ECGs were classified from normal to abnormal (G0–G5) according to the severity of ECG findings, and as GN when noise prevented a diagnosis. The results were G0 2,224 (85.7%), G1 49 (1.9%), G2 113 (4.4%) and G3 7 (0.3%). None was classified as G4 or G5. However, 203 (7.7%) were classified as GN. Therefore, abnormal findings were present in 169/2596 people (6.6%) in this study. The abnormal findings included 16 SVPC, 33 VPC, 19 AF, 1 A-V Block, 7 negative T waves, 50 RBBB, 1 LBBB, 2 WPW syndrome and 9 ST-T abnormalities.
Conclusion: The pocket size ECG recorder is useful for facilitating cardiac screening immediately before the beginning of a marathon.

http://dx.doi.org/10.1016/j.jelectrocard.2013.05.079

Simulation study of ventricular rate control therapy during atrial fibrillation using one-dimensional cable model with two conduction pathways

S. Inada[a], T. Ono[b], N. Shibata[c], M. Iwata[a], R. Haraguchi[a], T. Ashihara[d], A. Abe[e], T. Ikeda[e], K. Mitsui[b], M.R. Boyett[f], H. Dobrzynski[f], K. Nakazawa[a]
[a]*National Cerebral and Cardiovascular Center Research Institute*
[b]*Tokyo Denki University*
[c]*Shinjuku Mitsui Building Clinic*
[d]*Shiga University of Medical Science*
[e]*Toho University Faculty of Medicine*
[f]*University of Manchester*

Introduction: The atrioventricular (AV) node lies between the atria and ventricles and is the only conduction pathway between the upper and lower chambers in a normal heart. During atrial fibrillation (AF), the AV node has an important role in adjusting ventricular rate. In addition, calcium channel blockers, digitalis and beta-blockers are used for controlling the ventricular rate clinically. However, the mechanisms of these drugs on excitation conduction in the AV node have not been clarified. To investigate the effects of drugs on AV nodal conduction, we constructed a mathematical model of the AV node and simulated excitation conduction between the right atrium and the bundle of His.
Methods: Recently, we have developed action potential models for the AV node including atria-nodal, nodal and nodal-His cells of the rabbit. Using these models, we have constructed a one-dimensional model from the right atrium to the bundle of His through the AV node. The model has fast and slow conduction pathways in the AV node. To simulate action potential conduction, stimuli were applied into the atrial string. In addition, the effect of beta-blockers was also simulated.
Results: Because of long refractoriness in the fast pathway, high frequency excitations in the right atrium were partially blocked in the AV node. As a result, the excitation rate in the bundle of His corresponding to that in the ventricle was decreased during AF. The slow pathway acts as subsidiary conduction pathway. When a drug such as a calcium channel blocker was applied to the AV node, the ventricular rate was even further decreased. Although all kinds of drugs used in this study could alter ventricular rate during AF, the mechanisms were different. For example, a calcium channel blocker alters conductivity in a slow pathway and a compact AV node, while a beta-blocker alters refractoriness in the fast pathway.
Conclusions: Our simulations suggest that two conduction pathways play important roles during AF. Furthermore, our model is a useful tool for analysing drug-mediated complex conduction patterns in the AV node.

http://dx.doi.org/10.1016/j.jelectrocard.2013.05.080

Investigation of interrelation between heart rate and blood pressure using wavelet transform coherence

R. Kaur, D. Singh
Dr. B. R. Ambedkar National Institute of Technology, Jalandhar

Introduction: The spontaneous assessment of physiological phenomena can be inferred from the bivariate spectral analysis of the variability in the RR interval (RRI) and systolic blood pressure (SBP). Wavelet transform coherence (WTC) has previously been used for the bivariate analysis of cardiovascular signals due to its potential to offer additional information about the complex functioning of autonomic regulatory mechanisms.
Methods: In the present work, a complex Morlet wavelet with WTC has been used to evaluate wavelet coherence between RRI and SBP signals using the standard Eurobavar dataset.
Results: Wavelet coherence was determined between RRI and SBP in only the LF and HF frequency ranges. In healthy volunteers, high coherence was observed at LF (SBP leading RRI $<90^{o}$) and at HF (with a very small lead of SBP). In hypercholesterolemia patients, high coherence at LF (SBP leading) and almost negligible coherence at HF were seen. In hypertensive patients, low coherence at LF (SBP leading) and significantly high coherence are found at HF (very small lead of RRI). In hypertensive (treated) patients, high coherence at LF (SBP leading) and much less or almost negligible coherence at HF (very small lead of RRI) were seen. In diabetic patients without neuropathy, low coherence at LF (small lead of SBP) and high coherence at HF (almost in-phase) were seen. In diabetic patients with neuropathy, high coherence at LF (RRI leading $<90^{o}$, a case of baroreflex failure) and much less coherence at HF (RRI leading) were found. In heart transplant patients, less coherence at some instants at LF (RRI leading $<90^{o}$, case of baroreflex failure) and much less coherence at HF (RRI leading) were found. In pregnant women, high coherence at LF (SBP leading $< 90^{o}$) and high coherence at HF (small lead of SBP) were noted. In 6/7 outpatients, high coherence at LF (SBP leading $< 90^{o}$) and at HF (small lead of SBP) were seen.
Conclusion: In this study, the WTC using a complex Morlet wavelet was successfully used to analyze the interrelation between RR interval and SBP by providing the magnitude and phase information simultaneously on the wavelet coherence plot.

http://dx.doi.org/10.1016/j.jelectrocard.2013.05.081

Comparative study of the mussel's cardiac activity

B.I.N. Bakhmet Igor
Institute of Biology, Karelian Research Centre, Russian Academy of Science

Introduction: In spite of the relatively simple structure of the mussel's cardiac system, it has rather interesting details. First, it has three chambers – two auricles and one ventricle. Second, recently it was proved that the ultrastructure of the mussel's myocardium is very similar to that of the mammalian. Thus, for comparative investigations, it is very helpful to study the characteristic properties of the mussel's cardiac activity and physiology. For the first step, we decided to estimate the heart rate of the four different species of bivalvia.
Methods: HR was recorded using remote monitoring of cardiac muscle volume (plethysmogram) based on infra red radiation of the heart region and reflected light recording. Optical sensors (CNY-70) were used. A specially developed amplifier with a system of filters and a portable digital oscillograph (Fluke 125) transmitted the signal to a personal computer to be recorded as consecutive heart rate (HR) oscillations which were processed using FlukeView 3.0 software. We investigated HR of four species of Bivalvia – *Mytilus edulis* L., *Hiatella arctica* L., *Modiolus modiolus* L. and *Arctica islandica* L. – under field conditions at moderate and extremely low temperatures (+10.0° and −1.5 °C).
Results: During moderate temperatures, the HR of blue mussels was significantly higher than those of *H. arctica* and *M. modiolus*. The extremely unstable character of cardiac activity in *A. islandica* should be underlined. Moreover, abrupt cardiac arrest lasting 1–9 h was observed in every clam. During the winter season (−1.5 °C), the HR of all species fell up to 5.43; 3.09 and 5.25 beats per min in *H. arctica*, *M. modiolus* and *M. edulis* consequently.
Conclusion: The reason for such original physiology of *A. islandica* is still unclear. Cardiac activity of the other animals is discussed from the point of view of their ecology and growth rate and consequently, level of metabolism.

http://dx.doi.org/10.1016/j.jelectrocard.2013.05.082

Reference intervals of late potentials and association with the autonomic nervous system in healthy subjects using Holter ambulatory electrocardiogram

K. Hashimoto, Y. Kasamaki, Y. Okumura, T. Nakai, S. Kunimoto, T. Hiro, I. Wtanabe, M. Nagashima, T. Nakayama, A. Hirayama, M. Soma
Nihon University School of Medicine

Introduction: It has been reported that late potentials (LP) were useful in detecting malignant arrhythmias and identifying the risk of sudden cardiac death in patients with organic heart disease and idiopathic ventricular fibrillation syndrome. Recently, it has become possible to measure LP throughout 24 hours using a newly developed Holter ambulatory electrocardiogram recorder. However, there are few studies describing reference intervals for LP over a 24 hour period, and little is known about their association with the autonomic nervous system in healthy subjects.
Methods: LP were recorded on 48 normal healthy subjects (men 25, women 23), aged 11–87 years (mean ± SD, 45 ± 7). LP parameters (fQRS, RMS40, LAS40) obtained using Holter ambulatory electrocardiography (Ela medical. Inc.) were measured before and after each meal and going to bed (4 points in daytime and 4 points at other times: total 8 points per 24 hours). We measured the RR interval and analyzed the component of HF, LF/HF for heart rate variability (HRV) at the same time on 24-hour ambulatory ECG.
Results: The normal limits of LP parameters during daytime were:

For men: upper limit (90th percentile) fQRS = 118 ms,
LAS 40 = 41 ms;
lower limit (10th percentile) RMS40 = 20 μV;
For women: upper limit (90th percentile) fQRS = 114 ms,
LAS 40 = 42 ms;
lower limit (10th percentile) RMS40 = 17 μV.
The normal limits of LP parameters at night time were:
For men: upper limits (90th percentile) = fQRS 124 ms,
LAS 40 = 48 ms;
lower limit (10th percentile) RMS40 > 18 μV;
For women : upper limit (90th percentile) = fQRS 126 ms,
LAS 40 = 44 ms;
lower limit (10th percentile) RMS40 = 14 μV.

There was a significant positive correlation between LAS40 and HF (Men: $p < 0.01$, $r = 0.4$ and Women: $p < 0.05$, $r = 0.4$). On the other hand, there was a significant negative correlation between RMS40 and HF (Men: $p < 0.05$. $r = -0.4$ and Women: $p < 0.05$. $r = -0.3$).
Conclusion: In healthy subjects, there was circadian variation in LP which might be augmented by the autonomic nervous system. These factors should be taken into account in setting of reference intervals of LP parameters.

http://dx.doi.org/10.1016/j.jelectrocard.2013.05.083

Dynamics of AV synchronization in patients with paroxysmal AF: role of atrial rate

M. Masè[a], M. Del Greco[b], M. Marini[b], F. Ravelli[a]
[a]*Department of Physics, University of Trento*
[b]*Division of Cardiology, Santa Chiara Hospital*

Introduction: The role of atrial activity in the generation of ventricular rhythm during atrial fibrillation (AF) in humans is poorly understood. To investigate the mechanisms of atrioventricular (AV) conduction in AF patients, we quantified the level of AV synchronization and reconstruct AV response curves at changing atrial rate during the short-term evolution of AF episodes.
Methods: Atrial electrograms and ECG signals were recorded in 10 patients with paroxysmal AF. Statistically significant AV synchronization epochs of *n:m* order (i.e., *n* atrial beats in *m* ventricular cycles) were automatically identified by AV synchrogram analysis, and quantitatively characterized in terms of overall percentage of significantly coupled beats (p_{lb}), maximal length (l_{max}) and conduction ratio ($CR = m/n$) of synchronized epochs. AV response curves were reconstructed in each patient by displaying the identified *CRs* as a function of the corresponding atrial cycle length (*AA*).
Results: Synchrogram analysis revealed the presence of several short-length ($l_{max} = 3.7 \pm 1.6$ s) epochs of AV synchronization in AF, which involved $p_{lb} = 21.5 \pm 8.3\%$ of atrial beats. Atrial rate significantly affected AV conduction, since the spontaneous 13.6 ± 6.0% shortening of atrial cycle length (*AA* = 198.3 ± 24.0 vs 171.0 ± 21.4 ms, $p < 0.001$) in the first minutes of the episodes determined a 20.5 ± 10.0% decrease in AV conduction ratios (*CR* = 0.34 ± 0.09 vs 0.27 ± 0.06, $p < 0.001$). AV response curves revealed a Farey sequence organization of synchronization orders at changing atrial rate, where *(n + N):(m + M)* patterns appeared between *n:m* and *N:M* patterns. This ordering is suggestive of a scaling effect of nodal recovery on atrial beats.
Conclusions: The presence of a significant percentage of atrial beats synchronized with ventricular activity and the dependence of AV response on atrial rate provide evidence for the contribution of atrial activity, filtered by nodal refractoriness, to the generation of ventricular response in AF.

http://dx.doi.org/10.1016/j.jelectrocard.2013.05.084

New ECG index as a marker of poor prognosis in acute pulmonary embolism: ST segment elevation in lead aVR with ST segment depression in lateral leads

P. Kukla[a], Z. Zhan Zhong-qun[b], A. Baranchuk[c], L. Bryniarski[d], E. Mirek-Bryniarska[e], M. Jastrzêbski[d]
[a]*Departament of Cardiology and Internal Diseases, Gorlice, Poland*
[b]*Taihe Hospital Hubei University of Medicine, China*
[c]*Division of Cardiology, Kingston General Hospital, Queen's University, Kingston, Ontario, Canada*
[d]*First Department of Cardiology and Hypertension, University Hospital, Cracow, Poland*
[e]*Department of Cardiology, Dietl Hospital, Cracow, Poland*

Introduction: ST segment elevation in lead aVR (STE-aVR) with ST segment depression in lateral leads (STD-lat) is associated with a poor prognosis in acute coronary syndromes. The aim of the study was determine the prognostic role of STE-aVR with STD-lat in patients with acute pulmonary embolism (APE).
Methods: We analyzed ECG and clinical data of 470 patients (pts) with APE, mean age 65.9 years, male/female: 196/274 and noted 50 (10.6%) cardiac deaths. The new ECG index STE-aVR with STD-lat was observed in 96 (20.8%) patients. By considering the first ECG on admission to hospital and the presence or absence of the ECG index mentioned above, we divided all patients into 2 groups: new ECG index (+) (n = 96 pts) or new ECG index (−) (n = 374 pts).
Results: We analyzed the presence or absence of the new ECG index in the context of complications (cardiac death, cardiac arrest, respirotherapy or catecholamines used) using the hospitalization index. Results are shown in the Table 1.

Table 1

	New ECG index (+)N = 96	New ECG index (−)N = 374	p value
AF	18 (18.7%)	70 (18.7%)	NS
RBBB	19 (19.8%)	39 (10.4%)	0.012
Complications	42 (43.8%)	74 (19.8%)	0.00002
Cardiac death	18 (18.8%)	32 (8.6%)	0.0038
Catecholamines	33 (34.4%)	43 (11.5%)	0.00001
Respirotherapy	20 (20.8%)	20 (5.3%)	0.00001

AF – atrial fibrillation; RBBB – right bundle branch block.

Conclusions: The new ECG index: STE-aVR with STD-lat predicts poor prognosis in patients with APE. Patients with a positive index present a two-fold greater risk of complications, a 2-fold greater risk of cardiac death, a 3-fold greater risk depending on catecholamines used and a 4-fold greater risk of respiratory insufficiency that requires intensive respirotherapy.

http://dx.doi.org/10.1016/j.jelectrocard.2013.05.085

Towards computational modelling of the human foetal electrocardiogram: normal sinus rhythm: AV conduction block and re-entrant tachycardia

A.P. Benson[a], B. Hayes-Gill[b], A.V. Holden[a], E. Pervolaraki[a]
[a]*University of Leeds*
[b]*Univerity of Nottingham*

Introduction: The 10-100 μV foetal electrocardiogram can be recorded from the maternal abdominal surface from ~12 weeks gestational age (WGA), and RR, PR, QR and QT intervals, and T and P wave dispersions extracted. These non-invasive measures provide quantitative information on sino-atrial node pacemaking rate (*via* RR), propagation times and velocities (*via* PR, QT), and ventricular action potential duration and its restitution (QT-RR) during foetal normal sinus rhythm. Arrhythmias are observed in <5% of recordings.

Methods: The parameters of biophysically detailed models of adult human cardiac cell electrophysiology, based on voltage clamp, immune-histochemical and mRNA expression data were modified, informed by data from the literature on animal foetal tissue and cardiomyocytes derived from human stem cell lines, to reproduce human foetal RR and QT intervals. One dimensional partial differential equation models of SAN, atrial, AVN and ventricular tissue, with lengths from MRI and intercellular coupling informed by PR and QR intervals, were constructed for hearts from 15–40 WGA. Numerical solutions, with zero-flux boundary conditions, were by the explicit Euler method with time and space steps $\Delta t = 0.005$ ms and $\Delta x = 0.1$ mm.

Results: The 1D model at 15, 30 WGA gave NSR intervals RR: 400, 450; QR: 200, 280 ms. Spatially uniform progressive reduction of $\{g_{Ca,L}$ and $g_{Ca,T}\}$ slowed the SAN, and led to AV conduction blocks. Self terminating and persistent re-entry with a period of 340–350 ms within a 1-D ring ventricular tissue model.

Conclusion: The preliminary 1-D family of models reproduces the observed timings of fECG intervals from 15–40 WGA, the characteristics of development of foetal AV block, and self terminating ventricular tachycardia.

http://dx.doi.org/10.1016/j.jelectrocard.2013.05.086

T-wave axis deviation and left ventricular hypertrophy interaction in diabetes and hypertension (MOLI SANI Project)

A.D. Assanelli[a], R.L. Rago[b], D.C.A. di Castelnuovo.[b], B.F. Badilini[c], V.M. Vaglio[c], G.F. Gianfagna[b], S.M. Salvetti[d], Z.F. Zito[b], D.M.B. Donati[b], D.G.G. de Gaetano[b], I.L. Iacoviello[b]
[a]*Chair of Internal/Sport Medicine University of Brescia*
[b]*Laboratory of Genetic and Environmental Epidemiology, Research Laboratories, Fondazione di Ricerca e Cura "Giovanni Paolo II"*
[c]*AMPS LLC, New York, NY, USA*
[d]*Chair of Internal/Sport Medicine*

Background: T wave axis deviation (TA) is a known independent predictor of fatal and non fatal events. The mechanisms underlying the relationship with events have not been extensively investigated. The evaluation of TA might be useful to identify asymptomatic patients at increased cardiovascular (CV) risk.

Aim: We aimed at evaluating the prevalence of TA according to the presence or absence of diabetes (DM) and/or hypertension (HT), two conditions characterized by an increased CV risk, in a large sample of the adult general Italian population.

Methods: 10,184 women (54 ± 11 years) and 8,775 men (54 ± 11 years) were analysed from the Moli-sani cohort, a database of randomly recruited healthy adults (age >35) from the general population of Molise, a central region of Italy where standard 12-lead resting ECGs are collected. Subjects with previous AMI, angina, cerebrovascular disease or left bundle brunch block or missing values for TA or LVH were excluded. T-wave axis deviation was measured from the standard 12-lead resting ECG and was defined as the angle of the T wave in the frontal plane as computed by a proprietary algorithm (CalECG/Bravo, AMPS-LLC, NY). LVH was defined as Sokolow Lyon voltage (SLv) >35 mm or Cornell Product (CP) ≥2440 mV * sec.

Results: TA was abnormal in 1.1% of subjects without both HT and DM, in 1.4% in subjects without HT but with DM, in 2.7% of subjects with HT but without DM, in 4.2% of subjects with both HT and DM (Table 1).

Table 1

	N	T-axis deviation	
		Normal or borderline	Abnormal
a) Hypertension NO and Diabetes NO	11504	11379 (98.9%)	125 (1.1%)
b) Hypertension YES and Diabetes NO	5920	5760 (97.3%)	160 (2.7%)
c) Hypertension NO and Diabetes YES	575	567 (98.6%)	8 (1.4%)
d) Hypertension YES and Diabetes YES	960	920 (95.8%)	40 (4.2%)

p for effect of Hypertension (a + c *versus* b + d) <0.0001; p for effect of Diabetes (a + b *versus* c + d) 0.46; p for interaction effect Hypertension * Diabetes p = 0.39.

Conclusion: Our data suggest that T axis deviation, a demonstrated marker of increased CV risk, is associated with the presence of arterial hypertension, may or may not be associated with diabetes, but is not associated with diabetes alone.

http://dx.doi.org/10.1016/j.jelectrocard.2013.05.087

The positive T-wave: insights from a 3D anatomical and electrophysiological model of the rabbit ventricles

S.J. Castro[a], J. Higham[a], R. Sleiman[a], A.V. Holden[b], M.R. Boyett[a], H. Zhang[a]
[a]*University of Manchester*
[b]*University of Leeds*

Introduction: Ionic mechanisms underlying the upright positive T-wave are controversial and incompletely understood. It is believed that the regional difference in the action potential duration (APD) of ventricular cells arising from electrophysiological heterogeneity plays an important role. The aim of this study is to investigate possible contributions of transmural (TM), apico-basal (AB) and interventricular (IV) heterogeneity to the positive T-wave.

Methods: A family of single cell models for rabbit left ventricle (LV) has been developed in our previous study. The model was further modified to incorporate experimental data on transmural heterogeneity in the right ventricles, forming cell models for the right ventricular endocardial and epicardial cells. These single cell models were incorporated into an anatomical model of the rabbit ventricles generated by a DT-MRI scan. In the 3D model, apico-basal heterogeneity was modelled by including gradients of I_{CaL}, I_{Ks} and I_{Kr} as seen experimentally.
Simulations were run for a ventricular wedge preparation, isolated LV and whole ventricles under varying degrees of heterogeneity (using combinations of AB, TM and IV heterogeneity). ECGs were calculated at multiple electrode sites located in three planes orthogonal to the apico-basal axis: i) above the base, ii) round the mid-region and iii) below the apex.

Results: In the wedge preparation, TM heterogeneity is necessary to produce a positive T-wave. In the LV preparation AB and TM heterogeneity both play a role in the positive T-wave, although only AB heterogeneity was capable of producing an upright T-wave by itself. In the whole ventricular preparation, IV heterogeneity significantly increased T-wave amplitude.

Conclusion: Our results show all three types of heterogeneity play a role in T-wave genesis, albeit with TM heterogeneity playing a less significant role.

http://dx.doi.org/10.1016/j.jelectrocard.2013.05.088

Sample entropy is unable to explore spatial and temporal fluctuations in physiologic time series!!

P. Marwaha, R.K.S. Ramesh Kumar Sunkaria
Dr. B R Ambedkar National Institute of Technology, Jalandhar (PB)

Introduction: Non linear methods of heart rate variability (HRV) analysis are becoming more popular. It has been observed that complexity measures quantify the regularity and uncertainty of cardiovascular RR-interval time series. In the present work, sample entropy (SampEn) has been evaluated in healthy normal sinus rhythm (NSR) and congestive heart failure (CHF) groups for different data lengths N and tolerance level r.
Methods: SampEn is used to measure the regularity and uncertainty in a time series. It is the negative natural logarithm of the conditional probability that two sequences similar for m points remain similar for one more point. Here self-matches are excluded while calculating probabilities. The lesser the SampEn, the more regular is the time series. SampEn is applied on RR interval time series derived from 14 NSR and 11 CHF subjects.
Results: SampEn is evaluated for template lengths of m = 2, template matching tolerance r = 0.10, 0.15, 0.20, 0.25, 0.3 of standard deviation of data series and data length N = 1000 to 20000. It is demonstrated that SampEn is small for higher values of tolerance r. Moreover, SampEn in patients with CHF has been observed to be higher than that of NSR for the data length varying from 1000 to 5000. Afterwards, with increase in data length N = 10000 and 20000, both groups overlap each other and it is difficult to distinguish between them.
Conclusion: SampEn exhibits higher complexity for pathologic subjects than for healthy subjects, which is a misleading observation. This may be due to the fact that SampEn does not account for multiple time scales inherent in the physiologic time series, and the hidden spatial and temporal fluctuations remain unexplored. The recently proposed method of multiscale entropy has the potential to overcome these shortcomings.

http://dx.doi.org/10.1016/j.jelectrocard.2013.05.089

Linear-nonlinear heart rate variability analysis and SVM based classification of normal and hypertensive subjects

M.G. Poddar[a], V. Kumar[a], Y.P. Sharma[b]
[a]*Indian Institute of Technology, Roorkee, Uttarakhand, India*
[b]*Post Graduate Institute of Medical Education and Research, Chandigarh, India*

Introduction: The goal of this study is to analyze and compare the heart rate variability (HRV) ontology of normal (NOR) and hypertensive (HTN) subjects using time domain (TD), frequency domain (FD) and nonlinear methods. Thereafter, all features are used to classify findings using a support vector machine (SVM), to identify HTN clearly, which is a major cause of mortality.
Methods: We collected ECG data from 57 NOR and 56 HTN of 5 minutes duration with prior verification of clinical status by a cardiologist. TD features Variance, SDNN, RMSSD, pNN50 were estimated and FD features like Power over the full frequency range, VLF, LF, HF and hence LF/HF were calculated by PSD using FFT (256 data samples, Hann window with 50% overlapping). Nonlinear features SD1 and SD2 of Poincare plots, coefficients of approximate and sample entropy were also estimated. SVM classification was done with initial normalization between 0 and 1, $C \in \{2^{-4},..,2^{15}\}$ and $\gamma \in \{2^{-12},..,2^{5}\}$ using tenfold cross-validation to optimize C and γ values. Data sets of 25 for both NOR and HTN for training and testing were used.
Results: All TD features have higher values in NOR as compared to HTN [(Variance: 1736.2 v. 1117.75), (SDNN: 37.69 v. 30.19), (RMSSD: 31.83 v. 26.36) and (pNN50: 12.0 v. 8.99)], while all FD features have decreased values of HTN in comparison with NOR while only LF/HF is increased as it is a ratio [(Power in VLF in ms^2: 269.36 v. 139.15), (P-LF: 183.93 v. 70.13), (P-HF: 108.37 v. 45.09), (P-Total: 561.66 v. 254.38) and (LF/HF: 2.19 v. 2.54)]. In nonlinear methods, again all measures were lower in HTN than in NOR [(Poincare Plot SD1: 22.99 v. 18.67), (SD2: 51.87 v. 37.39), (ApEn: 1.0885 v. 0.9902) and (SAMPEN: 1.5541 v. 1.5152)]. Using these features, the SVM classifier produced 100% classification accuracy with 100% sensitivity.
Conclusion: The proposed method distinguishes patients with HTN from healthy subjects using HRV analysis and SVM classification; hence it may work as a better predictor for all cause mortality in patients with HTN.

http://dx.doi.org/10.1016/j.jelectrocard.2013.05.090

Ventricular repolarization indices as predictors of fatal arrhythmias in ischemia/reperfusion model

O.G. Bernikova[a], J.E. Azarov[a], K.A. Sedova[b], S.N. Kharin[a], D.N. Shmakov[a]
[a]*Institute of Physiology, Ural Branch, Russian Academy of Sciences, Syktyvkar, Russia*
[b]*Czech Technical University, Kladno, Czech Republic*

Introduction: Dispersion of repolarization has long been recognized as a factor predisposing to reentrant ventricular arrhythmias. Similarly, the duration of repolarization could favor the after depolarization proarrhythmic mechanism. The objective of the study was to assess what repolarization parameters contribute significantly to the genesis of ventricular tachycardia and/or ventricular fibrillation (VT/VF) with the aid of an experimental preparation and multiple regression model.
Methods: The experiments were done in 24 anesthetized domestic cats which underwent a coronary occlusion-reperfusion (30 min–30 min) sequence. A synthetic antioxidant agent echinochrome was given to 10 animals to modify the reperfusion injury and dispersion of repolarization. In each of about 80 intramyocardial leads, the activation time (AT), the end of repolarization time (RT), and the activation-recovery interval (ARI) were determined as was the dV/dt min during QRS, dV/dt max during ST-T, and the time difference between the former and the latter, respectively.
Results: VT/VFs arose in a total of 10 animals at the onset of reperfusion. During an ischemia/reperfusion episode, the VT/VF group of animals demonstrated the greater global ARI and RT dispersion, RTs in nonischemic areas, QRS and Tpeak-Tend interval, and the lower heart rate as compared with the nonVT/VF animals ($p < 0.05$). Transmural dispersion of repolarization did not change in the course of experiment and did not distinguish between VT/VF and nonVT/VF cats.
Conclusion: The multiple regression model showed that global, but not transmural, repolarization dispersion determined the Tpeak-Tend interval which along with the heart rate and QRS could predict VT/VF occurrence. The genesis of VT/VF in this ischemia/reperfusion model could also be independently influenced by the repolarization duration in nonischemic areas.
The study was supported by the Ural Branch of Russian Academy of Sciences (Projects 12-I-4-2059, 12-P-4-1003, 12-C-4-1009).

http://dx.doi.org/10.1016/j.jelectrocard.2013.05.091

ST elevation in high-resolution BSPM measured at stress test to assess myocardial ischemia

M. Kania[a], R. Zaczek[b], H. Zavala-Fernandez[a], D. Janusek[a], G. Opolski[b], R. Maniewski[a]
[a]*Nalecz Institute of Biocybernetics and Biomedical Engineering, Warsaw, Poland*
[b]*Department of Cardiology, Medical University of Warsaw, Poland*

Introduction: The aim of this study was to evaluate the ST segment changes in high-resolution body surface potential maps (HR-BSPM) measured at rest and during an exercise stress test for assessment of myocardial ischemia.
Methods: The study was carried out on a group of 28 patients with coronary artery disease and 15 healthy volunteers. A 67-channel high-resolution electrocardiographic system was used. HR-BSPM was recorded at rest and during supine exercise stress testing using an ergometer. The workload was increased by 25 W every 2 minutes, beginning at 50 W. Wavelet transforms and ICA were applied to reduce noise artifacts in the ECG signals. The integral maps of ST segment were calculated from time averaged two-minute recordings at rest and at maximal workload. Finally, the results obtained for detection of myocardial ischemia were compared with the outcomes of a standard 12-lead ECG stress test with the gold standard being findings at coronary arteriography.
Results: The results of analysis of ST segment depression in HR-BSPM for ischemia detection were in agreement with the findings at coronary arteriography. For some patients, significant changes in the ST segment were observed at stress HR-BSPM but were not visible in the standard 12-lead ECG recorded under the same conditions.

Conclusion: Results suggest that integral maps of ST segment calculated from high-resolution BSPM measured at rest and during exercise test can improve detection of patients with ischemic heart disease in comparison to the standard electrocardiographic stress test examination.

http://dx.doi.org/10.1016/j.jelectrocard.2013.05.092

Detrended fluctuation analysis for measuring heart rate variability during different phases of menstrual cycle in young healthy women

K. Rawal, B.S. Saini, S. Luthra, I. Saini
Dr.B R Ambedkar National Institute of Technology, Jalandhar, India

Introduction: Measuring heart rate variability (HRV) is a way to assess the autonomic nervous control of heart through sympathetic and parasympathetic regulation. The extent to which HRV is influenced by the phases of the menstrual cycle has been a subject of interest. In this work, a nonlinear technique, Detrended Fluctuation Analysis (DFA), has been proposed for assessing the changes in HRV during the menstrual cycle. It is a method for detecting the long range correlations of a signal.

Methods: The algorithm was validated on an HRV dataset acquired using BIOPAC® MP 150 system having a sampling frequency of 500 samples/sec. In this study, the electrocardiogram (ECG) of 20 young healthy women aged 20–30 years were recorded in the supine position for 15 minutes in a laboratory setting during the luteal, menstrual and follicular phases of the menstrual cycle. The RR-intervals were then obtained using a wavelet transform method. The scaling exponent (α) was calculated using DFA for detecting the stress in the menstrual cycle.

Results: Mean values of α during the luteal phase, menstrual phase and follicular phase were 0.77, 0.88 and 0.86 respectively (Table 1). The difference in values of α in these three phases of the menstrual cycle demonstrated that HRV decreases in the luteal phase which leads to more stress as compared to other two phases of the cycle.

Table 1
DFA results during three phases of menstrual cycle.

Menstrual Cycle Phases (20 Subjects)	Scaling Exponent (α)
Luteal Phase	0.77
Menstrual Phase	0.88
Follicular Phase	0.86

Conclusion: The results of this study have confirmed that DFA of HRV is useful in classifying the stress in three phases of menstrual cycle. The DFA parameter alpha (α) had a low scaling exponent value during the luteal phase meaning that the subjects experienced more stress during that phase compared to the menstrual and follicular phases.

http://dx.doi.org/10.1016/j.jelectrocard.2013.05.094

Electro-mechanical modelling of in-vivo human left ventricle

H. Gao[a], B.E. Griffith[b], D. Carrick[c], C. McComb[c], C. Berry[c], X.Y. Luo[a]
[a]*School of Mathematics and Statistics, University of Glasgow, UK*
[b]*Division of Cardiology, Department of Medicine, New York University School of Medicine, USA*
[c]*Institute of Cardiovascular and Medical Science, University of Glasgow, UK*

Introduction: Reliable and accurate computational models of the left ventricle (LV) with multiphysics capabilities are urgently needed for identifying high-risk patients and stratifying therapy. In this study, we have developed subject specific LV models by coupling myocyte contraction and nonlinear biomechanics, and applied them to a healthy volunteer and a patient with a myocardial infarction (MI).

Methods: LV geometries are reconstructed after cardiac magnetic resonance imaging studies. For the patient, the MI is segmented and incorporated into the model with much higher stiffness and no contractility compared to normal myocardium. Myocardial fibres are generated by a rule-based method. A simple model of intracellular calcium dynamics is used to trigger myocardial contraction uniformly, and the active contractile tension T is modelled as a function of time, intracellular calcium concentration, sarcomere length (SL) and the maximum isometric tension (T_{ref}) at the resting SL. T_{ref} is optimized by matching the measured *in-vivo* end-systolic volume with a systolic pressure loading inside the LV.

Results: Both the healthy and diseased LV models are able to simulate the LV dynamics from end diastole to end systole, and the deformed LV geometries agree well with the MRI measurement. The maximum isometric tension T_{ref} is found to be nearly doubled in the LV with MI (309 kPa) compared to the healthy LV (169 kPa), in order to compensate the reduced contractility in the MI region. However, the active contracting force T at end systole increases only moderately in the normal myocardium in the infarcted LV (87.9 kPa) compared to the force in the same area of the healthy LV (79.7 kPa). This may be associated with adverse remodelling, which may lead to heart failure in the longer term.

Conclusion: The developed LV model is capable of electro-mechanical simulation of *in-vivo* LV dynamics, and is able to characterize subject specific parameters, such as T_{ref}. Further validations are needed.

http://dx.doi.org/10.1016/j.jelectrocard.2013.05.095

QT/RR dynamic coupling in LQT syndrome patients

P.L. Pavel Leinveber[a], J.H. Josef Halamek[b], J.P.C. Jean-Phillipe Couderc[c], P.J. Pavel Jurak[b], V.V. Vlastimil Vondra[b]
[a]*St. Anne's University Hospital, ICRC, Brno, Czech Republic*
[b]*Institute of Scientific Instruments, AS CR, Brno, Czech republic*
[c]*Center for Quantitative Electrocardiography and Cardiac Safety, University of Rochester Medical Center, Rochester, NY, USA*

Introduction: The long QT syndrome patients are susceptible to life-threatening arrhythmias triggered by sudden change of RR interval. Their QT interval reacts abnormally. The description of the dynamic QT/RR coupling in genotyped LQT patients has not been thoroughly investigated.

Methods: We propose an analysis of the static and dynamic QT/RR coupling based on ambulatory Holter recordings. Three parameters are used to characterize the QT/RR coupling: the gain for fast (GainF) and slow RR variability (GainL), and the time constant of QT adaptation (τ). These parameters have a physiological significance. We investigated the values of these parameters across genders, and in genotyped LQT-1 and 2 patients.

Results: QT/RR parameters are statistically significant and genetically dependent (gender, LQT genotype) over the data. Women have steeper GainL (0.17 vs. 0.19 $p < 0.01$) and faster adaptation τ (186 vs. 156, $p < 0.05$) than men. LQT1 patients have steeper GainL (0.22) and GainF (0.05) and faster adaptation (122), all $p < 0.001$, than controls. LQT2 patients have even steeper GainL (0.25, $p < 0.05$) than LQT1, while τ is similar (193) to that in healthy subjects.

Conclusion: Genetic dependence of QT parameters together with modelling of QT behavior in response to sudden change of RR may explain the higher prevalence of arrhythmias in women and LQT subjects, even in subjects with similar values of QTc. The parameters presented may also be used to eliminate QT/RR hysteresis and to predict QT behaviour in any sudden change of RR or enable analysis of QT irregularity hidden behind the dynamic QT/RR coupling. We presume that the dynamic description of QT/RR coupling will contribute to understanding of abrupt induction of life threatening arrhythmias during physical and psychological stress. This technique may also find an application in stratification of patients with risk of sudden cardiac death and in testing of pro-arrhythmogenic effects of drugs.

http://dx.doi.org/10.1016/j.jelectrocard.2013.05.096

IKr blocker dofetilide promotes Ashman phenomenon in patients with atrial fibrillation

M.R. Sardar, A. Khaji, R. Ju, C. Patel, J. Bradley
Lankenau Medical Center

Introduction: The Ashman phenomenon is aberrant ventricular conduction that often occurs during a short-long-short R-R interval in patients

with atrial fibrillation. The aberrant conduction is caused by prolongation of the refractory period of the ventricular conducting system and myocardium due to a long R-R interval of a preceding beat. Dofetilide, an I_{Kr} blocker, exhibits a strong reverse use-dependence effect on prolonging the refractory period. We investigated effects of dofetilide on the Ashman Phenomenon.

Methods: 10 consecutive patients (age: 67 ± 7, males: 5) with atrial fibrillation who were admitted for dofetilide loading (250 to 500 micrograms q12h) were investigated.

Results: Dofetilide significantly prolonged the QTc intervals from baseline 434 ± 24 ms to 480 ± 25 ms after a second dose ($p < 0.01$), accompanied by an increase in the longest RR interval at which Ashman beats occurred. The total number of Ashman beats increased from 42 ± 24 at baseline to 93 ± 79 after the 1st dose ($p < 0.05$) and 133 ± 101 after the 2nd dose ($p < 0.05$) during the 6 hour time period following each dose. Episodes of consecutive Ashman beats (≥3), which are often misinterpreted as non-sustained ventricular tachycardia, significantly increased from 1 ± 2 pre-dofetilide to 3 ± 3 post-dofetilide. An abrupt increase in Ashman beats in one patient was associated with the development of Torsades de Pointes post DC cardioversion. Interestingly, change of atrial fibrillation to atrial flutter led to a reduction in Ashman beats probably related to relative regularization of ventricular rates.

Conclusions: Pure I_{Kr} blockade promotes the Ashman phenomenon during atrial fibrillation likely via reverse use-dependent prolongation of the ventricular refractory period.

http://dx.doi.org/10.1016/j.jelectrocard.2013.05.097

Novel ECG criteria for the diagnosis of arrhythmogenic right ventricular cardiomyopathy

V.N. Batchvarov[a], R. Bastiaenen[a], P. Macfarlane[b], E. Clark[b], E.R. Behr[a]
[a]*St. George's University of London*
[b]*University of Glasgow, Scotland*

Introduction: In order to improve the electrocardiographic (ECG) diagnosis of arrhythmogenic right ventricular cardiomyopathy (ARVC), we evaluated novel parameters of the terminal QRS complex and the value of bipolar chest leads with a negative left foot electrode (CF leads) computed from the standard 12 leads.

Methods: We analysed digital 12-lead ECGs in 44 patients with ARVC (44 ± 15 years, 73% men) and 276 healthy subjects (32 ± 12 years, 50% men), 44 of them age and sex-matched with patients. The duration (DS_{V1} to DS_{V3}), length (LS_{V1} to LS_{V3}) and area (AS_{V1} to AS_{V3}) of the terminal S wave in leads V1 to V3 were measured automatically. The presence of T wave negativity as a major or minor diagnostic sign of ARVC was assessed in V1 to V6 and in the CF leads computed from the standard 12 leads.

Results: DS_{V1}, DS_{V2} and DS_{V3} were longer ($p < 0.0001$), LS_{V1} and LS_{V2} were shorter ($p = 0.001$) and AS_{V1} was smaller ($p = 0.006$) in ARVC patients without RBBB compared to controls. In ARVC patients, T wave negativity as a major or minor diagnostic sign was more common in the CF leads than in the unipolar precordial leads (77% vs 58%, $p = 0.008$). In healthy controls ($n = 273$, excluding 3 subjects aged 16 years or younger), T wave negativity in leads CF1 and CF2 was more common than in V1 and V2 (3.7% vs 1.1%, $p = 0.016$) whereas T wave negativity beyond leads V2 or CF2 was equally rare (0.7%). The negative T waves in the CF leads had generally different morphology in ARVC patients compared to healthy controls. A composite parameter including the terminal S wave duration and length in V1 and V2 and diagnostic T wave negativity in the CF leads separated ARVC patients from controls (both groups without RBBB) with 92% sensitivity and 90% specificity.

Conclusions: The automatically measured terminal S wave duration and length in V1 and V2 are useful for the diagnosis of ARVC. The CF leads are diagnostically more sensitive and practically equally specific compared to the unipolar precordial leads.

http://dx.doi.org/10.1016/j.jelectrocard.2013.05.098

Improved EASI ECG model as a result of using various regression and machine learning techniques

W. Oleksy, E. Tkacz, Z. Budzianowski
Silesian University of Technology

Introduction: In 1988, Dower and his team introduced the 5 electrode EASI lead system, which can be used for continuous electrocardiogram (ECG) monitoring as an alternative to both the commonly used 5-electrode lead bedside monitoring system and the traditional 10-electrode Mason-Likar 12-lead ECG system. The 12 lead ECG derived from the EASI system was proven to have a high correlation with the standard 12 lead ECG. In addition, it is less susceptible to artifacts and waveform interference, it increases mobility and comfort of patients and it is also easier and faster to use because of the smaller number of electrodes used.

Methods: Our work was focused on improving the Dower transformation from 3 to 12 leads by using some regression and machine learning techniques to obtain a new EASI model and as a result, improve the EASI method. Linear Regression, Artificial Neural Networks, Support Vector Regression, Pace Regression, Least Median of Squares Regression, Gradient Boosting and Isotonic Regression methods were used to create a better model.

Results: The new model obtained was compared with the Dower model and an improved model created by Feild, Feldman and Horacek. To determine the performance of all models, the correlation coefficient, root mean square error (RMSE) and mean absolute error (MAE) were calculated for each of them. Each model calculation was 10 fold cross validated. All results are based on data from the PhysioNet database and from data that were artificially generated.

Table 1
RMSE comparison for all 12-leads.

	aVF	aVL	aVR	I	II	III	V1	V2	V3	V4	V5	V6
New model	27.45	22.02	16.03	18.01	26.13	31.41	21.01	40.54	46.62	55.60	24.66	10.77
Dower model	28.41	35.45	31.86	40.75	32.57	37.19	99.24	177.75	120.25	144.60	119.93	93.17
Other test model	66.29	34.22	55.30	42.47	78.20	60.03	86.42	119.61	141.69	129.96	49.90	33.10

Conclusion: Regression techniques and machine learning algorithms help to improve the basic EASI method. The newly obtained model in linear form could easily be applied in a new hardware device.

http://dx.doi.org/10.1016/j.jelectrocard.2013.05.100

Patient specific modelling of atrial fibrosis and conduction

R. Morgan, K. Rhode, O. Aslanidi
Kings College London

Introduction: Experimental evidence suggests that areas of fibrosis in the atria can cause disturbances to the electrical excitation waves, potentially leading to arrhythmogenic re-entrant waves. Current ablation treatments cauterise large damaged areas of the atria, based on statistical data. Patient specific areas of atrial fibrosis may be used to model the resultant conduction abnormalities, and guide more accurate interventions.

Methods: Patient specific atrial geometry is reconstructed from clinical MRI images. The MRI signal of the blood volume within the atria is dilated to reconstruct appropriate wall thickness. Such a dilation is specific to regions of the atrial wall (its thickness can also be obtained from MRI), resulting in a realistic reconstruction of the 3D atrial geometry. This is then combined with manually segmented pre-ablation fibrosis MRI data. Using modified Courtemanche et al. (1998) and MacCannell et al. (2007) equations to simulate the electrophysiology of the atrial myocytes and fibroblasts respectively, wave conduction through the atrial tissue was simulated. Variation of the number of fibroblasts coupled to each myocyte allows for different levels of fibrosis.

Results: Simulations show up to 20% decrease in wave propagation velocity in areas of fibrosis (compared to healthy atrial tissue), depending on the number of fibroblasts (0–10) coupled to myocytes. This can be explained by different electrophysiological properties of the fibroblasts that are non-excitable, but have a resting potential of about −50 mV. Electrotonic load from the fibroblasts alters the action potential properties of the coupled myocytes, slowing down the conduction.

Conclusion: The model developed combines patient specific atrial geometry and distribution of fibrosis with detailed electrophysiological

modelling, and can be used for studying the effect of fibrosis on atrial conduction in health and disease.

http://dx.doi.org/10.1016/j.jelectrocard.2013.05.101

Application of higher order spectra for estimation of rehabilitation progress in case of patients suffering from ischemic brain stroke

W. Oleksy[a], E. Tkacz[a], I. Provaznik[b]
[a]*Silesian University of Technology*
[b]*Brno University of Technology*

Introduction: This study aimed to estimate the progress of rehabilitation in patients after an ischemic brain stroke (IBS). The classic approach utilizes the EEG and different signal processing tools for analysis and classification of patients. In this paper, a totally different, indirect approach is considered. Instead of using the EEG, the relatively easier to acquire heart rate variability signal (HRV) is applied. Furthermore, a classic analysis method like power spectral estimation is replaced with the use of the second order statistics and calculation of both bispectrum and bicoherence.
Methods: There were 21 patients in whom an IBS was diagnosed. Each patient had a Holter ECG recorded during the first, tenth and sixtieth day after the IBS. For 5 patients, the last recording was not performed due to the death of the patient. Finally, a database consisting of 16 patients was created. All signals in the database were analyzed using higher-order polyspectra. Such a method has been chosen to avoid losing the information about phase which is the important limitation of signal analysis based only on the power spectrum. The bispectra have been computed using a direct (FFT-based) estimation method implemented in Matlab's Higher-Order Spectral Analysis Toolbox.
Results: From the results obtained, it appears that, on the basis of the most irregular shape of the acquired bispectra, the critical moment in the rehabilitation procedure appeared somewhere around the tenth day after the IBS. Calculating the simple power spectrum density (PSD) of the HRV signals does not produce such a result as PSD loses phase information which is probably important from the interpretation point of view.
Conclusion: Preliminary results appear promising, suggesting that the method merits further investigation.

http://dx.doi.org/10.1016/j.jelectrocard.2013.05.102

Improved averaging of multi-lead ECGs and electrograms

B. Erem[a], R. Martinez Orellana[a], P. Stovicek[b], D.H. Brooks[a], R.S. MacLeod[c]
[a]*Northeastern University*
[b]*Charles University Hospital*
[c]*University of Utah*

Introduction: Averaging is a ubiquitous technique for improving electrocardiographic signal quality in both clinical and research environments. Standard methods depend heavily on accurate time alignment, sometimes difficult to achieve. Moreover, changes in phase timing can decrease averaging fidelity. We propose a new averaging method for multi−electrode heart and body surface signals that allows local timing variability and does not require time alignment.
Methods: We treat each multi−lead snapshot in time as a spatial pattern, and thus signals as a sequence of patterns. Where the standard method averages spatial patterns at equivalent sequence times, our method groups spatial patterns based on spatial similarity of the patterns themselves, averaging across similar patterns, thus allowing time warping across individual measured beats.
Results: Experiments were conducted on ECGs recorded from 120 leads on the body surface during pacing on the LV and RV endocardial surfaces with an ablation catheter. We time-aligned ECGs by pacing times and averaged with both our method and the standard method. We found that the timing variability during QRS can adversely affect the results of the standard method, whereas our results were less affected. We will show this timing variability and differences between averages with body surface potential maps. We also undertook experiments with ECGSIM-synthesized 12-lead ECGs. Random phase shifts were used to simulate time-alignment errors and pseudo-random noise was added for measurement errors. We measured the performance of the averaging methods by comparing them to the original signals, and found that our method results in better signal-to-noise ratio.
Conclusions: The proposed averaging method can reduce alignment and phase variability errors in averaging by optimally time-warping to match similar spatial patterns. The method also works on standard 12−lead ECGs.

http://dx.doi.org/10.1016/j.jelectrocard.2013.05.103

Noninvasive reconstruction of potentials on endocardial surface from body surface potentials and CT imaging of partial torso

B. Erem[a], J. Coll Font[a], R. Martinez Orellana[a], P. Stovicek[b], D.H. Brooks[a], R.S. MacLeod[c]
[a]*Northeastern University*
[b]*Charles University Hospital*
[c]*University of Utah*

Introduction: We illustrate reconstruction of epicardial and endocardial potentials from body surface measurements and CT images of the cardiac region only. Standard methods cannot reconstruct endocardial potentials during activation and require full torso imaging.
Methods: Prior to a pace mapping procedure, limited axial X-Ray CT images of the volume containing the subject's heart were acquired. The images were used to fit a generic torso surface, extract the shape of a subject-specific joint epicardial-endocardial ventricular surface, and then construct a mathematical forward model relating heart to body surface potentials. Pacing locations were recorded using the CARTO system. Body surface potentials were recorded from 120 torso electrodes. QRS complexes of beats from the same pacing train were averaged using a novel time invariant spatial averaging technique, and supplied as input to an inverse reconstruction algorithm employing a novel transmural regularization constraint.
Results: The procedure was carried out for a total of 22 pacing locations on the left and right ventricles. Reconstructed potentials were related to the expected propagation of activation wavefronts from pacing locations. We obtained isopotential maps of the reconstructed potentials on the endocardial and epicardial surfaces as well as activation maps from reconstructed potentials, which were used to identify pacing locations and determine the mean and standard deviations of localization errors.
Conclusions: Using only partial CT imaging, noninvasive reconstructions of the electric potentials on endocardial and epicardial ventricular surfaces may be feasible when using combined novel averaging and regularization algorithms.

http://dx.doi.org/10.1016/j.jelectrocard.2013.05.104

Electrocardiographic source estimation in patients with acute myocardial ischemia

T. Konttila, V. Mäntynen, M. Stenroos
Aalto University, Department of Biomedical Engineering and Computational Science

Introduction: The first method used for detecting ischemia is often the ECG. The 12-lead ECG is robust for detecting acute ischemia caused by occlusion of the LAD artery, but its sensitivity to RCA and LCx artery occlusions is worse. Additional leads have been shown to increase the sensitivity to ischemia, but the interpretation of such measurements requires an expert clinician.
In our prior work, we have introduced approximate methods for estimating and visualizing the cardiac source or potential distribution during acute myocardial ischemia. The purpose of these methods is to robustly visualize ischemia with freely selectable electrode-locations even if patient-specific geometries are not available. In this study, we apply these methods to measured and simulated body surface potential mappings (BSPMs) of ischemia.
Methods: We used the Helsinki boundary element method library for forward modelling, and minimum-norm estimation (MNE) and minimum-variance beamforming for inverse computations. We first simulated ischemia in each main artery with ECGSIM software. We then computed inverse solutions of simulations and compared the results to the inverse solutions of

measurements during balloon angioplasty. All measurements were done with 123-lead BSPM, and we analysed 10 ST segments from each patient.
Results: Beamformer works only for small sources, while MNE excels in reconstructing the extent of ischemia. MNE cannot distinguish between sources on endocardial and epicardial surfaces, but the source surface can be estimated by the direction of the reconstructed sources. Transmural ischemia may show as a positive area surrounded by a negative area if the ischemia near the endocardial surface is larger.
Conclusions: From our reconstructions of ischemia measurements and simulations, MNE appears to be usable for reconstructing the ST-segment changes caused by ischemic myocardium.

http://dx.doi.org/10.1016/j.jelectrocard.2013.05.105

Considering gender differences for cardiac safety
C.L. Green[a], C.E. Garnette[b], A. Parekh[b], P. Kligfield[c]
[a]Duke University Medical Center
[b]Food and Drug Administration
[c]Weill Cornell Medical College

Introduction: Gender differences in QT interval duration have been noted since Bazett's initial description during the 1920s. Even though differences are known to exist, most thorough QT (TQT) studies conducted in healthy volunteers are pooled across gender, ignoring possible differences in baseline measures and heart rate correction methods. To increase our understanding of gender differences affecting the performance of TQT studies, we aimed to quantify gender differences in QT behaviour, including the baseline normal range and gender-specific responses to moxifloxacin, and to compare the effective utility of different heart rate corrections for QT by gender and gender differences at baseline, including variability and determination.
Methods: ECG interval data available from the Cardiac Safety Research Consortium (CSRC) ECG Data Warehouse were used for this project. RR and QT were evaluated using pooled data from the CSRC sponsor-reported ECG database, and where available, from automated re-analyses of the TQT datasets. The QT interval was corrected for heart rate by Fridericia's, Bazett's, Sagie's, Hodges', Individual and a Population (overall and by gender) correction formulae (QTcF, QTcB, QTcS, QTcH, QTcI and QTcP, respectively).
Results: QT interval gender differences, including heart rate correction methods and baseline variability, were detected suggesting that gender should be considered during evaluation of new drugs. Known gender-specific differences, including non-drug normal ranges and response to moxifloxacin were confirmed.
Conclusions: The results could advance public health and further the mission of the CSRC by providing definitive gender-specific differences in QT behaviour and recommendations for considering these differences in future TQT studies, resulting in more accurate analyses and ultimately, drugs shown to be safe in both men and women.

http://dx.doi.org/10.1016/j.jelectrocard.2013.05.106

F wave analysis using magnetocardiography in the patient who has a long-standing persistent atrial fibrillation
D. Kim
Seoul Veterans Hospital

Introduction: Atrial fibrillation (AF) is known as an irregular electrical activity in the atrial wall. The maze procedure for blocking macro-nodular re-entry and EP ablation for lesion sets (such as complex fractionated atrial electrograms, pulmonary vein (PV) or non PV foci) shows clinical success respectively. If the F wave activity has some regularity in its characteristics, it could be used for successful treatment. We introduced magnetocardiography (MCG), which is a non-contact and more sensitive method for detecting atrial F-waves than conventional ECGs. In the patient who has a long standing persistent AF, we analysed and now report F wave characteristics using the MCG method.
Methods: We utilized a highly sensitive, low-Tc, 64-channel MCG system and recorded data in the supine position for about 5 minutes (30 seconds a session, several sessions) at pre and postoperative periods of AF surgery. From the MCG registry data, F waves were selected from the period between the T wave and the next R wave. We calculated and clustered the distance of the F wave source origin from selected channel, the intensity of each F wave and the time interval between consecutive F waves for determining the regularity of AF.
Results: From the 10s 64-channel MCG data registry, there were 56 F waves and 12 R waves detected. After removing overlaps from QRST activity, 32 F waves remained. There were three frequent distances detected as clusters from the distance calculation, and their mean distances were 19.7 mm in 9 F waves (28%), 33.1 mm in 7 (22%) and 9.7 mm in 3 (9%), respectively. In intensity, three frequent amplitudes are detected as clusters within 10% ranges, such as 0.216 ± 0.007 V in 10 waves (31%), 0.163 ± 0.005 V in 8 waves (25%) and 0.132 ± 0.001 V in 3 waves (6%). Among the 19 time intervals between 31 consecutive F waves (two consecutive waves in 5 pairs, three consecutive waves in 4 series, and four and five consecutive waves in each, respectively), 17 intervals (89%) were clustered within 10% ranges of time interval, having a mean value of 0.173 ± 0.015 seconds. They showed overall 59% clustering in distance and 62% in intensity.
Conclusion: Using MCG F wave analysis, we found some regularities of distance from source, intensity and time interval of F waves in terms of clustering.

http://dx.doi.org/10.1016/j.jelectrocard.2013.05.107

Topical diagnosis of polymorphic ventricular arrhythmias by noninvasive electrocardiographic imaging
M.P. Chmelevsky, S.V. Zubarev, T.V. Treshkur, D.S. Lebedev
Almazov Federal Heart, Blood and Endocrinology Centre

Introduction: The aim of the study was to determine localization of polymorphic ventricular arrhythmias (PVA) using noninvasive electrocardiographic imaging.
Methods: Three patients according to Holter ECG monitoring revealed PVA (3 to 5 ventricular ectopic morphologies; from 1,500 to 19,000 per day). All patients underwent topical diagnosis of PVA prior to radiofrequency catheter ablation (RFCA) with an Amycard 01C System for noninvasive electrophysiological studies. Afterwards, RFCA of ectopic foci was performed using a Carto 3 electrophysiological navigation system.
Results: Based on preoperative noninvasive mapping of 2 patients with 4 PVA morphologies, only two foci for VA were revealed. The first (dominant) was in the front wall of the outflow tract of the right ventricle and the second was in the posterior-basal area of the left ventricle. One patient with 5 morphologies was identified with one VA focus in the anterior-septal area of the right ventricle with small fluctuations in its position depending on PVA shape. When comparing these data with the results of intraoperative mapping during RFA, coincidence of localization centres of ventricular ectopy was obtained.
Conclusions: Coincidence of results from noninvasive and intraoperative mapping allows us to hope that even at the preoperative stage in patients with PVA, the real number of foci can be established. A theoretical explanation for the coincidence of foci with different types of PVA on the ECG requires further research.

http://dx.doi.org/10.1016/j.jelectrocard.2013.05.108

CT angiography identifies coronary venous anomaly resulting in successful ablation of an epicardial pathway
P.C.D. Dorostkar, H.R. Roukoz, C.W.S. Shepard
University of Minnesota
Introduction: Several congenital anomalies have been associated with a predisposition to specific tachycardias. Difficult accessory pathways have been associated with Ebstein's anomaly, L-Transposition of the great arteries, and especially venous anomalies of the coronary sinus.
Methods: We describe a case where CT angiography defined detailed coronary sinus anatomy that was not noted by echocardiography, supporting successful repeat ablation of a middle cardiac vein accessory pathway in a 10 year old boy. ECG-gated, breath-hold Flash CT angiography of the chest was performed with 80 kV care dosing to reduce patient radiation exposure. Images underwent post-processing on a Voxar 3D visualization system.
Results: We report the case of a 10 year old boy with Wolff-Parkinson-White syndrome and supraventricular tachycardia and failed ablation 2 years prior. The surface ECG was suggestive of an epicardial postero-septal accessory

pathway. A CT angiogram was done to screen for coronary sinus anomalies. It showed ectasia of the proximal segment of the middle cardiac vein that was not noted by echocardiography. The pathway was then easily located at the proximal part of the ectatic segment and successfully ablated.
Conclusions: CT angiography of the heart can delineate and define anatomical structures and associated anomalies that support tachycardia in the young. This diagnostic test can be used as an adjunct for planning, reconstruction and subsequent successful ablation of the substrate(s) that support tachycardia in patients with congenital heart disease.

http://dx.doi.org/10.1016/j.jelectrocard.2013.05.109

Association between endomyocardial tissue biopsies and right ventricular conduction delays

D. Pickham[a], K. Hickey[b], L. Doering[c], B. Chen[c], C. Castillo[b], B. Drew[a]
[a]*University of California, San Francisco*
[b]*Columbia University*
[c]*University of California, Los Angeles*

Introduction: Repeated cardiac catheterization with endomyocardial tissue biopsies of right ventricular myocardium is routinely used to monitor for cellular rejection after heart transplantation. The aim of our study was to determine whether there is an association between endomyocardial tissue biopsy and ventricular conduction abnormalities in the first year following transplant surgery.
Methods: A single reviewer blinded to outcome analyzed serial standard 12-lead ECG data for adults (n = 43) after hospital discharge following heart transplant at two institutions. Digital ECGs (n = 207, = 5/pt) were manually interpreted with onscreen magnification. Biopsy data were abstracted directly from cardiac catheterization reports.
Results: Forty-three patients had both ECG and biopsy data (72% men). Mean age was 50 (±13) years and varied by sex (M, 54 years vs F, 41 years, $p = .002$). In all, 338 biopsy procedures (= 8/pt, range 1–12) were performed, extracting 1319 tissue samples (= 30/pt, range 2–49); these did not vary by sex ($p = .366$ and $p = .136$, respectively). Evidence of mild allograft rejection (International Society for Heart Lung Transplant Grade 1R) was present in 26% of all biopsies, involving 67% of patients. Evidence of right ventricular conduction delay was present in 53% of ECGs, involving 27 (63%) patients: 2 patients with new onset RBBB and 4 with variable right ventricular conduction delays. Patients with 8 or more biopsy procedures were associated with an increase in right ventricular conduction delays (Fisher's exact $p = .026$); however, the number of tissue samples were not significantly associated ($t = -1.4$, $p = .14$). A biopsy burden score (# procedures × # tissue samples) dichotomized at 200 was associated with more right ventricular conduction delays (Fisher's exact $p = .011$).
Conclusions: Right ventricular abnormalities are common in heart transplant recipients undergoing frequent endomyocardial tissue biopsies. A biopsy procedure burden score >200 is associated with higher prevalence of right ventricular conduction delays. More data are needed to determine any causal relationship between endomyocardial tissue biopsy and right ventricular conduction delays and to determine whether there is progression of blocks that require pacemaker therapy.

http://dx.doi.org/10.1016/j.jelectrocard.2013.05.110

P wave in healthy Nigerians using automated analysis

I. Katibi[a], P. Macfarlane[b], E. Clark[b], B. Devine[b], S. Lloyd[b], S. Latif[b], M.A. Araoye[a], A.B.O. Omotoso[a], P.M. Kolo[a], O.S. Aiyedun[a], W. Olaofin[a]
[a]*University of Ilorin, Nigeria*
[b]*University of Glasgow, Scotland*

Introduction: The P wave of the normal ECG has been well studied for several racial groups except indigenous Black Africans. All previously reported ECG studies among Nigerians have been through manual rather than automated analysis.
Methods: 12 lead ECGs were recorded using a Burdick Atria 6100 electrocardiograph in and around Ilorin, Nigeria. Apparently healthy volunteers were recruited from the University of Ilorin and from surrounding villages. Each was medically examined by a physician and a detailed medical history obtained. Data were gathered locally on a PC and sent to the University of Glasgow for further analysis. ECGs were reviewed to exclude any that were technically unsatisfactory and others that had an unexpected abnormality. The ECG measurements underwent statistical analysis using SAS v9.1. Plots and summary statistics were used to assess, informally, the relationship of P amplitude with age and sex. Regression techniques addressed formal relationships. Normal ranges were established by splitting the data into age-sex subgroups and by calculating the 96th percentile range within each subgroup.
Results: The study included 782 males and 479 females, all apparently healthy, with a relatively even spread of ages between 20 and 87 years. A single upright P wave is the commonest type and is mostly seen in lead II (96.0%). A single inverted P wave is seen in lead aVR. A biphasic P wave with initial upright component is seen in lead V1 (60.9%) mostly. A biphasic P wave with initial inverted component is another variety which was very uncommon in this study (0.2%). The upper limits of P wave amplitude varied with gender, ECG lead and age. They were also slightly higher than earlier reported upper limits of normal in the same population and indeed, British and Chinese populations. Age and gender trends in P wave duration were not statistically significant.
Conclusion: This is the first large study of automated ECG recording in healthy Blacks living in West Africa. The findings reported here contrast somewhat to those seen in Caucasians, thereby requiring further evaluation.

http://dx.doi.org/10.1016/j.jelectrocard.2013.05.111

12-lead ECG analysis based on composite lead signal

A. Dohare[a], V. Kumar[a], R. Kumar[b]
[a]*Indian Institute of Technology, Roorkee, Uttrakhand, India*
[b]*Rajendra Institute of Medical Science, Ranchi, Jharkhand, India*

Introduction: Cardiologists diagnose heart disorders by interpreting ECG recordings on the basis of their knowledge and expertise. In the present work, an enhanced composite ECG lead signal (generated by preprocessing all the 12 individual leads) is used for detection and marking of all ECG wave components. The analysis was carried out on the original and artificial cases of CSE data sets, 3 and 4.
Methods: The morphology of the composite lead signal consists of all ECG components such as P, QRS and T wave. The ECG components in the composite lead signal are noise free and enhanced in comparison to all of the individual 12 leads. The calculation of the composite lead ECG is carried out in two steps. In step 1, preprocessing is carried out for removing base line wander

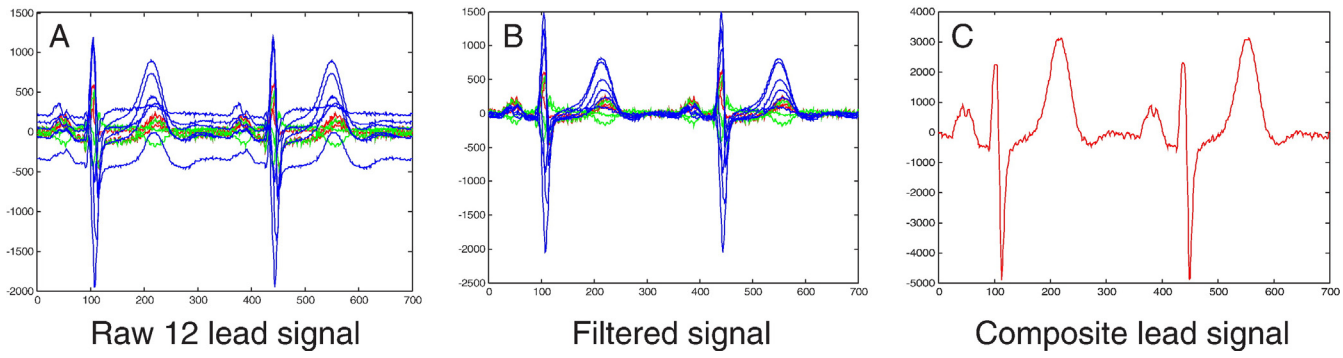

using a median filter in two stages (window '*fs/2*' in the first stage and window '*fs*' in the second stage). In the second step, all the 12 preprocessed leads are added to generate a noise free and enhanced composite ECG lead as shown in the figure. In the present work, a composite lead has been used for detection of the QRS complex and the usual fiducial points using the CSE datasets 3 and 4 (for detection) and CSE dataset 3 (for marking).

Results: The proposed composite lead signal yields a QRS detection sensitivity of 99.92% and a positive predictive value of 99.87% on CSE datasets 3 and 4. The boundary marking using the composite lead in comparison with the original and artificial cases of CSE data set 3 is in agreement with referee markings.

Conclusion: The ECG wave complexes in the composite lead are noise free and enhanced in comparison to all 12 individual leads. The proposed composite lead yields a higher sensitivity and positive predictive value on standard benchmark datasets which indicate its usefulness for identifying various ECG wave components and for rhythm analysis in a clinical environment in order to assist cardiologists.

http://dx.doi.org/10.1016/j.jelectrocard.2013.05.112

Diagnosis of intraventricular conduction disturbances with BSPM using band patterns

M. Sobieszczanska[a], D. Polak-Jonkisz[b], H. Filipowski[a], L. Rusiecki[a], A. Janocha[c], K. Laszki-Szczachor[a]
[a]*Department of Pathophysiology, Wroclaw Medical University*
[b]*Department of Pediatric Nephrology, Wroclaw Medical University*
[c]*Department of Physiology, Wroclaw Medical University*

Introduction: Isochrones (VAT) maps are used for assessing intraventricular activation. Here, VAT maps-based patterns of colorful bands for easy recognition of bundle branch blocks (BBB) are presented.

Methods: The study group consisted of 57 patients (60 ± 11.6 years) with various BBB diagnosed by ECG. There was also a control group of 31 normal subjects (age: 48 ± 9.7 years) with no ECG abnormalities. BSPM recordings using an 87-lead Fukuda Denshi system gave isochrone maps, called also VAT (Ventricular Activation Time) maps, that reflect precisely the sequence of depolarization of the ventricles. Analyses of VAT maps inspired us to apply a new manner of displaying differences on VAT maps specific for a particular BBB type in one figure. This idea was realized through creating band patterns derived from VAT maps.

Results: In order to assess the differences in ventricular activation time values, the patterns consisting of coloured bands as well the reference of the mean VAT values for particular BBB types, were prepared. Each row of the matrix (the band), constituted by a set of ventricular activation time values recorded in each patient at all BSPM leads, is represented in the pattern figure as a single horizontal line. Recognition of individual BBB type is performed by comparison of the coloured areas arrangement reflecting VAT values from the given patient with the reference band patterns. This enables enrolment of a patient into the diagnostic group. While analyzing the band patterns, it was noticed that the mean values of VAT data did not differ significantly from the source values, which was verified by statistical analyses, and therefore makes the diagnosis more reliable.

Conclusions: Coloured VAT band patterns display features of intraventricular conduction disturbances of various types. Visual analysis of band patterns is a useful tool for quick diagnosis of bundle branch blocks.

http://dx.doi.org/10.1016/j.jelectrocard.2013.05.113

Sensitivity of epicardial electrical markers to ischemia detection

K. Aras, B. Burton, D.J. Swenson, R.S. MacLeod
University of Utah

Introduction: The goal of this study was to evaluate the sensitivity of electrogram markers on the cardiac surface to acute ischemia induced by complete or partial coronary occlusion combined with rapid atrial pacing in open chest canine and swine models.

Methods: The anesthetized open chest animals received coronary blood by means of a cannulated left anterior descending artery and pacing from atrial stimulus electrodes. We induced demand ischemia (i.e., maintaining reduced coronary flow and increasing the heart rate in steps) or supply ischemia (i.e., maintaining elevated heart rate and reducing coronary flow in steps) in episodes lasting 4–12 minutes followed by 20–30 minutes of reperfusion. A 247 electrode sock and up to 300 transmural needle electrodes captured epicardial and transmural electrograms. We determined onset of ischemia by ST elevation in the needle electrodes and then evaluated when it was detected on the epicardial surface by means of ST-segment, T-wave, R-wave, S-wave and QRS amplitudes.

Results: There was delay of 30–300 s between the onset of non-transmural ischemia (based on intramural electrograms) and its detection on the epicardial surface. The extent of the delay depended primarily on the ultimate degree of ischemia achieved for the particular combination of pacing rate and coronary flow. Of all the epicardial markers, epicardial T-wave changes were detected earliest.

Conclusion: Non-transmural ischemia can develop locally throughout the ventricular wall and often remain electrocardiographically silent on the epicardial surface and, by extension, from the ECG, until the ischemic region reaches a critical volume. From all the electrogram features, we found the epicardial T-wave amplitude to be the most sensitive to ischemia, more so even than the ST segment.

http://dx.doi.org/10.1016/j.jelectrocard.2013.05.114

Ventricular epicardial repolarization pattern in diabetic rabbits

M.A. Vaykshnorayte, A.O. Ovechkin, K.A. Sedova, J.E. Azarov
Laboratory of Cardiac Physiology, Institute of Physiology, Komi Science Center, Ural Branch, Russian Academy of Sciences

Introduction: The purpose of the study was to find out the spatial pattern of cardiac ventricular repolarization in diabetes mellitus (DM) in situ and to estimate the contribution of sympathetic tone to its development.

Methods: DM was indusced in rabbits with alloxan (100 mg/kg). At 4–5 week follow-up, the ventricular electrical potentials were mapped with the 64-electrode epicardial sock array in zoletil-anesthetized (10 mg/kg) animals, 13 of which were diabetic and 8 were healthy. Activation-recovery intervals (ARIs) serving as repolarization duration indices were measured in each lead prior to and after the injection of esmolol (0.5 mg/kg).

Results: The left ventricular (LV) apical ARIs were shorter than the basal ARIs in controls ($P < 0.046$), whereas the converse was found in DM ($P < 0.022$). Additionally, an interventricular ARI gradient was found in the DM group with the right ventricular (RV) ARIs being longer than the LV ARIs ($P < 0.022$). Esmolol abolished all the repolarization gradients within the ventricles in healthy and DM rabbits by the preferential prolongation of the initially shorter repolarization durations.

Conclusion: DM caused the remodelling of ventricular repolarization which at least in part could be ascribed to sympathetic dysfunction.

The study was supported by the grant for young scientist of Ural Branch of the Russian Academy of Sciences.

http://dx.doi.org/10.1016/j.jelectrocard.2013.05.115

Morphology-based characterization of rapid electrogram activity in atrial fibrillation patients

F. Ravelli[a], M. Masè[a], A. Cristoforetti[a], M. Del Greco[b], M. Centonze[c], M. Disertori[b]
[a]*Department of Physics, University of Trento*
[b]*Division of Cardiology, S. Chiara Hospital*
[c]*Division of Radiology, S. Chiara Hospital*

Introduction: Although the role of high-frequency (HF) sources in sustaining atrial fibrillation (AF) is widely recognized, the underlying mechanisms of rapid electrical activity have not been fully characterized. These may comprise focal/reentry mechanisms resulting in regular and repetitive patterns (rapid and repetitive sources, RR), as well as more complex propagation patterns yielding highly fragmented potentials (rapid and fragmented sources, RF). In this work, we aimed to combine a wave morphology (similarity index, S) analysis of atrial electrograms with an atrial cycle length (ACL) measurement, to distinguish the two types of

HF sources and investigate their spatial distribution in patients with persistent AF.

Methods: Biatrial electroanatomic mapping was performed in 14 patients with persistent AF. ACL and S indexes were calculated from atrial electrograms at each mapping point location, and ACL/S values were integrated on CT atrial reconstructions. RR and RF were identified as areas displaying a higher activation rate than the surrounding tissue, with similarity values of $S \geq 0.5$ and $S \leq 0.25$, respectively.

Results: 15 RR sources (1.1 ± 0.9 sources per patient, range 0–3) and 29 RF sources (2.1 ± 1.5, range 0–5) were found in our population of patients. While rapid sources displayed no preferential location, RR and RF sources clustered in specific atrial regions. RR sources were grouped in the region of the pulmonary veins and left atrial appendage (12/15), while RF sources were mainly located in the left atrial body (20/29). A lower number of sources was detected in the right atrium, with 3 RR sources located on the antero-lateral wall and superior caval vein region and 3 RF sources in the postero-septal region.

Conclusion: These results show the potential of the combined morphology/cycle length analysis to characterize the different nature of HF sources and to disclose their spatial distribution, which may have implications in the development of effective AF ablation strategies.

http://dx.doi.org/10.1016/j.jelectrocard.2013.05.116

Panoramic imaging of isolated rabbit hearts using a single camera system

A. Allan, F. Burton, G. Smith
University of Glasgow

Introduction: Mapping electrical activation over the whole cardiac surface has previously been achieved using multiple (typically 3) cameras. However, this can be done at lower cost using a single camera by rotating the heart through fixed angles and acquiring data sequentially from each viewpoint. Although this method cannot map irregular activity such as ventricular fibrillation, it can still be used to reconstruct fixed activation patterns resulting from repetitive stimulation.

Methods: Isolated Langendorff-perfused rabbit hearts were suspended in a custom chamber that allowed the heart and aortic cannula to be rotated to ± 120° from a central position using a stepper motor. Torsional movement of the heart was prevented by anchoring the apex. Activation timing was determined by external stimulation at rates higher than intrinsic pacemaker activity, applied to the right atrium (RA) or to ventricular myocardium. Epicardial voltage was monitored using voltage sensitive dye di-4-ANEPPS, loaded into the myocardium by bolus injection via the aortic cannula. Excitation at 480 nm was provided with LEDs (OptoLED, Cairn Research Ltd.). Emitted fluorescence was collected, filtered via a 590 nm long-pass filter and focused on a CCD chip (RedShirtImaging, Decatur, GA). Images (80 × 80 pixels) were acquired at 1 kHz. An idealised heart model was used to exclude overlapping sites from the 3 images. Excluded sites were identified by specifying a threshold angle of 60° normal to the surface of the heart in the model, and the resulting three unique images were then projected on to a single image representing the panoramic view.

Conclusion: The system can be used to: 1) map activation and repolarisation during RA pacing in the presence of an electromechanical uncoupler (blebbistatin) in normal conditions and in the presence of a ventricular infarct after ligation of the left circumflex artery, and 2) track movement of the ventricular wall without uncouplers with a high resolution camera in parallel to monitor electrical activity in the beating heart.

http://dx.doi.org/10.1016/j.jelectrocard.2013.05.117

A system for analysing thermal induced effects of propagation direction dependent features in field potentials of cardiomyocyte monolayers using multi-electrode arrays

R. Kienast, G. Fischer, M. Stöger, M. Handler, F. Hanser, C. Baumgartner
UMIT, Institute of Electrical and Biomedical Engineering

Introduction: Primary cultures of cardiomyocytes often contain multiple active pacemaker centres. This can lead to a changing origin of excitation. To analyse propagation direction dependent features such as the excitation velocity, it is important to have detailed information about spatial and temporal distribution of pacemaker centres and associated changes of direction in wave front propagation. However, a prerequisite for the analysis of such characteristics is the availability of a suitable temperature controlled measurement system and a computational approach to estimate the location of active excitation sources and their temporal changes.

Methods: Primary cultures of chicken cardiomyocytes are cultured directly on high-resolution multi-electrode arrays. A sensor array comprises 60 electrodes and is connected to an appropriate data acquisition system (Multi Channel Systems MCS GmbH, Reutlingen). To regulate the temperature of the cardiomyocyte monolayer during signal recording a temperature controlled extension module based on a water-cooling system was built. For an automated separation of excitation sources in time and space a novel algorithm based on the two dimensional spatial gradient of the wave front's arrival time was developed and successfully applied to our experimental data.

Conclusion: Our system allows a reproducible registration of thermal induced effects in field potentials of cardiomyocytes in-vitro using a multi-electrode array system. The computational method introduced provides detailed information of the temporal and spatial distributions of multiple active pacemaker centres in the cell culture. This information can be used to investigate thermal effects of propagation direction dependent features such as the excitation velocity or field potential rise time.

http://dx.doi.org/10.1016/j.jelectrocard.2013.05.118

Exercise training reduces life-threatening arrhythmias in heart failure rats: the importance exercise training intensity

T.S. Stølen[a], M.A.H. Høydal[a], A.B.J. Johnsen[a], S.E.G. Gaustad[a], E.S. Skogvoll[a], G.L.S. Smith[b], U.W. Wisløff[a]
[a]*NTNU*
[b]*University of Glasgow*

Introduction: Exercise is an effective treatment for heart failure (HF), but the relative beneficial and detrimental effect of moderate vs. high intensity training is uncertain. The aim of the study was to examine myocardial electrical activity in isolated hearts and excitation-contraction coupling in cardiomyocytes from rats with HF after exposure to moderate intensity (MOD) and high intensity aerobic interval training (AIT) regimens.

Results: Ventricular fibrillation (VF) was induced in all HF sedentary hearts (8/8). Exercise training reduced VF susceptibility in an intensity dependent manner (VF in 5/8 MOD hearts and 1/9 AIT hearts, $P < 0.001$). Prolonged action potential duration in HF hearts was normalized after MOD and further reduced after AIT ($P < 0.01$). Diastolic sarcoplasmic reticulum (SR) Ca^{2+} leak was highest in cardiomyocytes from the sedentary HF group ($P < 0.01$) and abolished by CaMKII inhibition, as well as AIT, whereas MOD had an intermediate effect. In a subsequent set of experiments, 2 isolated HF sedentary hearts were perfused with the CaMKII inhibitor AIP and 2 HF AIT hearts were perfused with the hERG inhibitor E4031 to observe whether CaMKII or hERG channel inhibition influence VF inducibility in HF. CaMKII inhibition did not change the VF threshold in HF sedentary rats, whereas hERG inhibition abolished the effect of AIT in HF. Depressed inotropy and lusitropy were present in the sedentary HF group ($P < 0.01$) and associated with depressed SR-Ca^{2+}ATPase (SERCA2a) and increased Na^{+}/Ca^{2+}-exchanger (NCX) activity. Both were normalized by exercise training in a dose dependent manner.

Conclusions: Exercise training reduced VF susceptibility and normalized Ca^{2+} cycling and inotropy. Inhibition of the hERG channels abolished the protected effects of high intensity exercise training on VF susceptibility. No adverse effects accompanied AIT in the post-MI HF rats.

http://dx.doi.org/10.1016/j.jelectrocard.2013.05.119

Intramural LV afterdepolarisations and arrhythmias during calcium overload in the intact rabbit heart

A. Kelly[a], G.L. Smith[b]
[a]*Norwegian University of Science and Technology*
[b]*University of Glasgow*

Introduction: The complex interaction between membrane potential (V_m) and intracellular calcium (Ca_i) governs excitation contraction coupling in the heart and is essential for normal regulation of the heartbeat. Spontaneous calcium release from the sarcoplasmic reticulum is thought to underlie after-depolarisations and triggered activity but the V_m/Ca_i relationship under these conditions is poorly understood. Using 2P laser scanning microscopy, we investigated action potentials (AP) and Ca^{2+} transients (CaT) at discrete transmural layers in the intact rabbit heart under conditions of Ca^{2+} overload.
Methods: Male New Zealand White rabbits (3–3.5 kg) were euthanized with an injection of sodium pentobarbital and heparin. Hearts were removed, mounted horizontally beneath a 2P microscope and retrogradely perfused at 37 °C. Pacing was initiated (250 ms PCL) from the LV endocardial surface. Hearts were loaded with the voltage and intracellular Ca^{2+}-sensitive dyes di-4-ANEPPS and Fura2-AM, respectively. Ca^{2+} overload was induced by perfusion with 1 μM ouabain. AP and CaT recordings were made at 100 μm intervals down to a depth of 600 μm using 2 kHz line scans.
Results: After 5 min of ouabain perfusion, slow increases in diastolic Ca^{2+} were evident indicating Ca^{2+} overload. This was accompanied by significant shortening of AP duration (APD_{90}) (162 ± 2 vs 142 ± 1 ms, PRE-vs POST ouabain, -200 μm; $P < 0.05$) and formation of a ~10 ms repolarisation gradient between the surface (100 μm) and deeper layers (200–600 μm). CaT rise time was significantly prolonged close to the surface (100–200 μm) but not deeper (300–400 μm). However CaT decay (CaT_{90}) demonstrated a gradual prolongation between 100 and 400 μm.
Conclusion: These preliminary data demonstrate depth-dependent behaviour of AP-CaT coupling in the intact heart during Ca^{2+} overload that is absent under normal conditions. The cause of these gradients is unknown but may reflect transmural differences in electrophysiology and Ca^{2+} handling underlying ectopic electrical events in the ventricle.

http://dx.doi.org/10.1016/j.jelectrocard.2013.05.120

The sequence of depolarization and structural organization of the myocardium in rats with hypertrophy of different genesis

I.M. Roshchevskaya, O.V. Suslonova, M.P. Roshchevsky
Laboratory of Comparative Cardiology of the Komi Science Centre, UD RAS, Syktyvkar, Russia

Introduction: Among chronic diseases of the cardio-vascular system, arterial hypertension of heterogeneous etiology leading to myocardial hypertrophy is the most common.
Methods: The sequence of depolarization and architecture of the myocardial left ventricle (LV) and interventricular septum (IVS) of normotensive Wistar rats (n = 30), Wistar rats with experimentally induced renovascular hypertension (n = 15, the Goldblatt model), and ISIAH rats with inherited stress-induced arterial hypertension (n = 7), were studied.
Results: In ISIAH rats, an even increase in thickness of the walls of the LV and IVS was revealed. The significant change of orientation of all myocardial layers did not occur due to the thickening of fibres of the circular layer. In rats with renovascular hypertension, the heterogeneous thickening of the walls of the LV and IVS, thickening of the subendocardial layer, the fibres of which are longitudinally oriented, and the change of thickness and orientation of the circular layer were revealed. In animals with myocardial hypertrophy of different genesis, the excitation wave in the ventricles spreads successively from the endocardium to epicardium as in the case of normotensive Wistar rats. In hypertensive animals, in the areas of most thickening of the circular layer, the excitation wave spreads unevenly with delays.
Conclusion: The increase of ventricular depolarization duration in animals with hypertrophy of different genesis is connected with hypertrophy of myocardial fibres and an increase of connective tissue volume compared to normotensive animals.
The study is supported by Program of UD and SO RAS, project No 12-C-4-1037.

http://dx.doi.org/10.1016/j.jelectrocard.2013.05.122

Cardioelectric field on the body surface of Wistar rats under postischemic reperfusion

M. Mazur, O. Suslonova, I. Roshchevskaya
Laboratory of Comparative Cardiology of the Komi Science Centre, UD RAS

Introduction: For early noninvasive diagnosis of ischemia and restoration of myocardial function, we use multichannel simultaneous cardioelectrotopography for receiving exact information on the localization, area and depth of the damage related to the functional condition of the reperfused myocardium.
Methods: We investigated body surface potential mapping (BSPM) on male Wistar rats (n = 19), anesthetized with urethane (1.2 g/kg, i/m) after 15-minutes occlusion and 60-minutes reperfusion of the left anterior descending coronary artery. Cardioelectric potentials were registered from 64 subcutaneous electrodes distributed on the thoracic surface of rats before and during occlusion as well as under reperfusion. Morphology of the reperfused myocardium was studied.
Results: During ventricular depolarization under coronary artery reperfusion, amplitude characteristics of BSPM changed unevenly in rats relative to the initial state. During the ascending phase of RII, the value of the positive and negative extrema noticeably increased. During the descending phase of RII, the amplitude of only the positive extremum clearly increased. During the maximal initial ventricular electrical activity, the BSPM amplitude characteristics did not significantly change compared with the initial state. During ventricular repolarization compared with the initial state during occlusion, a marked increase of the amplitudes of the positive and negative extrema was revealed. During reperfusion, the positive extremum reduced only during the ascending phase of the TII-wave. Histological changes of the reperfused myocardium were revealed in rats.
Conclusion: The experimental modelling of post-ischemic reperfusion of the coronary artery in Wistar rats leads to a significant change of amplitudes of the BSPM extrema between the initial and end phase of ventricular activity, along with morphological changes of the reperfused myocardium.
The study is supported by Program of UD RAS, project No 13-4-SP-442.

http://dx.doi.org/10.1016/j.jelectrocard.2013.05.123

Vectorcardiographic patterns for differential diagnosis in right end-conduction delay, early repolarisation and Brugada syndrome

C.A. Pastore, N. Samesima, E. Kaiser
Heart Institute (InCor) – Hospital das Clínicas da Faculdade de Medicina – Universidade de São Paulo

Introduction: Electrocardiographic (ECG) and vectorcardiographic (VCG) events occurring almost concomitantly during electrical activation of the heart may exhibit similar electrocardiographic aspects that confuse the correct diagnosis, as in the case of the QRS loop right end-conduction delay (RECD), early repolarisation (ER) phenomenon in anterior leads, and J-point elevation in leads V1–V3 in Brugada syndrome (BS). The objective of the present study was to analyse the three planes of the VCG to establish differential aspects that could identify these entities.
Methods: ECGs/VCGs of patients with BS (n = 18), ER (n = 15) and RECD (n = 10) were analysed and specific characteristics were compared.
Results: ECG appearances were as usual for these abnormalities, but with difficulties to differentiate right end-conduction delay from ER notch/delay or J point elevation in BS. In the horizontal plane, VCG loops showed slowing at the end of ventricular electrical activation in all cases, followed by a very neat gap between the end of QRS and beginning of T-wave loops, in all BS and ER cases. This gap was not evidenced in RECD (0/10). The QRS loop in RECD was always located in the right posterior quadrant (10/10). In BS, this location was 100% in the right anterior quadrant, while in ER it was 100% in left posterior quadrant. Also, with respect to ER and BS cases, a "break" in the QRS loop, very much resembling a "nose", was seen immediately before the beginning of the T-wave loop in BS (18/18). In ER, however, there was the clear presence of a "fishhook" shape at the end of the QRS loop in 100% cases.

Conclusion: The presence of a notch, especially in the horizontal plane, between the end of QRS and beginning of T-wave loops featuring the appearance of a "nose" in Brugada, and a "fishhook" in early repolarization, and their location in the quadrants, can be the differential diagnostic elements in these conditions.

http://dx.doi.org/10.1016/j.jelectrocard.2013.05.124

Relevance of individualized qt interval correction in subjects with large heart rate fluctuations

V. Jacquemet[a], R. Cassani Gonzalez[b], B. Dubé[b], A. Vinet[a], A.R. Le Blanc[b], M. Sturmer[b], G. Becker[b], T. Kus[a], R. Nadeau[b]
[a]*Université de Montréal*
[b]*Hôpital du Sacré-Coeur de Montréal*

Introduction: Careful measurement and individualized correction of the QT interval for heart rate are necessary to provide a stable physiological value, as demonstrated by Malik and colleagues. Our aim is to provide further arguments to support the use of this subject-specific approach when large fluctuations in heart rate are caused by atrial arrhythmias or induced by a treadmill stress test.

Methods: Four healthy subjects and ten patients with ventricular dysfunction underwent a stress test on a treadmill wearing a Holter ECG with pseudo-orthogonal leads. Twenty patients with atrial flutter undergoing catheter ablation were continuously recorded before, during and after the intervention using the same Holter monitoring system. In all cases, RR and QT time series were extracted and semi-automatically validated. QTc intervals were computed using Bazett's (QTc,B) and Fridericia's (QTc,F) correction formulae, and compared to a 3-parameter nonlinear subject-specific methodology incorporating transfer-function based hysteresis reduction (QTc,I). Stability in QTc determination was estimated as the intra-subject standard deviation (std) of the QTc time series.

Results: Table 1 shows the intra-subject QTc variability in each group for the three different QT correction formulae.

Table 1
Intra-subject QTc variability.

Group	std (RR)	std (QTc,B)	std (QTc,F)	std (QTc,I)
Stress test healthy	156 ± 34 ms	16.8 ± 2.4 ms	12.9 ± 4.4 ms	7.1 ± 2.1 ms
Stress test patients	125 ± 28 ms	22.1 ± 5.6 ms	15.7 ± 4.8 ms	10.4 ± 4.5 ms
Flutter patients	193 ± 55 ms	30.1 ± 9.1 ms	20.0 ± 5.1 ms	8.4 ± 3.5 ms

Conclusion: When large RR fluctuations occurred, hysteresis reduction and individualized QT correction significantly and consistently decreased intra-subject QTc variability.

http://dx.doi.org/10.1016/j.jelectrocard.2013.05.125

Detection of the role of anxiety in the genesis of idiopathic ventricular parasystole and the choice of pathogenetic therapy

T.E. Tulintseva, D.Y. Ilina, E.A. Tsurinova, T.V. Treshkur
Almazov Federal Heart, Blood and Endocrinology Centre

Introduction: High levels of anxiety are common in patients with idiopathic ventricular parasystole (VP). The aim of the study was to define the possibility of treatment of VP with an anxiolytic in patients with anxiety.

Methods: Inclusion criteria consisted of an abnormal amount of idiopathic VP during Holter ECG recording, and a medium or high anxiety level according to psychological questionnaires. All patients underwent a clinical examination, ECG, echocardiogram, ETT, psychological questionnaires, psychological counselling, and an emotional Stroop Colour and Word Test (SCWT). There were two groups formed out of 56 patients. Group I included 20 patients (12 women), mean age 46.6 ± 14.7 years, with ventricular ectopic complexes (VEC) totalling 11354.7 ± 536.3/day, who received an anxiolytic in a therapeutic dose for 30 days. The control group consisted of 20 patients (11 women), 45.2 ± 11.3 years, VEC 12467.2 ± 423/1 /day, without any therapy. Holter ECG, SCWT and psychological questionnaires were repeated in 30 days.

Results: The average number of VEC decreased significantly from 478.8 ± 47.2 to 155.7 ± 73.2 ($t_{cmp} = 2.4$, $p \leq 0.05$) in the first group according to Holter ECG findings, while in the control group, VEC decreased from 512.5 ± 67.5 to 467.3 ± 39.4 ($t_{cmp} = 0.5$, $p \geq 0.05$). A positive SCWT became negative in 95% of patients in the first group, i.e. an arrhythmia was not provoked ($\phi_{cmp} = 3.1$, $p \leq 0.01$). The number of patients with middle and high anxiety level decreased more than 3 fold ($\phi_{cmp} = 1.85$, $p \leq 0.05$), after therapy with an anxiolytic. There were no significant changes in the second group with respect to the results of the questionnaires and SCWT.

Conclusions: This study shows that psychogenic factors play an important, and sometimes a decisive role in the genesis of idiopathic VP. Anxiolytic therapy can be recommended for patients with VP and a high anxiety level.

http://dx.doi.org/10.1016/j.jelectrocard.2013.05.126

T wave alternans, detection, quantification and pattern definition

A.D.D. Aruna Deogire[a], S.T.H. Satish Hamde[b]
[a]*MET's Institute of Engineering*
[b]*SGGS Institute of Engineering and Technology, Vishnupuri, Nanded*

Introduction: T Wave Alternans (TWA), a ventricular repolarization phenomenon, can identify increased risk of sudden cardiac death. This study is a multilead principal component analysis technique to detect and quantify TWA with pattern classification ABAB or BABA.

Methods: The testing was done on the Physionet/CinC 2008 challenge database. This is a collection of 100 ECG records out of which 30 are synthetic, with known alternans magnitudes. The proposed method is aimed at detecting these positive alternans cases. ECG records are filtered moderately to preserve the alternans characteristics. Detection of R peaks and calculation of heart rate is then undertaken. T peaks are detected and T waves are isolated. Isolated T waves of eight independent leads are passed to a Principal Component Analysis (PCA) and the first PAC component is the signal for analysis. TWA detection is done by comparing amplitudes of alternative T waves. If a difference in amplitude is found, on alternate basis, consecutively for 1/4 of total detected beats and heart rate and variance criteria are matching, then alternans is considered as present. The alternans magnitude is calculated for detected records with pattern classification.

Results: After examining 100 records, 29 were detected as TWA positive, with no false detection, where 30 were expected. Our results were compared with those of Bortolan G, Christov I. (2012) and show considerable improvement, as indicated in the table. For those TWA records detected, the magnitude was calculated and compared with the actual values. This revealed that there were 9 records with 0% error, 12 records with <25%, 2 records with 30% and 6 records with 50% error out of the total of 29 detected records. Furthermore, the TWA pattern ABAB or BABA was also classified.

Method	Sensitivity (%)	Accuracy (%)
Proposed	96.66	96.66
Bortolan G, Christov I. (2012)	86.7	87.5

Conclusion: Thus, the present work is a step in the direction of understanding and contributing to TWA research where an attempt is made to detect the presence or absence of TWA, quantify its magnitude and define the pattern of alternans. The magnitude measurement and pattern classification part of this work need further improvement. This work is currently in progress.

http://dx.doi.org/10.1016/j.jelectrocard.2013.05.127

Autocorrelation maps of atrial activation in young adults—a preliminary study

K. Kozlikova
Institute of Medical Physics, Biophysics, Informatics and Telemedicine, Faculty of Medicine, Comenius University of Bratislava

Introduction: Atrial depolarization can be displayed in body surface isopotential maps (IPM) that may be analysed using autocorrelation maps (ACM). The aim of this work was to study the form of the ACM in young adults.
Methods: We constructed IPM from 24 leads after Barr in 92 controls (49 women, 43 men) without cardiovascular disease, aged 18–20 years, every 5 ms during the P wave. For each subject, every IPM was compared with every IPM using Pearson's correlation coefficient r. Comparisons were displayed in the form of ACM, square graphs with values r = 1 on the main diagonal. We analyzed the regions with high positive correlation $r \geq 0.9$ where the potential distribution changed slowly.
Results: The mean P wave duration was 84 ± 11 ms and the potentials ranged from 0.18 mV to 0.19 mV. The mean correlation coefficients of the ACM were 0.69 ± 0.09 ranging from 0.46 to 0.88. Negative correlation occurred in 56 ACM. We identified 4 types of ACM according the form of regions with high positive correlation. In type A (22 men, 10 women), the broadest region appeared at the beginning of the P wave; in type B (8 men, 14 women) at the end of the P wave; in type C (8 men, 8 women) approximately in the middle of the P wave. This broadening was always connected with narrow parts at its borders. In the remaining 22 cases (5 men, 17 women - type D), the region of $r \geq 0.9$ had approximately uniform width along the main diagonal.
Conclusion: We assume that different types of ACM probably display atrial activation represented by circular isochrones (slow changes) or preferential paths (fast changes). This hypothesis has to be verified in special studies.
(This study was partially supported by the grant KEGA 004UK-4/2011 from the Ministry of Education, Science, Research and Sport, Slovak Republic.)

http://dx.doi.org/10.1016/j.jelectrocard.2013.05.128

Does the inverse activation time/action potential duration relationship apply to the in vivo human heart?

M. Orini[a], B.M. Hanson[a], R. Bufacchi[a], M. Hayward[b], X. Jie[a], P. Taggart[a], P.D. Lambiase[a]
[a]*University College London*
[b]*University College London Hospital*

Introduction: Experimental evidence indicates an inverse relationship between action potential duration (APD) and activation time, attributed largely to local electrotonic current flow, which limits intrinsic dispersion of repolarization. However other factors may interact to modulate this response. The relationship between activation time (AT), repolarisation time (RT) and APD over the left and right ventricular epicardium in humans in vivo has not been reported.
Methods: 264 unipolar epicardial electrograms were recorded from 35 patients undergoing cardiac surgery for coronary artery disease. Pacing was established from the epicardial left ventricle over a range of cycle lengths (600 ms–350 ms). Activation recovery intervals were measured as a surrogate for APD as the time from the minimum derivative during depolarization phase to the maximum derivative during repolarization phase. Repolarization time was taken as RT = APD + AT. The linear correlations between AT and APD, and between AT and RT were studied with a robust bisquare method.
Results: Contrary to experimental work and previous observations in human endocardium, we observed the absence of a negative relationship between APD and local AT for all cycle lengths (median slope equal to −0.07 APD/AT, refer to Table 1 for details). As a result, the measured dispersion of repolarization was equal to or larger than the dispersion of depolarization.
Conclusion: Multielectrode mapping of left ventricular epicardium in humans revealed the absence of an inverse relation between APD and local activation time. This is in sharp contrast to most experimental work and in vivo human endocardiac data. As a result, the limitation of dispersion of repolarization conferred by a negative APD/AT slope was not present on the epicardium. This novel finding in humans in vivo may be relevant to arrhythmogenesis based on re-entrant mechanisms.

http://dx.doi.org/10.1016/j.jelectrocard.2013.05.129

Dual excitation wavelength optical imaging of transmural electrophysiological heterogeneity in pig ventricles

R.D. Walton, O. Bernus
Universite Bordeaux Segalen – LIRYC

Introduction: Transmural heterogeneity of the ventricular action potential duration (APD) is a major determinant of arrhythmogenic potential. However, challenges remain to measure transmural electrophysiologcal characteristics in the intact ventricles.
Methods: We utilised dual-wavelength excitation on pig (N = 22) left and right ventricular slabs stained with DI-4-ANBDQBS and used modulated LED illumination at 530 and 660 nm. Two CCD cameras imaged the epicardial (EPI) and endocardial (ENDO) surfaces, simultaneously recording reflected and transilluminated fluorescence for both excitation wavelengths, producing eight optical movies per experiment ($EPI_{0\text{-}3}$ and $ENDO_{0\text{-}3}$ in reference to the illuminated surface). The epicardium was paced from 1–4 Hz and optical action potentials (AP) recorded with dual-wavelength illumination at an effective frame rate of 750 Hz.
Results: Biophotonics simulations indicate that the respective optical signals originate from mean depths of 0.5, 1.5, 2.5 and 4 mm below the illuminated surface. EPI_0 therefore reflects primarily EPI activity, whereas EPI_3 contains significant contributions from the mid-myocardium (similar for ENDO). Overall, longer APDs were found in LV vs. RV (2-way ANOVA, p = 0.029). APD was significantly shorter in EPI_0 vs. $ENDO_0$ in LV (187.8 ± 7.4 ms vs. 215.0 ± 12.3 ms; p = 0.004). Similarly, an APD difference was found between EPI_0 and $ENDO_0$ in RV (173.2 ± 5.4 ms vs. 193.3 ± 10.8 ms; p = 0.045). Transmurally, a smooth increase in APD from EPI to ENDO was observed in the RV (2.1 ± 0.5 ms/mm). In the LV however, APD was found to be fairly constant throughout the mid-myocardium (192.3 ± 7.4 ms) at an intermediate level between EPI and ENDO. The steepest APD restitution curves were found within the sub-ENDO of LV ($ENDO_2$) and RV ($ENDO_1$).
Conclusion: Dual-wavelength excitation optical imaging with simultaneous acquisition of reflected and transilluminated signals has for the first time made it possible to infer transmural APD gradient in intact pig LV and RV.

http://dx.doi.org/10.1016/j.jelectrocard.2013.05.130

Table 1
Statistical results over 35 patients (median and interquartile range).

Cycle length [ms]	350	400	450	500	550	600
APD/AT slope [ms/ms]	−0.15/0.31	−0.02/0.30	−0.12/0.25	−0.08/0.26	−0.08/0.31	−0.11/0.43
RT/AT slope [ms/ms]	0.83/0.31	0.98/0.25	0.88/0.24	0.90/0.27	0.88/0.33	0.85/0.42
AT dispersion [ms]	89/34	85/37	90/33	88/33	89/30	82/30
RT dispersion [ms]	91/38	102/47[#]	109/43[#]	90/45	106/49[#]	106/38[#]

[#] Dispersion of repolarization is larger than dispersion of depolarization (P < 0.05, rank sum test).

Measurements of ventricular activation and repolarisation during deep hypothermia and rewarming using panoramic optical mapping of isolated Langendorff perfused rabbit hearts

E.S. Dietrichs[a], A. Allan[b], F. Burton[b], T. Tveita[c], G. Smith[b]
[a]*Norwegian Air Ambulance Foundation*
[b]*University of Glasgow*
[c]*University of Tromsø*

Introduction: Rewarming victims of accidental hypothermia is complicated by a high risk for arrhythmias and cardiac arrest, contributing to high mortality in these patients. The pathophysiology behind these arrhythmias is not yet fully understood. We therefore used our model of panoramic optical mapping to evaluate cardiac electrophysiology during cooling and rewarming from severe hypothermia.

Methods: Rabbit hearts were Langendorff-perfused with solution containing the mechanical uncoupler Blebbistatin (3 μM). Hearts were loaded with voltage sensitive dye to record membrane voltage from the epicardial surface and images were taken from 3 sides to record optical action potentials panoramically. Throughout recordings, hearts were right atrial paced at 300 ms (37 °C), 450 ms (31 °C) or 1700 ms (17 °C), based on intrinsic rates at these temperatures.

Results: Distribution of values was mostly uniform on all 3 views. Right ventricular (RV) activation time (T Act) was unaffected by cooling to 31 °C (37 °C vs. 31 °C, 154 ± 3 ms vs. 160 ± 9 ms, n = 6), while action potential duration (APD) increased (154 ± 7 ms vs. 243 ± 5 ms, n = 6 $p < 0.05$). Cooling to 17 °C increased T Act (37 °C vs. 17 °C, 154 ± 3 ms vs. 325 ± 28 ms, n = 6 $p < 0.05$) and APD (154 ± 7 ms vs. 423 ± 18 ms, n = 6 $p < 0.05$). Rewarming to 31 °C normalized TAct (37 °C vs. 31 °C, 154 ± 3 ms vs. 169 ± 10 ms, n = 6) but not APD (154 ± 7 ms vs. 253 ± 8 ms, n = 6 $p < 0.05$). Both T Act (initial vs. final, 154 ± 3 ms vs. 145 ± 5 ms, n = 6) and APD (154 ± 7 ms vs. 165 ± 3 ms, n = 6) normalized after rewarming to 37 °C.

Discussion: Hypothermia induced changes in action potential morphology with T Act being more affected by moderate hypothermia (31 °C) than APD. These differences were not accentuated by severe hypothermia (17 °C), but were even more pronounced during rewarming (31 °C). The present results demonstrate a condition similar to long QT syndrome at mild hypothermia and during rewarming from severe hypothermia.

http://dx.doi.org/10.1016/j.jelectrocard.2013.05.131

On complementary sensitivity distributions and resolution of MCG and ECG

V. Mäntynen, T. Konttila, M. Stenroos
Department of Biomedical Engineering and Computational Science, Aalto University

Introduction: Magnetocardiography (MCG) and electrocardiography (ECG) detect cardiac electrical activity in a complementary way. There are various mechanisms suggested for this difference. In this work, we characterize the sensitivity and resolution of the ECG and MCG with the help of numerical simulations and resolution analysis.

Methods: A realistically shaped volume conductor model for MCG and ECG was built using the boundary element method. The source of the electromagnetic field was modelled as freely-oriented primary current density spanned on the cardiac surface, and lead-field matrices for both modalities (body surface potential mapping, BSPM, and MCG) were built. Sensitivity was assessed in terms of L2 norm of the lead vector for each source location. Source-reconstruction capability of the modalities was assessed with minimum-norm current density estimation (CDE) and its point-spread function (PSF).

Results: On the anterior wall, MCG showed higher sensitivity to tangential currents than to normal currents, whereas BSPM was relatively more sensitive to normally-oriented currents. This relative difference was partially due to the proximity of cardiac blood masses. Sensitivity to posterior sources was clearly lower especially for MCG but also for BSPM. The PSF analysis results reflected the sensitivity distribution so that with MCG the anterior tangential currents were better localized and the corresponding source estimate was less spread compared to BSPM, whereas BSPM performed relatively better with posterior sources.

Conclusions: Volume conductor properties, especially due to the ventricular blood, contribute to produce complementary sensitivity distributions and resolution for MCG and ECG. This explains a part of observed differences between the two modalities. Simple numerical simulations and basic properties of linear estimators allow intuitive characterization of sensitivity differences.

http://dx.doi.org/10.1016/j.jelectrocard.2013.05.132

Dual analyses to identify best lead(s) on QT interval measurement for bedside ECG monitoring

S.L. Lo[a], H.S. Lo[b], H.C. Lo[c], F.C. Lin[d], S.J. Yeh[d]
[a]*Chang Gung University of Science and Technology*
[b]*Cathy General Hospital*
[c]*Taipei Veteran General Hospital*
[d]*Chang Gung Memorial Hospital*

Introduction: Adequate use of QT interval measurement in real time in hospital is a challenging aspect of bedside ECG monitoring due to the lack of a standardized and simple approach for finding the best measuring lead(s). Modern clinical practice relies on scientific, empirical and updated information. Thus, we aimed to investigate the best lead(s) for QT interval measurement for bedside ECG monitoring, through adopting a dual analysis approach.

Methods: A systematic review was undertaken in accordance with the Preferred Reporting Items for Systematic Reviews and Meta-Analyses. Search terms "QT interval, QT interval measurement, QT prolongation" in adult human studies were used on Web of Science, PubMed, EBSCO and Google Scholar. The outcomes assessed were the longest and most measureable across the 12 leads. We assessed the quality of evidence as recommended by Grading of Recommendations Assessment, Development and Evaluation. Secondly, we added a narrative review as an implicit process to compile evidence that supported the findings and statements being made.

Results: Twelve studies that involved 5927 subjects with 6635 ECGs for the period from 1966 to April 2012 were used. Despite several small sample sizes and moderate quality of these studies, the heterogeneity of study design and the diversity of collecting procedures were enhanced and precluded by the use of meta analysis. Lead V3 represented the most measureable and longest lead in ten of 12 studies; lead V4 was the longest in seven studies; and lead V2 appeared measureable in five studies. Lead II was found stable but unreliable.

Conclusion: Lead V3 was the best single lead for bedside monitoring for detecting a prolonged QT interval, and V4 can be used as an alternative. The authors suggest that future research should incorporate positron emission tomography imaging to determine whether results could be linked to a ventricular repolarisation effect and should re-examine these issues for current populations.

http://dx.doi.org/10.1016/j.jelectrocard.2013.05.133

ECG predictors of mortality among implantable cardioverter-defibrillator candidates for the primary prevention of sudden cardiac death

S. Al-Zaiti[a], J.A. Fallavollita[b], J.M. Canty[b], M.G. Carey[c]
[a]*University of Pittsburgh*
[b]*State University of New York, Buffalo*
[c]*University of Rochester*

Background: It has yet to be determined if the electrocardiogram (ECG) can provide prognostic information regarding the likelihood of sudden (SCD) versus cardiac non sudden death (C/NS) in high risk cardiac patients. Accordingly, we sought to evaluate the prognostic value of resting and ambulatory ECG parameters in patients with ischemic cardiomyopathy who were eligible for the primary prevention of SCD with an implantable cardioverter-defibrillator (ICD).

Methods: We prospectively evaluated 17 well validated high risk ECG parameters in PAREPET subjects (Prediction of ARrhythmic Events with

Positron Emission Tomography; n = 204, EF ≤ 35%, age 67 ± 11 years, 90% men). Twenty-four hour Holter ECG recordings were obtained in 97% of patients at the start of the study and were semi-automatically evaluated by a blinded reviewer. Patients were followed up by phone at 3-months intervals. Endpoints were determined by a blinded committee of cardiologists. ICD discharges due to ventricular fibrillation or tachycardia (≥240 beats/min) were considered equivalent to SCD.

Results: After a mean follow up of 51 ± 2 months, there were 33 (16%) SCD and 36 (18%) C/NS. In the multivariate analysis, QTc prolongation was predictive of SCD (hazard ratio 2.9 [1.2–7.3]) and depressed heart rate variability (HRV) was predictive of C/NS (hazard ratio 5.0 [1.5–17.1]). Persistent bi-ventricular pacing was associated with increased C/NS mortality, probably due to the strong correlation with a lower LVEF.

Conclusions: Among candidates for primary prevention of SCD, the ECG can yield further prognostic information independently from age and LVEF. Prolonged QTc predicted SCD and therefore potential ICD benefit. On the other hand, depressed HRV predicted C/NS death, suggesting that this risk factor may be particularly helpful to identify those who might benefit from bi-ventricular pacing in order to reduce the risk of heart failure death.

http://dx.doi.org/10.1016/j.jelectrocard.2013.05.134

Predicting the accuracy of cardiac pace mapping from lead field matrix characteristics

W.H.W. Schulze, D. Potyagaylo, O. Dössel
Institute of Biomedical Engineering, Karlsruhe Institute of Technology (KIT)

Introduction: In ECG imaging of transmembrane voltages, a lead field matrix is used that relates sources at an arbitrary position in the heart to the body surface potential map (BSPM). We assessed the ability of the lead field matrix to provide information on the similarity of extrasystoles originating from various locations in the heart. The proposed analysis can serve as a predictor for the accuracy of pace mapping studies.

Methods: A coarse subset of 3340 nodes was selected from a thorax mesh to create a map of stimulation sites in the heart (resolution: 4 mm). To simulate realistic extrasystoles starting from these sites, fibre orientations were introduced into the model and a cellular automaton was run until an elliptic volume with radius of 4.35 mm was reached. To resemble the simulated extrasystoles, a lead-field matrix was then created for the sum of all single point sources in the 1-step vicinity of the respective site. Both for the sources in the lead field matrix and the simulated extrasystoles, BSPM signals from one source were compared to those of other sources in the heart, with a single electrode signal difference of at least 10 microvolts serving as a criterion for similarity.

Results: Using the lead field matrix, 1652 out of 3340 sources were found to produce a unique BSPM that is characteristic for one single source in the heart (compared to 1747 out of 3340 single beats in the simulations). Points that could not be separated caused an overall localization error of 16 mm ± 25 mm (19 mm ± 29 mm). In the extreme case, when using the lead field matrix to find non-unique points, the distance to the next indistinguishable point in the simulation was 29 mm.

Conclusions: The lead field matrix serves well the purpose of predicting the average accuracy in pace mapping. Many ectopic beats can be localized precisely using the BSPM, but many others cannot be separated.

http://dx.doi.org/10.1016/j.jelectrocard.2013.05.135

Inter-catheter impedance variation during internal atrial defibrillation

P.R. Walsh[a], O.J. Escalona[b], D. Brody[c], J.M.C. Anderson[c]
[a]Waterford Institute of Technology, Ireland, and University of Ulster, Faculty of Engineering, UK
[b]University of Ulster, Engineering Research Institute, UK
[c]Heartsine Technologies Ltd., Belfast, UK

Introduction: According to the European Society of Cardiology, atrial fibrillation (AF) has a prevalence of 1–2% in the general population, rising to over 5.5% in individuals over 55 years of age and accounts for in excess of 30% of all arrhythmia related hospital admissions. For chronic AF sufferers (where all other therapies have proved ineffective), restoration of sinus rhythm through electrical shock remains the treatment of choice. Internal atrial defibrillation thresholds as low as 1.27 joules have been reported. However, at low energies, complex electro-mechanical interactions at the catheter-tissue interface have long been suspected as a major source of variation in the amount of electrical energy required to terminate this arrhythmia. The objective of this work was to characterise the variation of inter-catheter impedance during internal atrial defibrillation.

Methods: For this study, a custom low-power programmable impedance spectrometer was built to deliver a sinusoidal current of ±200 μA in magnitude from 1–100 kHz in frequency. Using this system, the complex impedance between a pair of defibrillation electrode poles (placed in the distal coronary sinus and wall of the right atrium) was recorded between successive atrial defibrillation attempts.

Results: A total of ten porcine models were investigated. Measurements detected inter-catheter impedance variations ranging from 15.5% to 28.9%. Subsequent data analysis revealed a mean inter-catheter impedance of 43.9 Ω with a variance of approximately 20.1% recorded.

Conclusions: Complex electro-mechanical interactions at the catheter-tissue interface have been identified as a cause of significant variation in inter-catheter impedance; which alters the associated cardioversion threshold during internal atrial defibrillation. Further research will be required to fully understand and mitigate adverse effects of the physical mechanisms involved.

http://dx.doi.org/10.1016/j.jelectrocard.2013.05.137

ECG management in Glasgow – from "patient to portal"

M.P. Watts, M. Gray, D.L. Murdoch, A. Cowe
NHS Greater Glasgow and Clyde Health Board

Introduction: Several years ago, as part of an ongoing service development in the Greater Glasgow and Clyde Health Board area, it was decided that ECGs from six acute and ambulatory care hospitals should be uploaded to a central GE Healthcare MUSE ECG management system and then made viewable to all clinical staff through the Glasgow Clinical Portal. The project was to be supported by a multidisciplinary team within the Health Board with external support from GE Healthcare.

Methods: The MUSE system was interfaced to the Health Board's SCI Store information repository to facilitate the automatic checking of patient demographic details prior to routing the ECG record to be viewed in the Clinical Portal. Fifty electrocardiographs from three different manufacturers are currently uploading a total of approximately 2000 ECGs per week from multiple sites, including three accident and emergency departments, with a cumulative total to date of 109,000 ECGs.

Results: The challenges encountered in setting up a large multi hospital ECG management system were substantial. The centralisation of ECG records across five Cardiology departments and the increasing number of ECGs being recorded by nursing staff required an approach to standardisation and a change of culture in moving from a paper case note environment to an electronic one. Multiple repeat ECGs for quality improvement over a short period of time and the many variants of demographic data input were found to be the major operational problems. Both ranged up to 12% of the total ECGs recorded in some clinical areas.

Conclusion: Whilst work continues to address these two issues, overall the system offers, in addition to the centralised storage and retrieval of ECGs over a wide area through the Clinical Portal, the advantages of validated patient ID on the ECG record, a large database for teaching and improvements in the collection of ECG management information.

http://dx.doi.org/10.1016/j.jelectrocard.2013.05.138